THESIS

INVESTIGATION OF ADIPOSE-DERIVED MESENCHYMAL STEM CELLS INTERACTION WITH ELECTROSPUN DEMINERALIZED BONE MATRIX NANOFIBER SCAFFOLDS

Submitted by

Selin Yaprak Akgul

Department of Chemical and Biological Engineering

In partial fulfillment of the requirements

For the Degree of Master of Science

Colorado State University

Fort Collins, Colorado

Spring 2016

Master's Committee:

Advisor: Matt Kipper
Co-Advisor: Ketul Popat

Travis Bailey
Nicole Ehrhart

ABSTRACT

INVESTIGATION OF ADIPOSE-DERIVED MESENCHYMAL STEM CELLS INTERACTION WITH ELECTROSPUN DEMINERALIZED BONE MATRIX NANOFIBER SCAFFOLDS

Nanofiber demineralized bone matrix (DBM) scaffolds were fabricated by electrospinning, and their ability to support cell adhesion and cell viability of murine adipose-derived mesenchymal stem cells (AD-MSCs) for short-term in culture media was investigated. Poly (ε-caprolactone) (PCL) scaffolds were used as control surfaces. Live cell stain calcein-AM and CellTiter 96® Non-Radioactive Cell Proliferation assays were used for cell adhesion and cell proliferation, respectively. DBM scaffolds supported greater cell adhesion compared to PCL nanofiber scaffolds. For cell viability, the two types of scaffolds behaved similarly. The results led to further research on DBM scaffolds. The ability to support osteoblastic differentiation of AD-MSCs for long-term (three weeks) in osteogenic differentiation media was also investigated. Both PCL scaffolds and DBM scaffolds seeded with no cells were used as control surfaces. The total protein content of viable AD-MSCs on the scaffolds was assessed by bicinchoninic acid (BCA) assay. Nanofiber scaffolds displayed increased levels of alkaline phosphatase (ALP) activity for the first week for all cases. ALP activity dropped after one week. Scanning electron microscopy (SEM) and alizarin calcium staining techniques were used to examine mineralization patterns qualitatively on DBM and PCL nanofiber scaffolds. DBM scaffolds deposited more calcium mineral than PCL scaffolds during three-week experiments. Mineralization was quantified by energy-dispersive X-ray spectroscope (EDS). After three weeks of culture, EDS revealed high calcium and phosphorus

deposition on DBM scaffolds compared to PCL controls. The DBM scaffolds exhibited increased mineralization over three weeks, both with and without cells. These results demonstrate that the adhesion, proliferation, and osteogenic differentiation of AD-MSCs were influenced by DBM scaffolds.

ACKNOWLEDGEMENTS

First and foremost, I would like to thank my advisors Dr. Kipper and Dr. Popat.

I would like to thank Dr. Kipper for accepting and welcoming me to his lab. I am deeply grateful for all his help and guidance, not only during my study in the program but also during my thesis work. Without his guidance and support, I would not be able to reach my goals.

I would like to express the deepest appreciation to Dr. Popat for his encouragement and continuous support throughout my thesis work. His trust and guidance gave me the opportunity to start and make progress on research. I am very thankful for his kindness and willingness to help me all the time.

I wish to thank Dr. Victoria Lezsczak. Dr. Laura Place, and soon to be Dr. Raimundo Romero for all their patience and valuable help as I progressed through my thesis. I would not be able to proceed as quickly as I did without their teachings.

Many thanks to my undergraduate assistants Michelle Ablutz, Jacob DeRoo, and Emilie Asbury for their efforts and assistance.

Finally, my sincere thanks go to my committee members Dr. Nicole Ehrhart and Dr. Travis Bailey for their availability and valuable insights.

DEDICATION

I would like to dedicate this work to my family, without whom none of this would have ever been possible, and to whom I am greatly indebted. To my husband, Emre Akgul, thank you for all your love and support during my exciting and challenging graduate school experience. I would like to extend to you my deepest appreciation for the encouragement you gave throughout my graduate study. To my mother, Guzin Yaprak, who has loved me unconditionally and supported me throughout my life. Thank you for all your sacrifices. To my father's memory, who is and will always be with me. Finally, to my brother, Sarper Yaprak, thank you for your love and trust throughout my life. Thank you all. I love you.

TABLE OF CONTENTS

LIST OF TABLES

LIST OF FIGURES

HYPOTHESIS AND SPECIFIC AIMS

Fundamental Hypothesis: Demineralized Bone Matrix (DBM) scaffolds can influence the osteoblastic behavior of adipose-derived mesenchymal stem cells.

Specific Aim 1: Development of electrospun nanofiber scaffolds from Demineralized Bone Matrix (DBM) and Poly (ε-caprolactone) (PCL).

Specific Aim 2: Characterize different Demineralized Bone Matrix (DBM) powder by using a thermal analysis technique.

Specific Aim 3: Investigate adipose-derived stem cell adhesion, proliferation and differentiation on DBM nanofiber scaffolds.

CHAPTER 1: LITERATURE REVIEW

1.1 Introduction

Tissue engineering is a developing science that combines biology, medicine, chemical engineering, mechanical engineering, and materials science. This field is a substitute for tissue transplantation. Tissue transplantation has many challenges; harvesting tissues and transplanting them from one area to another in the same person can be hurtful and costly, and may also have other constraints. Likewise, transplanting tissues from another person may be risky because of the immune system's responses. However, biological substitutes can be produced to restore, maintain, and improve tissue function by using tissue engineering applications. These applications increase the well-being of many people [1]. Examples of current research areas are engineering of skin, cartilage, bone, nerves, corneal epithelia, heart myocardium, blood vessels, arteries, and heart valves. There has been significant progress in tissue engineering of skin and cartilage. Artificial skin is produced from human skin cells in hydrogel form for burn injuries (microfab) and scaffold-free cartilage is successfully obtained from a construct that is just made of cells [2]. Other tissues like blood vessels and heart myocardium are more complex, thus engineering these type of tissues are more challenging [3].

The primary concept of tissue engineering is isolating cells or cell substitutes, then seeding these to scaffolds, so that they can culture a specific tissue. The cultured tissue is then transplanted to the damaged site. Figure 1.1.1 illustrates the central tissue engineering paradigm. There are three important factors that contribute to the success of tissue engineering applications: cells, scaffold, and cell-matrix (scaffold) interactions [4-6].

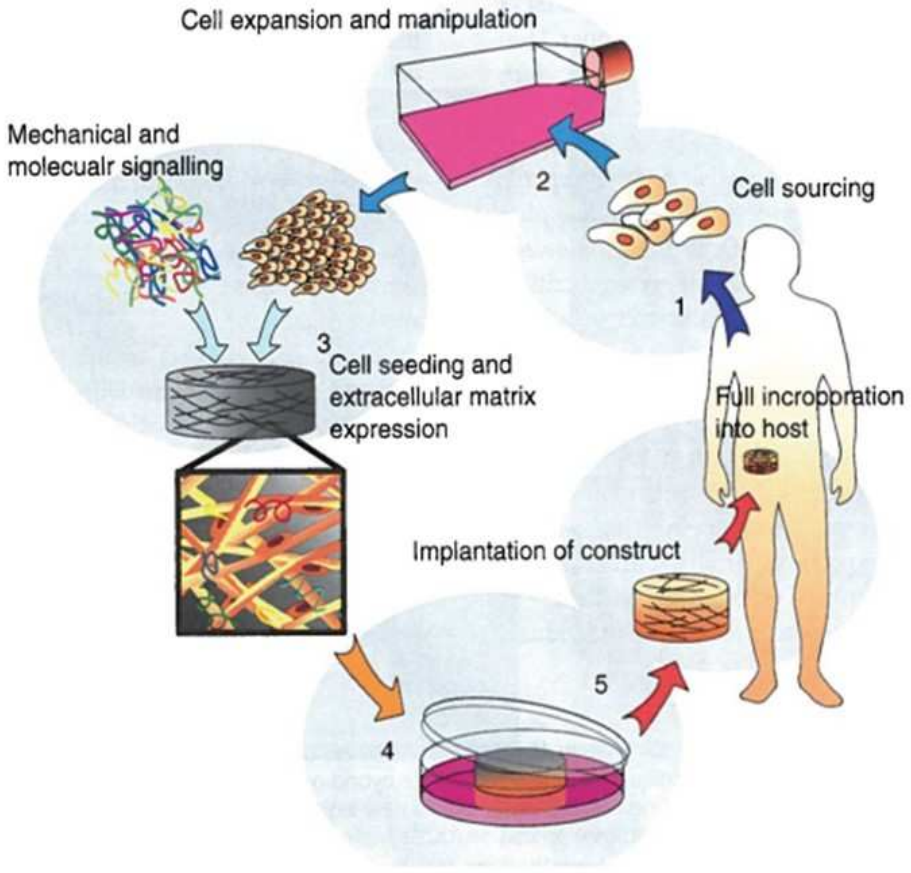

Figure 1.1.1: The central tissue engineering paradigm [7]. The primary concept of tissue engineering is isolating cells or cell substitutes, then seeding these to scaffolds, so that they can culture a specific tissue. 1: cell sourcing, 2: cell expansion and manipulation, 3: cell seeding, 4: implantation, 5: incorporation into host. Reprinted from Tissue Engineering, Blitterswijk, C. V. Burlington, MA: Elsevier, p. xv, Copyright 2008, with permission from Elsevier.

Most bone injuries and defects are caused by traumas and are easy to cure. But, in cases of malformation, tumors, and osteoporosis, healing is more challenging. There is a high possibility of complications like mal-union and non-union when the defects and injuries are severe. In those cases, healing may not be possible naturally. Current medical treatments are mostly problematic. Invasive surgery may be a solution to stabilize the bone by using fixation devices such as pins, screws and etc. But more than one surgery may be needed. Furthermore, bone takes a long time to heal in this way. Metallic implants are also used to treat these serious defects. In this way,

mechanical strength and integrity is achieved, but there are some disadvantages like infections and chronic pain. Also bone grafting is used as a therapy, but there are some drawbacks for all bone grafting procedures as well [8, 9]. There were approximately 1,100,000 surgical procedures involving bone grafting, inpatient fracture repair and bone tumor excision in the U.S. in 2004, according to data from the U.S. Healthcare Cost and Utilization (HCUP) Nationwide Inpatient Statistics. It is estimated that these surgical procedures cost more than $5 billion [10]. The gold standard for bone healing is still autografts. There are no immune responses and rejections from the body for this type of bone graft procedure. But there are some limitations, including donor site morbidity and limited availability [11-14]. Bone allograft (bone from a tissue donor) is an alternative to bone autograft. However, allografts have been reported to have a high risk of disease transmission as well as postoperative immunologic rejection. Xenograft (tissue from one species to an unlike species) is not a practical solution for bone healing and this method is not an ideal method either, because of the same concerns as bone allografts [9, 13, 15].

All the current methods have important disadvantages. Bone tissue engineering is an alternative way to restore, maintain or improve tissue function by using many fields including biology, medicine, materials science, and engineering [16]. Bone tissue engineering is based on five strategies: cell transplantation, bioreactors, growth factor delivery, gene therapy and scaffolds. Some of these strategies may be used together to provide bone regeneration at the site of bone loss or injury [9].

1.2 Cells and Extracellular Matrix (ECM)

Tissues are formed by specialized groups of differentiated cells [17]. Thus, the selection of the cell type is a key factor for the success of engineering tissue. Stem cells are considered as a

repair kit for the body because of their properties. Stem cells have two specific properties. The first is that they have the ability to make identical copies of themselves; they self-renew. As the cell divides, one or both daughter cells maintain the stem cell phenotype. The other significant property of stem cells is differentiation. They have the ability to form other cell types of the body. For these reasons, they are very promising for tissue engineering applications.

The stem cells differentiate as follows. After signal initiation, a stem cell becomes a progenitor or a precursor cell. During the differentiation process, the cell is committed to a certain lineage transforming into a mature phenotype and it upregulates and downregulates characteristic genes. At the end, the cell differentiates into a new type which is a fully mature form. This process results in an irreversible change, hence, a fully mature cell cannot go back and become a stem cell.

Stem cells are categorized into two types based on their source of origination: embryonic stem cells and adult stem cells. Embryonic stem cells do not exist in the body; they can be obtained from embryos. Adult stem cells are undifferentiated cells that are among differentiated tissues. There are two types of adult stem cells in bone marrow. Hematopoietic stem cells (HSCs) are capable of forming blood cells, and mesenchymal stem cells (MSCs) are capable of forming bone, cartilage, fat, and stroma cells. Stem cells are also defined based on the number of cell types that they differentiate into: totipotent cells, pluripotent cells, multipotent cells, oligopotent cells, and unipotent cells. Cells that have the ability to form an entire organism are called totipotent cells. They have the ability to form any kind of cells and tissues (e.g. fertilized oocyte). Pluripotent cells are capable of forming all three germ layers and they can produce most of the cells and tissues (cells of the inner cell mass of the blastocyst). Oligopotent cells are capable of differentiating into two or more lineages (e.g. neural stem cells). Unipotent cells are capable of forming cells from a

single lineage. Multipotent cells are capable of forming multiple cell types, (e.g. mesenchymal stem cells). They have the ability to differentiate into bone, cartilage, etc. [5, 7].

Stem cells should have various specific properties to be suitable for use in tissue engineering. Among those are sufficient availability, reliable differentiation, and safe transplantation. Adipose-derived stem cells (AD-MSCs), a specific population of MSCs, have most of these properties. The waste product of liposuction surgery, lipoaspirate, is a good source from which to produce AD-MSCs. They can be harvested easily and in large amounts since adipose tissue is abundant in the body. These stem cells have the ability to differentiate into several other mesenchymal cells, like chondrocytes, adipocytes, osteoblasts, and myocytes, and may even be used in chronic wound healing. Furthermore, they easily adhere to plastic culture flasks, and can be expanded in vitro. Due to all these reasons, AD-MSCs are very promising for tissue engineering applications [5, 18, 19]. Figure 1.2.1 summarizes the cycle of adipose-derived stem cell (ASC) isolation and differentiation for human ASCs.

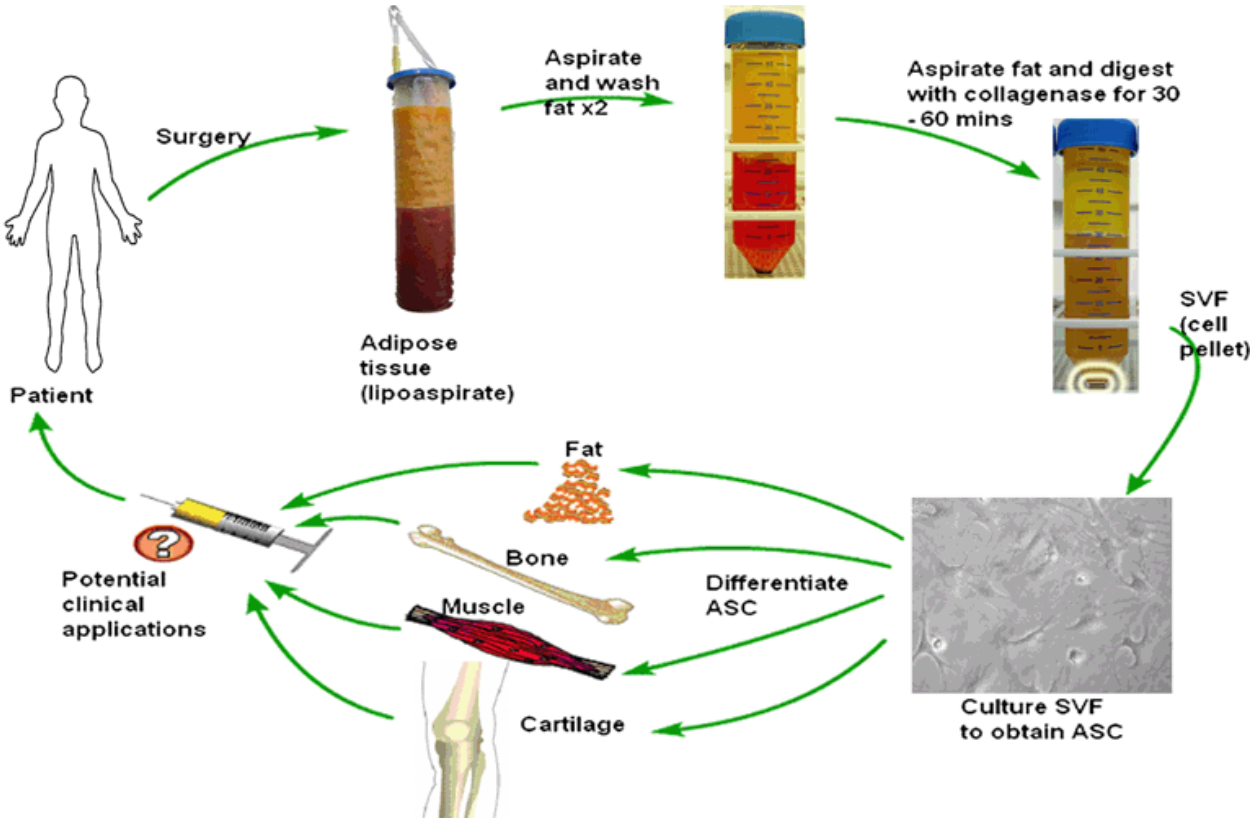

Figure 1.2.1: Summary of the cycle of human adipose-derived stem cell (ASC) isolation and differentiation for clinical usage [18]. Reprinted from ANZ J Surg, 79(4), Locke, M., Windsor, J., & Dunbar, P. R., Human adipose-derived stem cells: isolation, characterization and applications in surgery, 235-244, Copyright 2009, with permission from John Wiley and Sons.

Cells and the extracellular matrix (ECM) are the main constituents of tissue. There is a dependence between cells and ECM; ECM is synthesized and adjusted by cells, and cells use ECM as a medium to provide interaction within the components of the cells. ECM is composed of soluble and insoluble proteins. These proteins are interconnected in the ECM. ECM also controls many cellular fate processes. These processes are cell migration, cell adhesion, spreading, and death, and they vary with ECM density [20].

Blitterswijk explains ECM as follows [7]:

> [ECM] molecules, mainly proteins, which provide the mechanical strength required for proper function of each tissue and serve as a conduit for information exchange between adjacent cells and between cells and the ECM itself. The ECM is in a state of dynamic

> reciprocity and will change in response to environmental cues such as mechanical loading. In the context of tissue engineering applications therefore, use of ECM as a scaffold indeed provides structural support, but perhaps more importantly provides a favorable environment for constructive remodeling of tissue and organs (p. 123).

ECM provides a natural web of complex nanofibers to support and guide cells in the body [21-23].

Key features and main components of ECM can be seen in Table 1.2.1.

Table 1.2.1: Key Features of ECM and its major components [77]. Reprinted from Int J Biochem Cell Biol 29(1), Mutsaers, S. E., et al., Mechanisms of tissue repair: from wound healing to fibrosis, 5-17, Copyright 1997, with permission from Elsevier.

Component	**Function**	**Location**
Collagens	Tissue architecture, tensile strength Cell-matrix interactions Matrix-matrix interactions	Ubiquitously distributed
Elastin	Tissue architecture and elasticity	Tissues requiring elasticity, e.g. lung, blood vessels, heart, skin
Proteoglycans	Cell-matrix interactions Matrix-matrix interactions Cell proliferation Cell migration	Ubiquitously distributed
Hyaluronan	Cell-matrix interactions Matrix-matrix interactions Cell proliferation Cell migration	Ubiquitously distributed
Lamirin	Basement membrane component Cell migration	Basement membranes
Epilligrin	Basement membrane component (epithelium)	Basement membranes
Entactin (nidogen)	Basement membrane component	Basement membranes
Fibronectin	Tissue architecture Cell-matrix interactions Matrix-matrix interactions Cell proliferation Cell migration Opsonin	Ubiquitously distributed
Vitronectin	Cell-matrix interactions Matrix-matrix interactions Hemostasis	Blood Sites of wound formation
Fibrinogen	Cell proliferation Cell migration Hemostasis	Blood Sites of wound formation
Fibrillin	Microfibrillar component of elastic fibers	Tissues requiring elasticity, e.g. blood vessels, heart, skin

1.3 Scaffolds

Scaffolds are defined as synthetic extracellular matrices (ECMs) that support cells to proliferate, migrate and differentiate in three dimensions, which eventually lead to formation of tissue. Scaffolds can be cultured inside the body (in vivo) using the natural system of the body and/or can be cultured in culture flasks or petri dishes in laboratories and then be put inside the injured area.

Scaffolds are customized based on particular needs, and biomaterial selection is the most significant point in their design. O'Brien explains biomaterials [1]:

> In 1976, a biomaterial was defined as 'a nonviable material used in a medical device, intended to interact with biological systems'; however, the current definition is a 'material intended to interface with biological systems to evaluate, treat, augment or replace any tissue, organ or function of the body'. Biomaterials have moved from merely interacting with the body to influencing biological processes toward the goal of tissue regeneration. Typically, three individual groups of biomaterials, ceramics, synthetic polymers and natural polymers, are used in the fabrication of scaffolds for tissue engineering (p. 90).

One of the most important design issues is biocompatibility. Scaffolds should be accepted by the body and should not be rejected by the immune response, so that a suitable environment for the cell fate processes can be obtained. Another important issue in designing scaffolds is biodegradation. Scaffolds should be biodegraded over time so that new tissue can be regenerated and can replace these scaffolds. The balance between biodegradation rate and generation rate of new tissues is a challenge. Biocompatibility of biodegradation products should also be taken into consideration. These products should not cause any harm to the body. Scaffolds should have appropriate mechanical properties as well. They should have enough mechanical strength so that their properties are maintained during implantation into the body, especially for repairing tissues like bone and cartilage that are load-bearing and hard [24]. An effective scaffold should also have well-controlled microarchitectures, including well-controlled pore sizes and porosity [4]. Minimum

pore size is dictated by the diameter of cells in suspension and the complexity of cell behavior makes determining the optimum pore size challenging. Pore size must be carefully controlled to obtain an appropriate scaffold. The effect of implant pore size on tissue regeneration is emphasized by experiments and it is demonstrated that the optimum pore size is not constant across all types, but the optimal pore size for bone regeneration is 100-350 μm [24, 25].

Porosity is an important requirement for promoting vascularization, but this property may also weaken the strength of the scaffold if there is no balance between mechanical properties and porous architecture. The microarchitecture of scaffolds is very important for cells, because cells need nutrients and oxygen transport to live. These requirements can be obtained by vascularization. For vascularization, high porosity is the key, and interconnected pore structures are requirements for scaffold design [1, 27].

Polystyrene, poly-L-lactic acid (PLLA), polyglycolic acid (PGA) and poly-D,L-lactic-co-glycolic acid (PLGA) are the most common polymers that are used in synthetic polymer scaffolds. These polymers are very promising because of their tunable processability and kinetics [28]. Fabrication techniques such as solvent casting, particulate leaching, freeze drying, thermally induced phase separation, melt molding, phase emulsion, in situ polymerization and gas foaming can be used to tune the scaffold degradation rate, mechanical strength and degree of growth factor entrapment and obtain uniform and well-distributed porous synthetic polymer scaffolds [21]. These polymers also provide mechanical strength to the structure of scaffolds; however, there are many challenges in designing synthetic polymer scaffolds. First of all, these scaffolds may not be biocompatible within the human body, which means that they can be rejected by the immune system [1]. And also, these polymers may not support cell attachment, proliferation and differentiation since cells may not recognize them unless proteins and peptides are

introduced [29, 30]. For bone tissue engineering, poly (α-hydroxyl acids), poly (anhydrides), poly (phosphazenes), poly (ethylene glycol) (PEG), poly (ε-caprolactone) (PCL), poly (propylene fumarate) (PPF), poloxamer, polyurethanes and polyphosphate polymers have all been used as scaffolds [31].

Polyglycolic acid, PGA, is a highly crystalline polymer, compared to other biodegradable polymers. Due to this property, it is not soluble in most organic solvents; one exception, though, is hexafluoroisopropanol (HFIP). PGA also loses its mechanical strength relatively fast, in a two week period, and is absorbed after approximately four weeks of implantation.

Polylactic acid, PLA, is similar to PGA in structure, but differs in physical, mechanical, as well as chemical properties. Two isomers of PLA are poly-L-lactic (PLLA) and poly-D,L-lactic (PDLLA), with the latter having a faster degradation rate. Since processing at high temperatures may result in excess monomer formation, these materials should be processed at low temperatures.

Poly (ε-caprolactone) (PCL) is a low-cost, biodegradable polyester which is nontoxic and has good adhesion to a broad spectrum of substrates [32]. PCL is prepared by ring opening polymerization of ε-caprolactone using a catalyst such as stannous octoate, and this leads PCL to have low melting point (59-64°C) and a glass transition temperature of 260°C.

As mentioned above, when these type of polymers degrade, acidic degradation products can be released and this can lead to affect biocompatibility adversely. Furthermore, polyesters are stiff materials and this condition may be a significant drawback when mechanical compliance with soft tissue or blood vessels is required [24]. However, extensive research has been conducted on PCL's potential usage as a biomaterial because of its low melting point, slow degradation rate in vivo, good solubility and perfect blend-compatibility [33, 34]. Electrospun PCL scaffolds are fabricated as they have a potential to be used as bone and cartilage scaffolds [32, 33, 35]. Rigid

hydroxyapatite can be used for bone scaffolds to improve both the mechanical properties and the osteoconductivity of PCL scaffolds [35].

Synthetic polymers can be combined with natural polymers like collagen to facilitate processing into tissue scaffolds [36]. Natural polymers already have biodegradability and signaling mechanisms inherently, thus, there is no need to add growth factors or cytokines [6, 36]. Therefore, scaffolds made of both natural and synthetic polymers can be both biologically active and structurally strong. As many of the biodegradable materials today are based on natural polymers, collagen is a good example of these natural polymers. It is a very important protein in skin and bone, and enzymatic degradation of collagen produces amino acids in the human body. Collagenases and metalloproteinase enzymes are mainly responsible for this degradation [36].

Scaffolds are designed according to the tissue type that they will be applied. For bone applications, scaffolds should have the ability to provide signals that promote progenitor cell differentiation to osteoblasts; that means they should be osteoinductive. Scaffolds must also have integrative porosity so that osteoblasts can undergo an ideal process of bone formation. Cell migration and cell proliferation are also very important for new bone formation. That is why scaffolds should support cells for these activities as well. Scaffolds that will be used in this type of tissue engineering should also be degradable. The rate of regeneration of new tissue and degradation rate of the scaffold should be similar so that a healthy tissue growth can be achieved [1].

Cells and scaffolds are key factors for tissue engineering applications. Figure 1.3.1 shows the major elements factoring into engineered tissue development. The integration of these factors is essential. Integration of scaffolds and signals can be achieved by using raw materials strategies to obtain tissue engineering products. Raw materials are natural components of tissue's ECM.

Physical, chemical, adhesive and mechanical cues to cells can be provided by raw biomaterial usage. There is no need to add bioactive molecules to provide signaling mechanism since raw materials inherently can act as a signaling environment for differentiation. Also, raw materials can be combined with synthetic polymers or other raw materials and can be designed as a scaffold so that signaling mechanism is provided inherently, as well [6]. If scaffolds are made of synthetic polymers, they will be lack of this signaling mechanism, but signals can be introduced in a deliberate and controlled way by adding growth factors and cytokines [6].

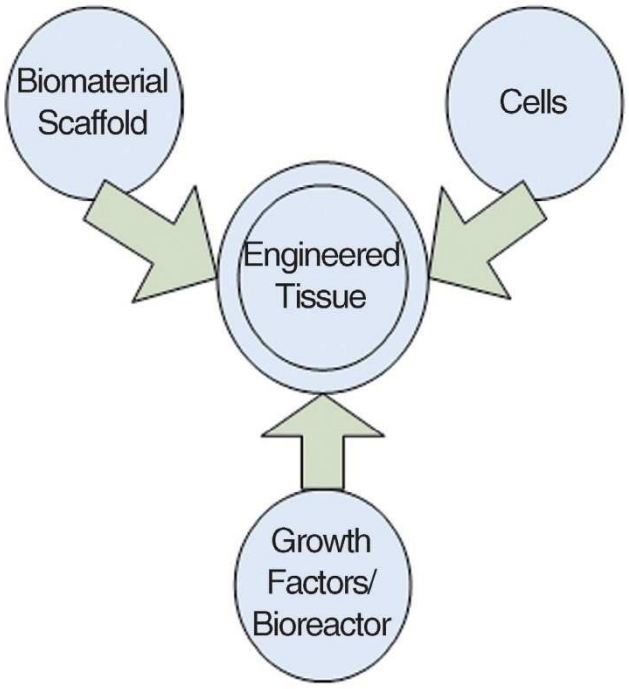

Figure 1.3.1: The major elements factoring into engineered tissue development: cells, signals (provided chemically by growth factors or physically by a bioreactor), and scaffolds [1]. Cells and scaffolds are key factors for tissue engineering applications and the integration of these factors is essential for successful applications. Reprinted from Materials Today, 14(3), O'Brien, F. J., Biomaterials & scaffolds for tissue engineering, 88-95, Copyright 2011, with permission from Elsevier.

1.4 Bone Tissue Engineering

In order to understand the required properties for a bone substitute, it is important to have knowledge about bones. Bone is a living, growing tissue that supports the systems in the human body. Bone is a complex composite material that has various levels of hierarchical structural organization, depicted in Figure 1.4.1. These levels and structures are listed in the study of Rho et al. as follows [37]: (1) the macrostructure: cancellous and cortical bone; (2) the microstructure (from 10 to 500 μm): haversian systems, osteons, single trabeculae; (3) the sub-microstructure (1-10 μm): lamellae; (4) the nanostructure (from a few hundred nanometers to 1 μm): fibrillar collagen and embedded mineral; and (5) the sub-nanostructure (below a few hundred nanometers): molecular structure of constituent elements, such as mineral, collagen, and non-collagenous organic proteins [37]. Micro and nanoscale structures of bone provide biochemical and biomechanical functions [25, 27, 37-40].

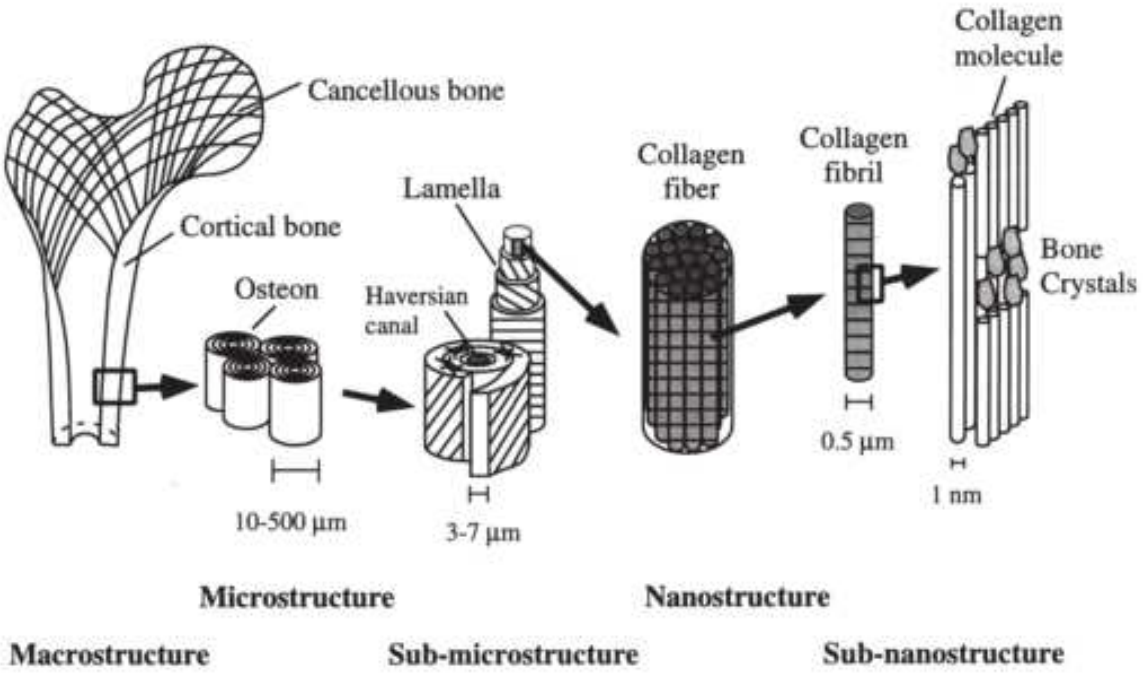

Figure 1.4.1: Hierarchical organization of bone [37]. The macrostructure: cancellous and cortical bone. The microstructure: haversian systems, osteons, single trabeculae. The sub-microstructure: lamella. The nanostructure: fibrillar collagen and embedded mineral. The sub-nanostructure: molecular structure of constituent elements, such as mineral, collagen, and non-collagenous organic proteins. Reprinted from Medical Engineering & Physics, 20(2), Rho, J.-Y., Kuhn-Spearing, L., & Zioupos, P., Mechanical properties and the hierarchical structure of bone, 92-102, Copyright 1998, with permission from Elsevier.

Biomechanically, bone is made of three phases: organic phase, mineral phase and water phase. Type I collagen constitutes the major part of the organic matrix of the bone. It is a nanoscale material that is responsible for vascular ingrowth, mineral deposition and binding of growth factors. There are also other collagen types, including types III, IV and V in this phase [41]. There are also several bone-related non-collagenous proteins (such as osteocalcin, matrix Gla protein, osteonectin, alkaline phosphatase, BAG-75 and osteopontin) that provide interaction with the mineral phase and several bone-related proteoglycans (such as biglycan and decorin). Collagen fibers deposit bone hydroxyapatite crystals and approximately 90% of mineral phase consists of these crystals. Bone hydroxyapatite has a form of nanosized mineral platelets. The thickness of

platelets ranges between 1 nm and 7 nm, the length between 15 nm and 200 nm, and the width between 10 nm and 80 nm [7, 42-44]. The mineral phase provides stiffness and the organic phase provides maintenance, elasticity and tensile strength [7, 43, 44]. Water is also an essential component of bone that is integrated into all hierarchical organization levels of the bone [41].

Structurally there are two types of bone: compact bone (dense, cortical) and cancellous (trabecular and spongy). Cancellous bones are very active and changes very often. They are placed in vertebral bodies and adjacent to articulating joints. The main locations of the compact bones are the shaft and peripheral lining of flat bones; they are more static and stronger than cancellous bones [7].

There are three main types of cells in bones: osteoblasts, osteocytes and osteoclasts. Osteoclasts are responsible for breakdown of the bone and this action initiates bone resorption [45]. Osteoblasts (bone-forming cells) are responsible for deposition of bone matrix. In addition, osteoblasts provide the RANKL/OPG balance which allows osteoclast differentiation. This condition shows that there is an interdependency that is mediated by the growth factors during bone resorption between these two bone cells. Osteocytes are the characteristic bone cell type, which are osteoblasts that reside on new bone matrix. They control the activities of osteoblasts and osteoclasts with the help of signaling pathways [7, 46].

Figure 1.4.2 shows the life span of an osteoblast. A large number of growth factors are involved in this process. Mesenchymal stem cells receive signals and differentiate to eventually become osteoblasts. Osteoblasts can differentiate further into osteocytes, they can die by apoptosis, or they can be a lining cell at the end of this process. The lining cells cover the inactive bone surfaces and do not take a part in bone formation [7, 47].

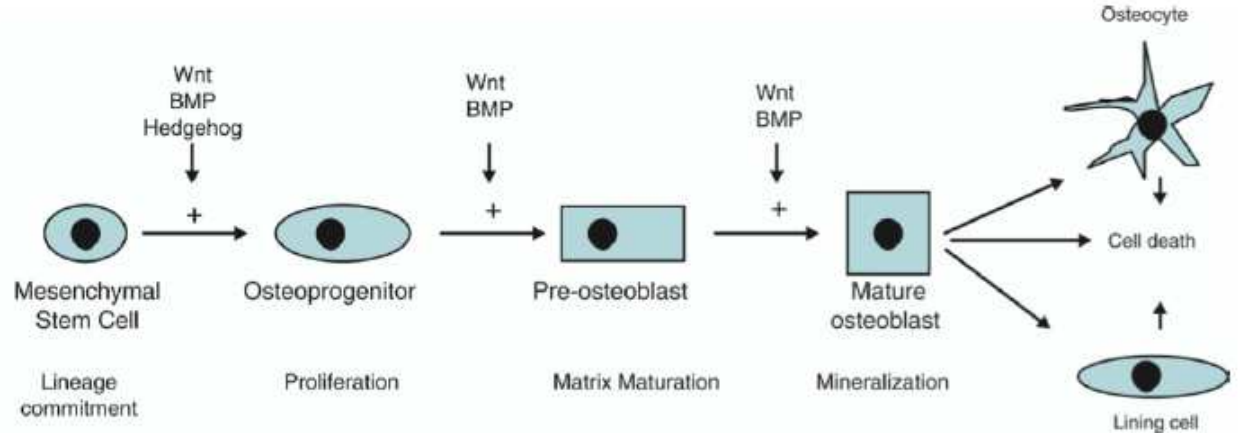

Figure 1.4.2: The life span of an osteoblast [7]. Mesenchymal stem cells receive signals and differentiate to eventually become osteoblasts. A large number of growth factors are involved in this process. Osteoblasts can differentiate further into osteocytes, they can die by apoptosis, or they can be a lining cell at the end of this process. Reprinted from Tissue Engineering, Blitterswijk, C. V. Burlington, MA: Elsevier, p. 62, Copyright 2008, with permission from Elsevier.

Bone tissue engineering is an alternative way to heal severe bone injuries and defects by using the body's natural biological response in conjunction with many fields like biology, engineering, material science, and medicine [9, 16]. Bone is hierarchically structured and there are many nanoscale and microscale materials in the bone. This may be the reason for bone cells to respond to nano and micro scale features [39, 48]. The influence of microscale on cellular and subcellular function is summarized in Figure 1.4.3. Extensive research has been conducted on using both natural and synthetic nanofibers and also blends of both types of nanofibers into their potential applications as tissue scaffolds. Nanofibers from natural polymers such as collagen, silk and DNA have been proposed [8, 25]. Elecrospun gelatin and poly (ε-caprolactone) (PCL) blend have been used as blend of natural and synthetic polymer by Heydarkhan-Hagvall et al., and it has been shown that this blend has a great potential to be used in cardiovascular tissue applications [49]. Synthetic polymers such as poly-L-lactic acid (PLLA) also have been used to fabricate nano-structured porous scaffolds. These porous, polymeric, nanofibrous scaffolds seeded with nerve stem cells can be used in nerve tissue engineering applications [61].

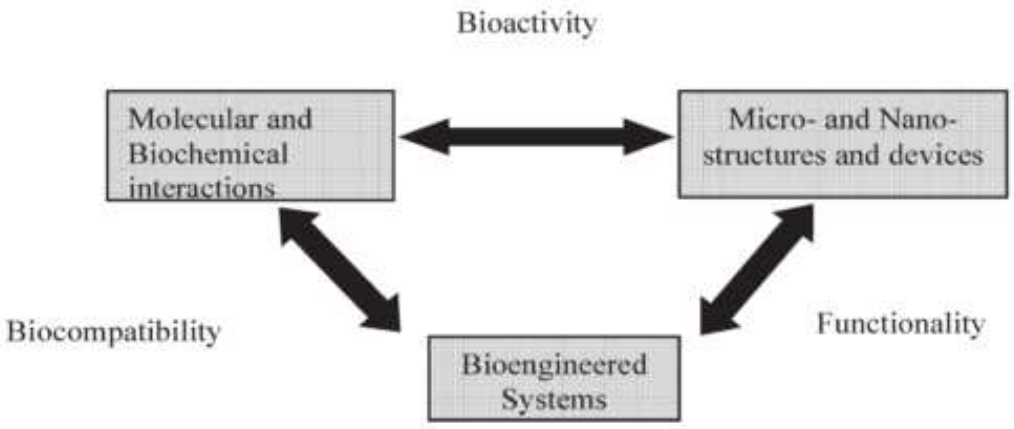

Figure 1.4.3: The influence of microscale on cellular and subcellular function [27]. Reprinted from Medical Engineering & Physics, 22(9), Desai, T. A., Micro- and nanoscale structures for tissue engineering constructs, 595-606, Copyright 2000, with permission from Elsevier.

As mentioned in the previous section, scaffolds are one of the key factors for bone tissue engineering applications and an effective scaffold should possess all required properties such as biocompatibility, porosity, biodegradability, mechanical properties, osteoconductivity and osteoinductivity [7, 50].

Osteoinduction is the process that induces the process of forming new bone tissues by osteoblasts. This process induces immature cells to differentiate into preosteoblasts and eventually to osteoblasts. Osteoinduction plays a key role in bone healing. An ideal scaffold for bone defects and injuries should be osteoinductive as it will be used as a bone substitute.

Osteoconduction and osteointegration are other significant required properties [51-57]. Glowacki and Mulliken explain osteoconduction as follows [58]:

> Osteoconduction occurs as the dead bone acts as a scaffold for the ingrowth of vessels, followed by resorption of the implant and deposition of new bone derived from the edges of the defect. This process is very slow and may require years to unite a large segmental defect.

Osteoinduction is a process that occurs regularly when bone implants are used. The response of bone implant may change according to the material that it is made of. Bone conduction cannot be achieved by using copper and silver [52]. Osteointegration is also on the response to a bone implant as osteoinduction. Osteointegration occurs when there is a direct connection between living bone and the surface of the implant [52, 60].

1.5 Demineralized Bone Matrix (DBM)

Demineralized bone matrix (DBM) has osteoinductive, osteoconductive and osteointegrative properties that lead to bone regeneration. These promising features of DBM attract considerable attention from bone grafting markets. According to the data provided by U.S. Market for Orthopedic Biomaterials in April 2010, about 15% of the over $1.4 billion bone grafting market (or about 220,000 procedures) focused on DBM products in 2009. Also, there is an approximately 5% increase in sales from 2008 to 2009 according to the same report [62].

DBM is an acellular composite material that is obtained from donor allograft bone. DBM is prepared as follows. Adherent soft tissues are debrided and blood and lipids are removed from the donor bone. Then an antibiotic soak is used for sterilization. Afterwards, the morselization is done to obtain a material in form of fibers and particles. After this process, acid demineralization is done by extracting mineral phase by using HCl, and then freeze-drying is applied one or more times. At the end of this procedure, a dry powder DBM is obtained. This material is mainly the organic matrix of the donor bone and it contains collagens and other non-collagenous proteins, growth factors, residual calcium phosphate, and small amount of cellular debris [63]. Acidic washing of DBM is very important, as native concentrations of organic materials and mechanical integrity following the demineralization process are inversely proportional to the length of this process. If

acidic washing process continues for too long, large amounts of minerals are removed. In this case, the amount of organic materials decreases and the mechanical properties weaken [6, 64].

Many DBMs are subjective and specific to laboratory since donor bones, from which DBMs are obtained, are from different animal models. DBM compositions may not be consistent. DBM particles that are in a range between 420-840 μm are more osteoinductive compared to the ones that are 250 μm [63, 65, 66].

Because of the inherently poor mechanical performance of DBM, it is not possible to use it as a single-component construct. This dry powder is typically combined with carriers so that high mass fractions, better handling, reliable delivery, and formulation of DBM products can be obtained [63]. There is no standardization and consistency of the DBM content in these products. Thus, it is not possible to deliver the same DBM dose from different products. This may be the reason for Acarturk and Hollinger's suggestion that the differences in carrier, the amount of DBM in the carrier, and the ability of the carrier cause differences in osteogenic activity among DBMs that are combined with carriers [67]. Furthermore, osteoinductivity of individual DBM lots that are processed by the same tissue bank may not be the same since these lots were obtained from different donor bones [63].

Carriers can affect compatibilities, applications and sterilization. Viscous carriers can be used to obtain a moldable putty from DBM. There are two types of viscous carriers: water-soluble polymers and water-miscible solvents. Glycerol can be an example for anhydrous water-miscible solvents and sodium hyaluronate can be given as an example for water-soluble polymers. DBM can be combined with carriers to obtain flexible sheets that may include both DBM and cortical bone chips. Thermoplastic, porcine collagen-based hydrogel is also used as a carrier for DBM. This non-water-soluble gel can be injected after being heated to 46-50 ºC. The composition

becomes firm at body temperature. Pluronic is another carrier; it is a product of BASF company and synonymous with poloxamer. This carrier is also temperature-sensitive and becomes firmer at body temperature [63].

As mentioned earlier, an effective bone scaffold should be osteoconductive, osteoinductive and osteointegrative to lead to bone regeneration and bone growth. Based on the results of the studies of Urist et al. in 1965 and 1971, DBM has sufficient amount of BMPs (bone morphogenetic proteins) which take part in the osteoblast differentiation process (Figure 1.4.2) [63, 68, 69]. Urist et al. also introduced the concept of osteoinduction in their study in 1971 [69]:

> The process of differentiation of pluripotential mesenchymal cells into osteoprogenitor cells and ultimately into osteoblasts that form as a consequence of a stimulating agent, that is, bone morphogenetic protein.

This shows that DBM already has strong inherent signaling capacity and has the signaling system that promotes cell proliferation and cell migration that will lead to bone matrix production, and that it can be used as a biomaterial for a bone scaffold [5].

DBM products that are commercialized can be in different forms, shapes and sizes. Putty, paste, strip, and cube products can be given as examples. For example, AlloSource has a commercial product, called AlloFuse™ that is injectable gel and putty. This product is comprised of heat sensitive copolymer and DBM. Medtronic also has a commercial product, called Osteofil®DBM, which is DBM in porcine gelatin and forms as an injectable paste and moldable strips [63]. There are many commercial products that contain DBM, but all of them are combined with carriers. Also, there are no products that have tunable nano-features. But it has been shown that nanoscale features directly affect bone cell behaviors and also promote cell adhesion and bone matrix production [48, 70-74]. In 2014, Leszczak et al. proposed that they can develop a novel material that is non-woven, highly porous nanofibers of bone matrix based on DBM [75]. This new highly

porous material has tunable nanofeatures and can be prepared without using a carrier. Thus, this novel material is claimed to be better than the other commercial products that is made of elecrospun DBM [75].

1.6 Electrospinning

Rapid prototyping, melt extrusion, salt leaching, emulsion templating, phase separation, and electrospinning are scaffold fabrication technologies that can be used to obtain porous polymer scaffolds. Electrospinning is a straightforward, cost-effective technique to fabricate biomimetic non-woven scaffolds that are constituted from a large network of interconnected fibers and pores [5, 49].

In the early 1900s, electrospinning was first developed for textile and filter applications. First, Doshi et al. used this method for tissue engineering applications [76]. After that study, which aimed at expanding the polymers that have the potential to be electrospun, electrospinning has started to become a common technique to obtain scaffolds [8]. The scaffolds that are obtained with this technique have high porosities, large surface area-to-volume ratios, and variable fiber diameters [26].

An electric field is created to overcome the surface tension of a polymer solution. A jet of the polymer solution is pushed out of a needle to a collector. As the polymer solution comes out, it spins because of the electric field and the solution vaporizes in the air. As it hits the collector, it deposits on there and polymer fibers with diameters that can range from tens of nanometers to microns can be obtained [8]. This process is influenced by polymer properties, solvent properties, solution flow rate, voltage, distance from needle to collector, and polymer concentration. The diameter and density of the fibers can be arranged by changing these parameters. For example,

solution viscosity is very important. If it is too viscous, droplets can dry out of the tip, and if the viscosity is too low, electrospraying may occur in the form of beads [26, 8]. Porosity and pore size are very critical since they affect cell attachment, migration, and proliferation, and surface area can be affected by fiber diameter [26]. Figure 1.6.1 the schematic for a typical electrospinning process.

In 2014, Leszczak et al. proposed that a novel material can be obtained by electrospinning DBM [75]. This new highly porous nanofibrous material is prepared by electrospinning DBM powder that is dissolved in 70:30 HFIP:TFA (hexafluoro-2-propanol / trifluoroacetic acid) solution blend . After electrospinning, the fibers are water-soluble, hence glutaraldehyde vapor treatment should be done to crosslink the nanofibers. In that study, it was observed that DBM concentration in the solution blend affects viscosity directly proportionally.

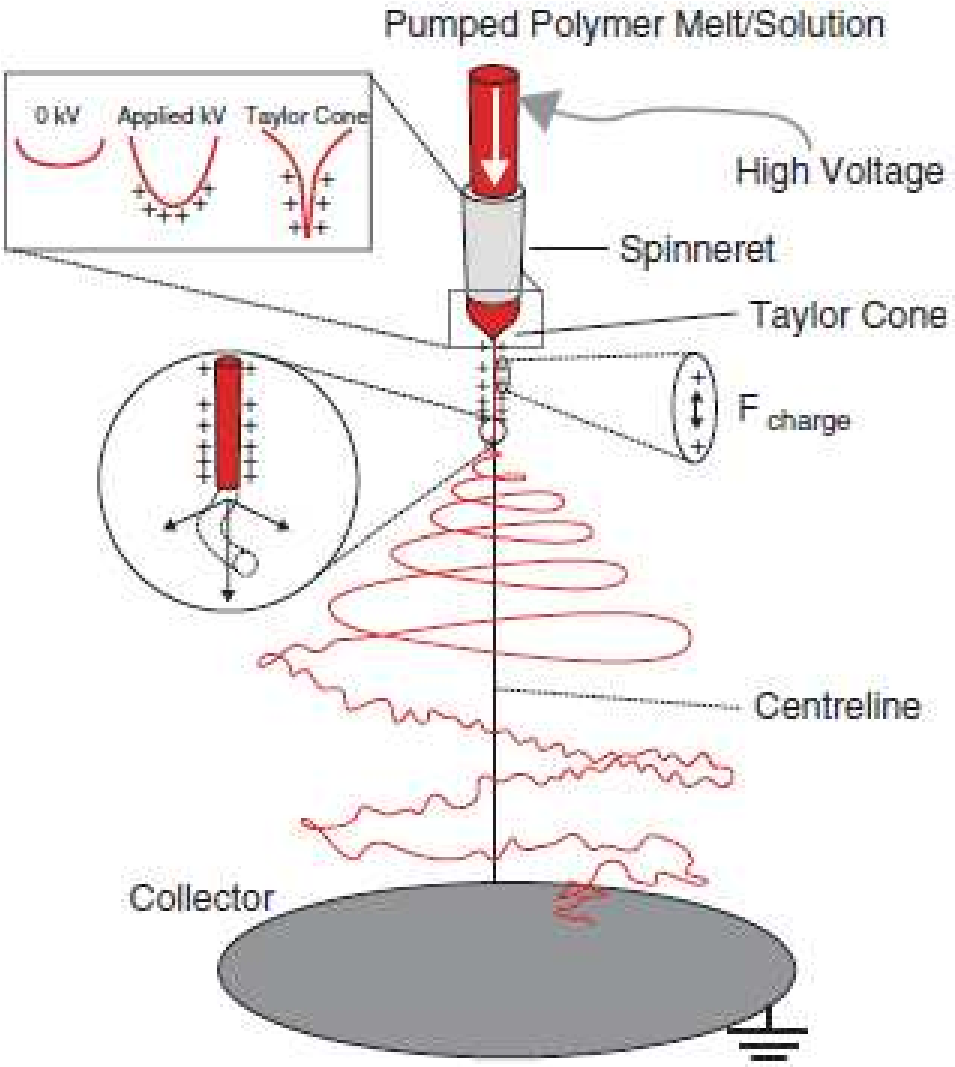

Figure 1.6.1: Schematic of the electrospinning process [7]. Reprinted from Tissue Engineering, Blitterswijk, C. V. Burlington, MA: Elsevier, p. 429, Copyright 2008, with permission from Elsevier.

REFERENCES

1. O'Brien, F. J. (2011). Biomaterials & scaffolds for tissue engineering. *Materials Today, 14*(3), 88-95.

2. Whitney GA (2012). Methods for Producing Scaffold-Free Engineered Cartilage Sheets from Auricular and Articular Chondrocyte Cell Sources and Attachment to Porous Tantalum. *BioResearch Open Access 1* (4): 157–165.

3. Andrews, D. L., Scholes, G. D., Wiederrecht, G. P. (2011). Comprehensive Nanoscience and Technology.

4. Cima, L. G., Vacanti, J. P., Vacanti, C., Ingber, D., Mooney, D., & Langer, R. (1991). Tissue engineering by cell transplantation using degradable polymer substrates. *J Biomech Eng, 113*(2), 143-151.

5. Murugan, R., & Ramakrishna, S. (2006). Nano-featured scaffolds for tissue engineering: a review of spinning methodologies. *Tissue Engineering, 12*(3), 435-447.

6. Renth, A. N., & Detamore, M. S. (2012). Leveraging "Raw Materials" as Building Blocks and Bioactive Signals in Regenerative Medicine. *Tissue Engineering Part B-Reviews, 18*(5), 341-362.

7. Blitterswijk, C. V. (2008). *Tissue engineering*. Burlington, MA: Elsevier.

8. Holzwarth, J. M., & Ma, P. X. (2011). Biomimetic nanofibrous scaffolds for bone tissue engineering. *Biomaterials, 32*(36), 9622-9629.

9. Mistry, A. S., & Mikos, A. G. (2005). Tissue Engineering Strategies for Bone Regeneration. In I. V. Yannas (Ed.), *Regenerative Medicine II: Clinical and Preclinical Applications* (pp. 1-22). Berlin, Heidelberg: Springer Berlin Heidelberg.

10. Khambete, H., Keservani, R. K., Kesharwani, R. K., Jain, N. P., & Jain, C. P. (2016). Chapter 3 - Emerging trends of nanobiomaterials in hard tissue engineering A2 - Grumezescu, Alexandru Mihai *Nanobiomaterials in Hard Tissue Engineering* (pp. 63-101): William Andrew Publishing.

11. Brown, K. L., & Cruess, R. L. (1982). Bone and cartilage transplantation in orthopaedic surgery. A review. *J Bone Joint Surg Am, 64*(2), 270-279.

12. Enneking, W. F., Eady, J. L., & Burchardt, H. (1980). Autogenous cortical bone grafts in the reconstruction of segmental skeletal defects. *J Bone Joint Surg Am, 62*(7), 1039-1058.

13. Erbe, E. M., Marx, J. G., Clineff, T. D., & Bellincampi, L. D. (2001). Potential of an ultraporous beta-tricalcium phosphate synthetic cancellous bone void filler and bone marrow aspirate composite graft. *Eur Spine J, 10 Suppl 2*, S141-146.

14. Betz, R. R. (2002). Limitations of autograft and allograft: new synthetic solutions. *Orthopedics, 25*(5 Suppl), s561-570.

15. Moore, W. R., Graves, S. E., & Bain, G. I. (2001). Synthetic bone graft substitutes. *ANZ J Surg, 71*(6), 354-361.

16. Langer, R., & Vacanti, J. P. (1993). Tissue engineering. *Science, 260*(5110), 920-926.

17. Lodish H., Berk A., Zipursky S.L., et al., Molecular Cell Biology. 4th edition. New York: W. H. Freeman; 2000. Section 1.5, Cells into Tissues.

18. Locke, M., Windsor, J., & Dunbar, P. R. (2009). Human adipose-derived stem cells: isolation, characterization and applications in surgery. *ANZ J Surg, 79*(4), 235-244.

19. Tsuji, W., Rubin, J. P., & Marra, K. G. (2014). Adipose-derived stem cells: Implications in tissue regeneration. *World J Stem Cells, 6*(3), 312-321.

20. Palsson B. (2003). Tissue organization, Tissue Engineering.

21. Stevens, B., Yang, Y., Mohandas, A., Stucker, B., & Nguyen, K. T. (2008). A review of materials, fabrication methods, and strategies used to enhance bone regeneration in engineered bone tissues. *J Biomed Mater Res B Appl Biomater, 85*(2), 573-582.

22. Zagris, N. (2001). Extracellular matrix in development of the early embryo. *Micron, 32*(4), 427-438.

23. Aumailley, M., & Gayraud, B. (1998). Structure and biological activity of the extracellular matrix. *J Mol Med (Berl), 76*(3-4), 253-265.

24. Yang, S., Leong, K. F., Du, Z., & Chua, C. K. (2001). The design of scaffolds for use in tissue engineering. Part I. Traditional factors. *Tissue Engineering, 7*(6), 679-689.

25. Pham, Q. P., Sharma, U., & Mikos, A. G. (2006). Electrospun Poly(ε-caprolactone) Microfiber and Multilayer Nanofiber/Microfiber Scaffolds: Characterization of Scaffolds and Measurement of Cellular Infiltration. *Biomacromolecules, 7*(10), 2796-2805.

26. Pham, Q. P., Sharma, U., & Mikos, A. G. (2006). Electrospinning of polymeric nanofibers for tissue engineering applications: a review. *Tissue Engineering, 12*(5), 1197-1211.

27. Desai, T. A. (2000). Micro- and nanoscale structures for tissue engineering constructs. *Medical Engineering & Physics, 22*(9), 595-606.

28. Gunatillake, P. A., & Adhikari, R. (2003). Biodegradable synthetic polymers for tissue engineering. *Eur Cell Mater, 5*, 1-16; discussion 16.

29. Yim, E. K. F., Pang, S. W., & Leong, K. W. (2007). Synthetic nanostructures inducing differentiation of human mesenchymal stem cells into neuronal lineage. *Experimental Cell Research, 313*(9), 1820-1829.

30. Henderson, L. A.; Kipper, M. J.; Chiang, M. Y. M. In Polymers for Biomedical Applications; Mahapatro, A., Kulshrestha, A. S., Eds.;*American Chemical Society*: Washington, D.C., 2008; Chapter 8, pp 118-152.

31. Puppi, D., Chiellini, F., Piras, A. M., & Chiellini, E. (2010). Polymeric materials for bone and cartilage repair. *Progress in Polymer Science, 35*(4), 403-440.

32. Yoshimoto, H., Shin, Y. M., Terai, H., & Vacanti, J. P. (2003). A biodegradable nanofiber scaffold by electrospinning and its potential for bone tissue engineering. *Biomaterials, 24*(12), 2077-2082.

33. Nam, J., Huang, Y., Agarwal, S., & Lannutti, J. (2007). Improved cellular infiltration in electrospun fiber via engineered porosity. *Tissue Engineering, 13*(9), 2249-2257.

34. Woodruff, M. A., & Hutmacher, D. W. (2010). The return of a forgotten polymer-Polycaprolactone in the 21st century. *Progress in Polymer Science, 35*(10), 1217-1256.

35. Wutticharoenmongkol, P., Pavasant, P., & Supaphol, P. (2007). Osteoblastic phenotype expression of MC3T3-E1 cultured on electrospun polycaprolactone fiber mats filled with hydroxyapatite nanoparticles. *Biomacromolecules, 8*(8), 2602-2610.

36. Nair, L. S., & Laurencin, C. T. (2007). Biodegradable polymers as biomaterials. *Science Direct. 32*, 762-798.

37. Rho, J.-Y., Kuhn-Spearing, L., & Zioupos, P. (1998). Mechanical properties and the hierarchical structure of bone. *Medical Engineering & Physics, 20*(2), 92-102.

38. Puleo, D. A., & Nanci, A. (1999). Understanding and controlling the bone–implant interface. *Biomaterials, 20*(23–24), 2311-2321.

39. Webster, T. J., & Ejiofor, J. U. (2004). Increased osteoblast adhesion on nanophase metals: Ti, Ti6Al4V, and CoCrMo. *Biomaterials, 25*(19), 4731-4739.

40. Lim, J. Y., Dreiss, A. D., Zhou, Z., Hansen, J. C., Siedlecki, C. A., Hengstebeck, R. W., . . . Donahue, H. J. (2007). The regulation of integrin-mediated osteoblast focal adhesion and focal adhesion kinase expression by nanoscale topography. *Biomaterials, 28*(10), 1787-1797.

41. Reznikov, N., Shahar, R., & Weiner, S. (2014). Bone hierarchical structure in three dimensions. *Acta Biomater, 10*(9), 3815-3826.

42. Zinger, O., Zhao, G., Schwartz, Z., Simpson, J., Wieland, M., Landolt, D., & Boyan, B. (2005). Differential regulation of osteoblasts by substrate microstructural features. *Biomaterials, 26*(14), 1837-1847.

43. Burr D.B. and Allen M.R. (Eds.). Basic and applied bone biology. Academic Press 2014.

44. Munro, N. H., & McGrath, K. M. (2015). Advances in techniques and technologies for bone implants. *Bioinspired, Biomimetic and Nanobiomaterials, 4*(1), 26-36.

45. Boyce, B. F., Yao, Z., & Xing, L. (2009). Osteoclasts have multiple roles in bone in addition to bone resorption. *Crit Rev Eukaryot Gene Expr, 19*(3), 171-180.

46. Caetano-Lopes, J., Canhao, H., & Fonseca, J. E. (2007). Osteoblasts and bone formation. *Acta Reumatol Port, 32*(2), 103-110.

47. Miller, S. C., de Saint-Georges, L., Bowman, B. M., & Jee, W. S. (1989). Bone lining cells: structure and function. *Scanning Microsc, 3*(3), 953-960.

48. Swan, E. E. L., Popat, K. C., Grimes, C. A., & Desai, T. A. (2005). Fabrication and evaluation of nanoporous alumina membranes for osteoblast culture. *Journal of Biomedical Materials Research Part A, 72A*(3), 288-295.

49. Heydarkhan-Hagvall, S., Schenke-Layland, K., Dhanasopon, A. P., Rofail, F., Smith, H., Wu, B. M., . . . MacLellan, W. R. (2008). Three-dimensional electrospun ECM-based hybrid scaffolds for cardiovascular tissue engineering. *Biomaterials, 29*(19), 2907-2914.

50. Habibovic, P., Yuan, H., van der Valk, C. M., Meijer, G., van Blitterswijk, C. A., & de Groot, K. (2005). 3D microenvironment as essential element for osteoinduction by biomaterials. *Biomaterials, 26*(17), 3565-3575.

51. Garcia, A. J., & Reyes, C. D. (2005). Bio-adhesive surfaces to promote osteoblast differentiation and bone formation. *Journal of Dental Research, 84*(5), 407-413.

52. Albrektsson, T., & Johansson, C. Osteoinduction, osteoconduction and osseointegration. *European Spine Journal, 10*(2), S96-S101.

53. Liu, S.-J., Chi, P.-S., Lin, S.-S., Ueng, S. W.-N., Chan, E.-C., & Chen, J.-K. (2007). Novel solvent-free fabrication of biodegradable poly-lactic-glycolic acid (PLGA) capsules for antibiotics and rhBMP-2 delivery. *International Journal of Pharmaceutics, 330*(1–2), 45-53.

54. Ruhé, P. Q., Kroese-Deutman, H. C., Wolke, J. G. C., Spauwen, P. H. M., & Jansen, J. A. (2004). Bone inductive properties of rhBMP-2 loaded porous calcium phosphate cement implants in cranial defects in rabbits. *Biomaterials, 25*(11), 2123-2132.

55. Bessho, K., Carnes, D. L., Cavin, R., & Ong, J. L. (2002). Experimental studies on bone induction using low-molecular-weight poly (DL-lactide-co-glycolide) as a carrier for recombinant human bone morphogenetic protein-2. *Journal of Biomedical Materials Research, 61*(1), 61-65.

56. Heckmann, L., Fiedler, J., Mattes, T., Dauner, M., & Brenner, R. E. (2008). Interactive effects of growth factors and three-dimensional scaffolds on multipotent mesenchymal stromal cells. *Biotechnology and Applied Biochemistry, 49*(3), 185-194.

57. Wilson, C. J., Clegg, R. E., Leavesley, D. I., & Pearcy, M. J. (2005). Mediation of biomaterial-cell interactions by adsorbed proteins: a review. *Tissue Engineering, 11*(1-2), 1-18.

58. Glowacki, J., & Mulliken, J. B. (1985). Demineralized bone implants. *Clin Plast Surg, 12*(2), 233-241.

59. Branemark, P. I., Hansson, B. O., Adell, R., Breine, U., Lindstrom, J., Hallen, O., & Ohman, A. (1977). Osseointegrated implants in the treatment of the edentulous jaw. Experience from a 10-year period. *Scand J Plast Reconstr Surg Suppl, 16*, 1-132.

60. Branemark, P. I. (1983). Osseointegration and its experimental background. *J Prosthet Dent, 50*(3), 399-410.

61. Yang, F., Murugan, R., Ramakrishna, S., Wang, X., Ma, Y. X., & Wang, S. (2004). Fabrication of nano-structured porous PLLA scaffold intended for nerve tissue engineering. *Biomaterials, 25*(10), 1891-1900.

62. Millennium Research Group, U.S. markets for orthopedic biomaterials (2010).

63. Gruskin, E., Doll, B. A., Futrell, F. W., Schmitz, J. P., & Hollinger, J. O. (2012). Demineralized bone matrix in bone repair: History and use. *Advanced Drug Delivery Reviews, 64*(12), 1063-1077.

64. Liu, G., Li, Y., Sun, J., Zhou, H., Zhang, W., Cui, L., & Cao, Y. (2010). In vitro and in vivo evaluation of osteogenesis of human umbilical cord blood-derived mesenchymal stem cells on partially demineralized bone matrix. *Tissue Eng Part A, 16*(3), 971-982.

65. Hollinger, J. O., Mark, D. E., Goco, P., Quigley, N., Desverreaux, R. W., & Bach, D. E. (1991). A comparison of four particulate bone derivatives. *Clin Orthop Relat Res(267)*, 255-263.

66. Schouten, C. C., Hartman, E. H., Spauwen, P. H., & Jansen, J. A. (2005). DBM induced ectopic bone formation in the rat: the importance of surface area. *J Mater Sci Mater Med, 16*(2), 149-152.

67. Acarturk, O., Hollinger, J.O.. (2006). Comparison of commercially available particulate demineralized bone products, *J. Plast. Reconstr. 118*, 862–873.

68. Urist, M. R. (1965). Bone: formation by autoinduction. *Science, 150*(3698), 893-899.

69. Urist, M. R., & Strates, B. S. (1971). Bone morphogenetic protein. *Journal of Dental Research, 50*(6), 1392-1406.

70. Popat, K. C., Leary Swan, E. E., Mukhatyar, V., Chatvanichkul, K.-I., Mor, G. K., Grimes, C. A., & Desai, T. A. (2005). Influence of nanoporous alumina membranes on long-term osteoblast response. *Biomaterials, 26*(22), 4516-4522.

71. Popat, K. C., Chatvanichkul, K.-I., Barnes, G. L., Latempa, T. J., Grimes, C. A., & Desai, T. A. (2007). Osteogenic differentiation of marrow stromal cells cultured on nanoporous alumina surfaces. *Journal of Biomedical Materials Research Part A, 80A*(4), 955-964.

72. Popat, K. C., Eltgroth, M., LaTempa, T. J., Grimes, C. A., & Desai, T. A. (2007). Decreased Staphylococcus epidermis adhesion and increased osteoblast functionality on antibiotic-loaded titania nanotubes. *Biomaterials, 28*(32), 4880-4888.

73. Popat, K. C., Eltgroth, M., LaTempa, T. J., Grimes, C. A., & Desai, T. A. (2007). Titania Nanotubes: A Novel Platform for Drug-Eluting Coatings for Medical Implants? *Small, 3*(11), 1878-1881.

74. Ruckh, T. T., Kumar, K., Kipper, M. J., & Popat, K. C. (2010). Osteogenic differentiation of bone marrow stromal cells on poly(ε-caprolactone) nanofiber scaffolds. *Acta Biomaterialia, 6*(8), 2949-2959.

75. Leszczak, V., Place, L. W., Franz, N., Popat, K. C., & Kipper, M. J. (2014). Nanostructured biomaterials from electrospun demineralized bone matrix: a survey of processing and crosslinking strategies. *ACS Appl Mater Interfaces, 6*(12), 9328-9337.

76. Doshi J, Reneker DH. (1995). Electrospinning process and applications of electrospun fibers. *J Electrost 35*:151-60.

77. Mutsaers, S. E., Bishop, J. E., McGrouther, G., & Laurent, G. J. (1997). Mechanisms of tissue repair: from wound healing to fibrosis. *Int J Biochem Cell Biol, 29*(1), 5-17.

CHAPTER 2: MATERIALS AND METHODS

2.1 Fabrication of DBM and PCL Scaffolds

Demineralized bone matrix (DBM) nanofiber scaffolds and poly (ε-caprolactone) (PCL) nanofiber scaffolds were fabricated using electrospinning. Electrospinning is a straightforward, cost-effective technique to fabricate biomimetic non-woven scaffolds that are constituted from a large network of interconnected fibers and pores [1, 2]. In 2014, Leszczak et al. designed experiments to obtain DBM nanofibers by using electrospinning [3]. The same technique, as well as parameters, were also used in this thesis study. 1.1 g of (11%) DBM (AlloSource, Figure 2.1.1) was dissolved in a 10 mL mixture of hexafluoro-2-propanol / trifluoroacetic acid (70/30) (Acros Organics) in a glass vial. The solution was heated and vortexed at 40°C in an oil bath for 22 hours, then was left to cool to room temperature. A sheet of aluminum foil was placed on the collector in the bottom of the electrospinning apparatus. Upon transferring into a syringe, the solution was immediately elecrospun at 1 mL/hr, 15 kV voltage, and needle tip to collector distance of 6 in (electrospinning apparatus: Harvard apparatus, Figure 2.1.2). After electrospinning the solution for three hours, the fibers were left to dry. Since these fibers were soluble with water, glutaraldehyde vapor was used to fix them. 10 mL of 50% glutaraldehyde (Sigma) was used at this step. The DBM nanofibers were left in glutaraldehyde vapor for three days. Glutaraldehyde vapor treatment setup can be seen in Figure 2.1.3.

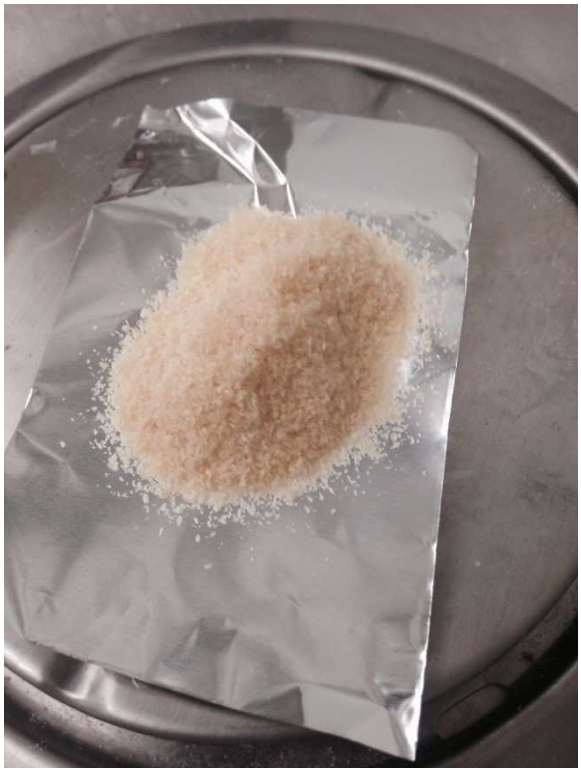

Figure 2.1.1: DBM powder.

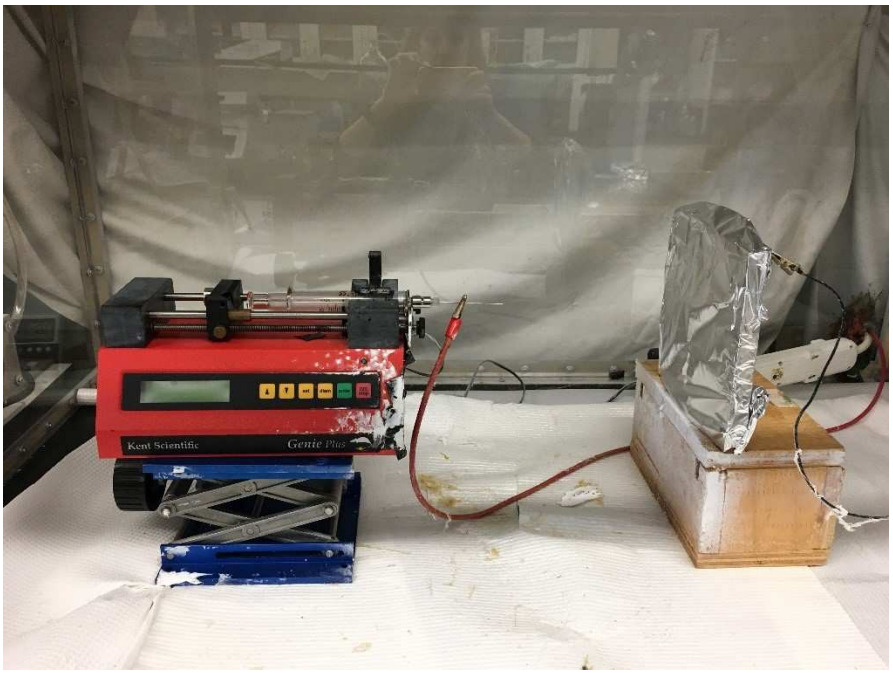

Figure 2.1.2: Electrospinning apparatus.

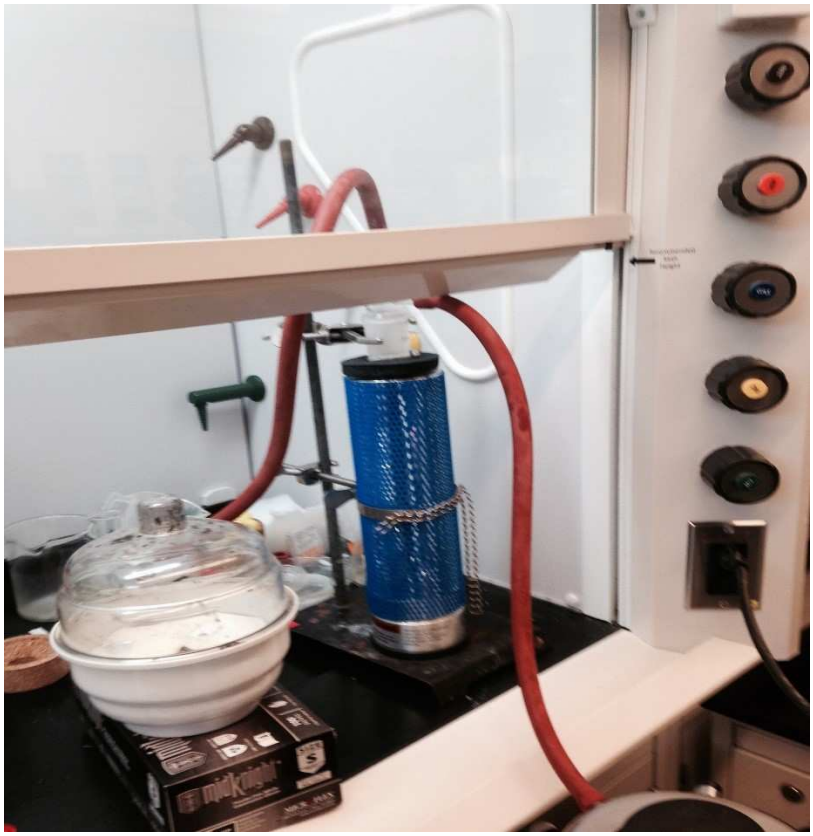

Figure 2.1.3: Glutaraldehyde vapor treatment setup.

PCL nanofiber scaffolds were prepared in a similar way. These scaffolds were fabricated as described previously in Ruckh et al. [4]. 1 g of (10%) PCL (Polysciences) was dissolved in 7.5 mL of chloroform, and 30.92 mg of oleic acid was mixed with 2.5 mL of methanol (Fisher Scientific). The two solutions were mixed and the final solution was directly electrospun at 2.5 mL/hr, 15 kV voltage, and needle tip to collector distance of 4 in, for approximately 20 minutes. When both DBM powder and PCL were electrospun, aluminum foil covering the collector, was completely covered with nanofibers and was completely white. The nanofibers could be easily recognized on aluminum foil for both cases. The nanofibers were imaged using field emission scanning electron microscopy (SEM, JEOL JSM-6500F) to determine whether the nanofibers had been produced successfully.

2.2 Culture and Seeding

Adipose-derived mesenchymal stem cells (AD-MSCs) were isolated from abdominal tissue of (FVB/NTsv-Tg (svyb-luc)-Xen) mice and cultured on DBM nanofiber scaffolds. For short term studies, AD-MSCs (Taconic, NY) were cultured in T75 culture flasks (Corning) in a medium supplemented with DMEM (HyClone) 15% fetal bovine serum (FBS) (HyClone), 2% mem vitamins, 1% anti-anti, and 1% mem amino acids at 37 ºC and 5% CO_2. The media was changed every 48 hours. Second passage confluent cells were split 1:2 and cells at fourth passage were used in all studies.

Before seeding cells, poly (ε-caprolactone) (PCL) nanofiber scaffolds were placed in tissue culture polystyrene (TCPS) disks, because it was very challenging to use PCL nanofibers that were placed directly on aluminum foil. Figure 2.2.1 shows TCPS disks. TCPS disks were cut from Corning multi-well culture plates. TCPS disks were chosen since they are non-toxic and they do not inhibit cell adhesion. TCPS disks were sterilized as follows. First, they were placed in a petri dish and sprayed with ethanol (70%) (Fisher Scientific) until they were totally covered with ethanol. After waiting 30 minutes, the disks were rinsed with PBS (Life Technologies) twice and then they were allowed to dry. Then, both sides of the disks were exposed to UV for 30 minutes. Carbon tape was used to stick PCL nanofibers on the foil to TCPS, because carbon tape is strong and solvent-free adhesive. Carbon tapes were sterilized in the same way and then were placed on TCPS disks. After this, PCL nanofiber scaffolds were placed on carbon tape that was attached to TCPS disks. PCL nanofiber scaffolds were placed in 48-well culture plates. Then, they were rinsed with PBS twice upon sterilization with ethanol.

Figure 2.2.1: Tissue culture polystyrene (TCPS) disks.

Demineralized bone matrix (DBM) nanofibers also were sterilized with ethanol and then rinsed with PBS. Then fourth passage AD-MSCs were seeded on both PCL and DBM nanofiber scaffolds in 48-well culture plates.

AD-MSC response was investigated in two phases:

- Cell adhesion and cell proliferation up to seven days of initial culture. Calcein-AM live stain and CellTiter 96® Non-Radioactive Cell Proliferation assay were used as described in Chapter 2.3 (25,000 cells/cm^2 for calcein-AM, 25,000 and 100,000 cells/cm^2 for CellTiter 96® Non-Radioactive Cell Proliferation assay were used).
- Cell osteogenic differentiation up to three weeks after osteogenic differentiation media was supplied (Alkaline Phosphate assay and Bicinchoninic Acid (BCA) protein assays, Alizarin

Red Staining, Cell Morphology), (100,000 AD-MSCs/cm^2 were seeded on nanofiber scaffolds for long term studies).

Osteogenic differentiation media was used for long term studies. Osteogenic differentiation media was prepared in complete culture medium (192 mL), was supplemented with 10 n*M* dexamethasone (Sigma), 200 µL of 1:100 dilution of 1 m*M* stock solution in DI water, 20 m*M* of β-glycerol phosphate (Sigma) and 50 m*M* L-ascorbic acid 2-phosphate (Sigma). This medium was replaced in every 48 hours for long term studies.

2.3 Cell Adhesion

After one, four, and seven days of culture, live cell adhesion was evaluated using calcein-AM (Life Technologies) staining (excitation 485 nm, emission 530 nm). Calcein-AM is a fluorogenic esterase substrate that is used as a membrane-permeable live-cell labeling. Intracellular esterases convert calcein-AM into fluorescein analogs and cleave the acetoxymethyl (AM) ester group, and the resulting calcein product becomes green. Apoptotic and dead cells do not retain calcein. DBM and PCL nanofiber scaffolds (three samples for each) were tested with this assay. After aspirating media, nanofiber scaffolds were rinsed with PBS twice. After this step, they were treated with 5 µ*M* calcein-AM in PBS. After being left 45 minutes in dark biosafety cabinet, the nanofiber scaffolds were imaged by using a fluorescence microscope (excitation 486 nm, emission 530 nm) (Zeiss) shown in Figure 2.3.1. Calcein was detected using the appropriate filter sets.

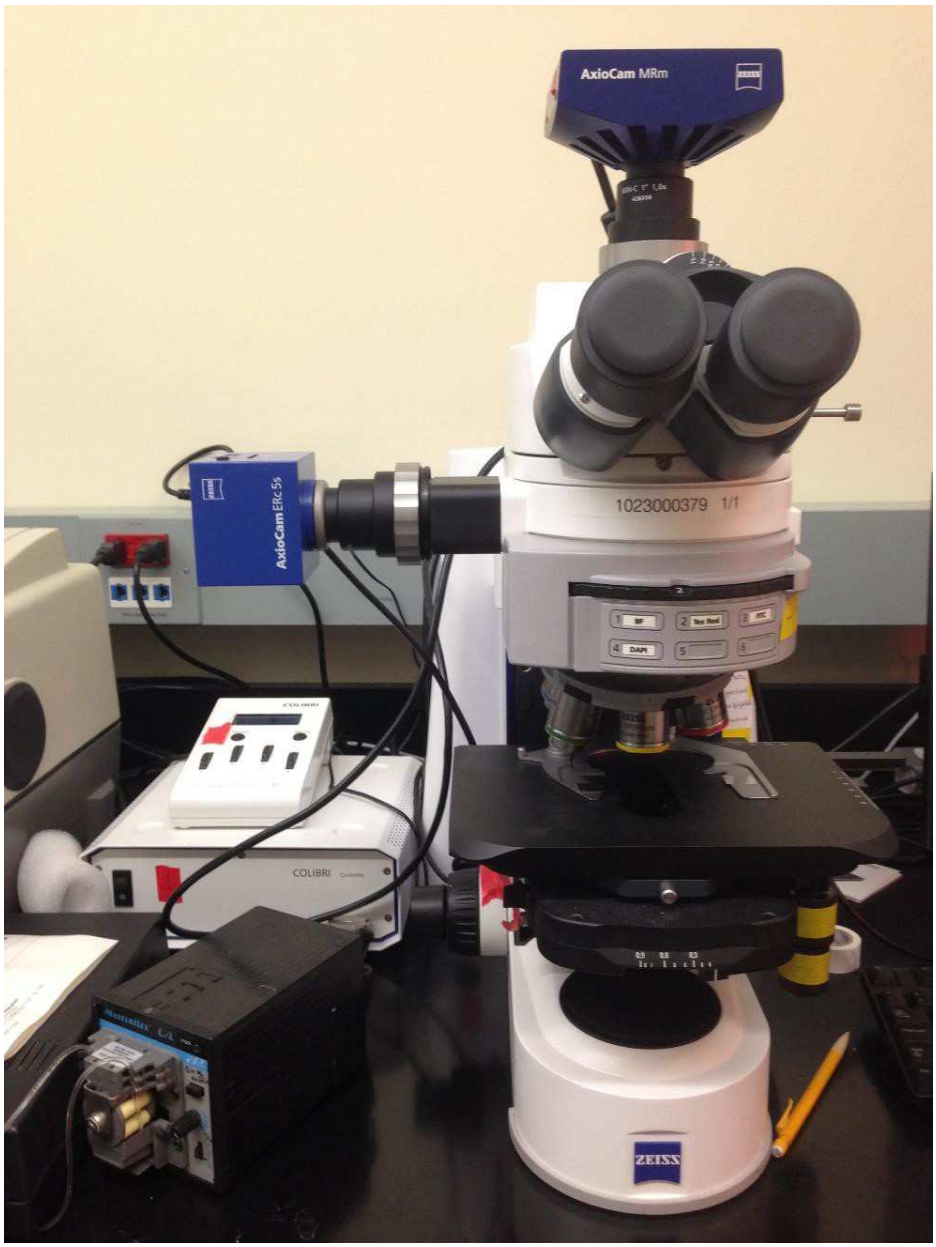

Figure 2.3.1: Fluorescent Microscope - Zeiss Imager.A2.

2.4 Cell Proliferation

After one, four, and seven days of culture, cell viability was measured by CellTiter 96® Non-Radioactive Cell Proliferation assay (Promega). CellTiter 96® Non-Radioactive Cell Proliferation assay is a 3-(4, 5-dimethylthiazol-2-yl)-2, 5-diphenyltetrazolium bromide)

tetrazolium (MTT) reduction assay. MTT is converted into a purple colored formazan product with an absorbance maximum near 570 nm by viable cells with active metabolism. The exact cellular mechanism of MTT reduction into formazan is not well understood, but likely involves reaction with nicotinamide adenine dinucleotide (NADH) (which is a coenzyme that is found in all living cells) or similar reducing molecules that transfer electrons to MTT [5]. According to Spinner's study, the mitochondrial succinate-dehydrogenases of viable cells cleave the tetrazolium ring in active mitochondria into formazan crystals [6]. Then formazan crystals should be dissolved in order to measure the quantity of formazan that is directly proportional to the number of viable cells.

DBM and PCL nanofiber scaffolds (three samples for each) were tested with this assay. After transferring the nanofiber scaffolds into another 48-well plate, 30 µL of dye solution was added on each well. After this step, the nanofiber scaffolds were incubated at 37°C for 4 hours. During the 4-hour incubation, the tetrazolium component of the dye solution was converted into a formazan product. After 4 hours, 100 µL of solubilization solution/stop mix was added to each well and the nanofiber scaffolds were incubated for an additional one hour. In this step, formazan product was solubilized. Lastly, a FLUOstar Omega plate reader was used to measure the quantity of formazan (presumably directly proportional to the number of viable cells). It was measured by recording changes in absorbance at 570 nm and 690 nm, using a plate reading spectrophotometer shown in Figure 2.4.1.

Figure 2.4.1: Plate reader (FLUOstar Omega).

2.5 Alkaline Phosphatase (ALP) and Bicinchoninic Acid (BCA) Protein Assays

Osteogenic differentiation media was provided for demineralized bone matrix (DBM) and poly (ε-caprolactone) (PCL) nanofiber scaffolds for one, two and three weeks. DBM nanofiber seeded with cells, DBM nanofiber scaffolds, PCL nanofiber scaffolds seeded with cells, and PCL nanofibers (three samples for each) were tested with alkaline phosphatase (ALP) and bicinchoninic acid (BCA) assays. After each time point, adipose-derived mesenchymal stem cells (AD-MSCs) were lysed from the nanofiber scaffolds, the nanofiber scaffolds were removed from media, and rinsed with PBS twice. 200 µL of RIPA buffer solution (Thermo Scientific) was added to each

well and then cell culture plate was allowed to cool on ice for 15 minutes. After 15 minutes, the contents of the wells were transferred into centrifuge tubes and the centrifuge tubes were centrifuged at 14,000 rpm for 5 minutes. Then, supernatants were transferred to different centrifuge tubes. These tubes were kept on ice during BCA and ALP assay studies.

The total protein content of each lysate was measured by Pierce™ BCA Protein assay kit (Thermo Scientific). This colorimetric assay is based on BCA. According to Wiechelman et al., the macromolecular structure of the protein, the number of peptide bonds and the presence of four amino acids (cysteine, cystine, tryptophan and tyrosine) form color with BCA [7]. There are two steps in total protein content evaluation. First, biuret reaction: cupric ion reduces to cuprous ion. The other step is the chelation of BCA with the cuprous ion, resulting in a purple color. Any wavelength between 550 nm and 570 nm is suitable for the color to be measured [7].

25 µL from each of the samples (standards and unknowns) were transferred into a 96-well plate, and 200 µL of working reagent was added to each well. Then, the plate was put into incubator (37°C) for 30 minutes. After 30 minutes, it was allowed to cool to room temperature and then a FLUOstar Omega plate reader was used for analysis (562 nm). The protein concentration of each sample was calculated as defined in the Thermo Scientific's Pierce™ BCA Protein assay kit instruction manual. The average 562 nm absorbance measurement of the blank standard replicates was subtracted from the 562 nm measurements of all other individual standard and unknown sample replicates, and then a standard curve was prepared by plotting the average blank-corrected 562 nm measurement for each BSA standard vs. its concentration in µg/mL. Then the standard curve was used to determine the protein concentration of each unknown sample.

ALP is one of the key components in the process of osteogenesis and ALP activity is a very early marker of differentiation of mesenchymal stem cells to osteoblasts [8, 9]. The ALP activity was

measured by a commercially available assay kit in order to understand if AD-MSCs support osteoblast differentiation on both DBM and PCL scaffolds. A colorimetric Alkaline Phosphatase Assay kit (Abcam) was used for this aim. ALP catalyzes the hydrolysis of 40 µL pNPP (p-nitrophenyl phosphate). 5 m*M* was diluted in 160 µL to obtain 1 m*M* standards and then standard curve dilution was prepared as described in the assay kit booklet. Then, 120 µL of standard dilutions and 40 µL of lysates with 40 µL of ALP assay buffer were added to a 96-well plate. 50 µL of pNPP solution was added to each well containing samples, and 10 µL of ALP enzyme was added to each well containing standards, and in the end, each well contained 130 µL of solution. After mixing wells carefully, the plate was kept in a dark place for 1 hour at room temperature. After 1 hour, 20 µL of stop solution was added to each well. A FLUOstar Omega plate reader was used for the analysis (OD405 nm). The duplicate reading was averaged for each standard and sample and then the mean absorbance value of the blank (standard #1) was subtracted from all standard and sample and the corrected absorbance was found. Then, corrected absorbance values for each standard were plotted as a function of the final concentration of pNPP. The trend line equation was calculated based on the standard curve data, and the concentration of alkaline phosphatase in the test samples was calculated according to the equation provided in the instruction manual.

2.6 Alizarin Red Staining

Calcium deposition is regarded as the final stage of osteoblast differentiation. It starts as the matrix matures and gradually increases until a stable bony structure is formed by the mineralized matrix [10, 11]. Alizarin red staining assay was conducted to evaluate the mineralization of calcium on demineralized bone matrix (DBM) and poly (ε-caprolactone) (PCL) scaffolds. This

staining is based on calcium formation of an alizarin red S-calcium complex, which is a bright red stain, in a chelation process.

To prepare Ringer's solution, 1.8 g NaCl (Fisher Scientific), 0.425 g $CaCl_2$ (Fisher Scietific) and 0.925 g KCl (Fisher Scientific) were dissolved in DI water and then the volume was brought to 250 mL by adding water. Then, the pH was measured and adjusted to 7.3-7.4. After this, the solution was filtered by using a 200 µL filter cup.

DBM and PCL nanofiber scaffolds were removed from the media and rinsed twice with cold (4°C) Ringer's solution. Then, the scaffolds were immersed in cold (4°C) paraformaldehyde (Sigma Aldrich) and PBS solution (4 g paraformaldehyde with 100 mL PBS) for 10 minutes. They were then rinsed with cold (4°C) DI water and submerged in cold Alizarin red (2% by wt) (Sigma Aldrich) and 0.1 *M* NaOH solution (with DI water) (Fisher Scientific) for 10 minutes. They were then rinsed three times with cold DI water and then allowed to dry in a desiccator. A Cannon Power Shot SD1000 was used for imaging.

2.7 Cell Morphology and Mineralization

Cell morphology and mineralization (calcium, phosphorus, oxygen, carbon, and nitrogen) on demineralized bone matrix (DBM) and poly (ε-caprolactone) (PCL) nanofiber scaffolds were evaluated after one, two and three weeks of culture. After removing the scaffolds from the osteogenic differentiation media, the scaffolds were immersed in PBS for approximately 5 minutes. After this step, to fix the cells on DBM and PCL scaffolds, a fixing solution was prepared as in the following procedure. 0.68 g sucrose (Aldrich) and 0.42 g of Na-cacodylate (Alfa-Aesar) were mixed with 19.4 mL of DI water (0.2 *M* Na-cacodylate and 0.1 *M* sucrose buffer). Then, this solution was separated into 2 aliquots (10 mL and 9.4 mL) and then placed into 2 centrifuge tubes.

0.6 mL of 30% glutaraldehyde (Sigma) was added to 9.4 mL of solution. This was the primary fixative. Scaffolds were immersed in primary fixative for 45 minutes. After this, the samples were placed in the 10 mL portion of Na-cacodylate buffer for 10 minutes. Then, samples were dehydrated by immersing in an increased graded ethanol series (35%, 50%, 70%, 100%) for 10 minutes for each concentration. Lastly, the scaffolds were placed in hexamethyldisilazane for 10 minutes and then the scaffolds were air-dried. They were stored in a desiccator until they were analyzed. For evaluation of fixed and dehydrated samples, field emission scanning electron microscopy (SEM, JEOL JSM-6500F) was used. The scaffolds were prepared for SEM as follows. They were attached to aluminum stubs with conductive adhesive tapes and then coated with 10 nm of gold. Then they were imaged by SEM. For analyzing the mineralization, samples were prepared as they were prepared for SEM as described and then an energy-dispersive X-ray spectroscope (EDS) (EDS-EDAX SDD) attached to the field emission scanning electron microscopy (SEM, JEOL JSM-6500F) shown in Figure 2.7.1 was used. The scaffold surfaces were examined at 10-15 kV and analyzed for approximately 10 minutes.

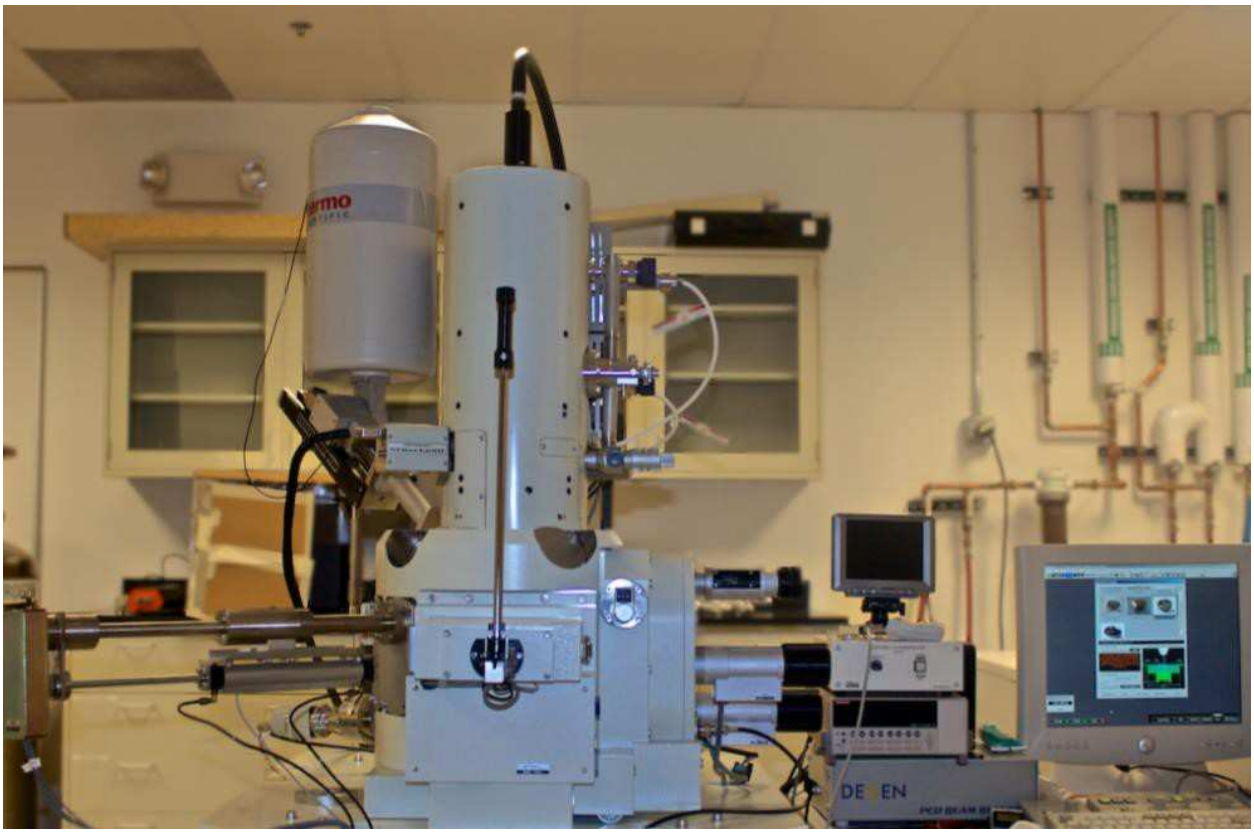

Figure 2.7.1: Scanning Electron Microscope (SEM), model JEOL JSM SEM 6500F.

2.8 Thermal Analysis of DBM

TGA (Thermogravimetric Analysis) is a thermal analysis method that measures weight changes of a sample as a function of temperature, i.e., when the sample is heated, cooled or held at constant temperature. This method was used to characterize six demineralized bone matrix (DBM) lots with regard to their composition. Upon preparing the DBM lot samples in a range between 5-20 mg, the lot samples were loaded to the TGA equipment (2950 TGA V5.4A) shown in Figure 2.8.1. Then, TA universal analysis software was used to arrange parameters.

Figure 2.8.1: TGA equipment.

2.9 Statistical Analysis

A two-tailed, unpaired t-test was used to evaluate the statistical significance at each time point for cell proliferation, alkaline phosphatase activity and protein content. Statistical significance was evaluated at $p < 0.05$.

REFERENCES

1. Heydarkhan-Hagvall, S., Schenke-Layland, K., Dhanasopon, A. P., Rofail, F., Smith, H., Wu, B. M., . . . MacLellan, W. R. (2008). Three-dimensional electrospun ECM-based hybrid scaffolds for cardiovascular tissue engineering. *Biomaterials, 29*(19), 2907-2914.

2. Murugan, R., & Ramakrishna, S. (2007). Design strategies of tissue engineering scaffolds with controlled fiber orientation. *Tissue Engineering, 13*(8), 1845-1866.

3. Leszczak, V., Place, L. W., Franz, N., Popat, K. C., & Kipper, M. J. (2014). Nanostructured biomaterials from electrospun demineralized bone matrix: a survey of processing and crosslinking strategies. *ACS Appl Mater Interfaces, 6*(12), 9328-9337.

4. Ruckh, T. T., Kumar, K., Kipper, M. J., & Popat, K. C. (2010). Osteogenic differentiation of bone marrow stromal cells on poly(ε-caprolactone) nanofiber scaffolds. *Acta Biomaterialia, 6*(8), 2949-2959.

5. Marshall, N. J., Goodwin, C. J., & Holt, S. J. (1995). A critical assessment of the use of microculture tetrazolium assays to measure cell growth and function. *Growth Regul, 5*(2), 69-84.

6. Spinner, D. M. (2001). MTT growth assays in ovarian cancer. *Methods Mol Med, 39*, 175-177.

7. Wiechelman, K. J., Braun, R. D., & Fitzpatrick, J. D. (1988). Investigation of the bicinchoninic acid protein assay: identification of the groups responsible for color formation. *Anal Biochem, 175*(1), 231-237.

8. Owen, T. A., Aronow, M., Shalhoub, V., Barone, L. M., Wilming, L., Tassinari, M. S., . . . Stein, G. S. (1990). Progressive development of the rat osteoblast phenotype in vitro: reciprocal relationships in expression of genes associated with osteoblast proliferation and differentiation during formation of the bone extracellular matrix. *J Cell Physiol, 143*(3), 420-430.

9. Liu, F., Malaval, L., & Aubin, J. E. (2003). Global amplification polymerase chain reaction reveals novel transitional stages during osteoprogenitor differentiation. *J Cell Sci, 116*(Pt 9), 1787-1796.

10. Lian, J. B., & Stein, G. S. (1992). Concepts of osteoblast growth and differentiation: basis for modulation of bone cell development and tissue formation. *Crit Rev Oral Biol Med, 3*(3), 269-305.

11. Shin, H., Zygourakis, K., Farach-Carson, M. C., Yaszemski, M. J., & Mikos, A. G. (2004). Modulation of differentiation and mineralization of marrow stromal cells cultured on biomimetic hydrogels modified with Arg-Gly-Asp containing peptides. *J Biomed Mater Res A, 69*(3), 535-543.

CHAPTER 3: RESULTS AND DISCUSSION

3.1 Fabrication of Nanofiber Scaffolds

Electrospinning was used to obtain both demineralized bone matrix (DBM) and poly (ε-caprolactone) (PCL) nanofibers. Electrospinning is a straightforward, cost-effective technique to fabricate biomimetic non-woven scaffolds that are constituted from a large network of interconnected fibers and pores [1, 2]. In 2014, Leszczak et al. obtained uniform DBM nanofibers by electrospinning [3]. After electrospinning, the fibers were water-soluble. Hence, glutaraldehyde vapor treatment was conducted to crosslink the nanofibers. In this study here, the same technique was used, with the same parameters. DBM was supplied by AlloSource (Centennial, CO). Six lots of DBM were used. The details are provided in Table 3.1.1 below.

Table 3.1.1: DBM lots. Lots were received from AlloSource. Lot numbers and their solubility (11% DBM) in a mixture of hexafluoro-2-propanol / trifluoroacetic acid (70/30).

DBM Lots		**DBM Lots**	
115561-601	Dissolved	104063-605	Not dissolved
132270-6505	Dissolved	116719-603	Dissolved
115679-601	Not dissolved	92112	Not dissolved

First, 1.1 g of DBM lot 104063-605 in a 10 mL solvent blend of hexafluoro-2-propanol / trifluoroacetic acid (70/30) was prepared at 40 ºC, but it could not be dissolved. Then, DBM lot 115561-601 was used and uniform nanofibers were obtained. In order to crosslink the water soluble nanofibers, glutaraldehyde vapor treatment was conducted. Scanning electron microscopy

(SEM) was used to image these nanofibers. Glutaraldehyde vapor stabilized the fibers successfully as can be seen in Figure 3.1.1.

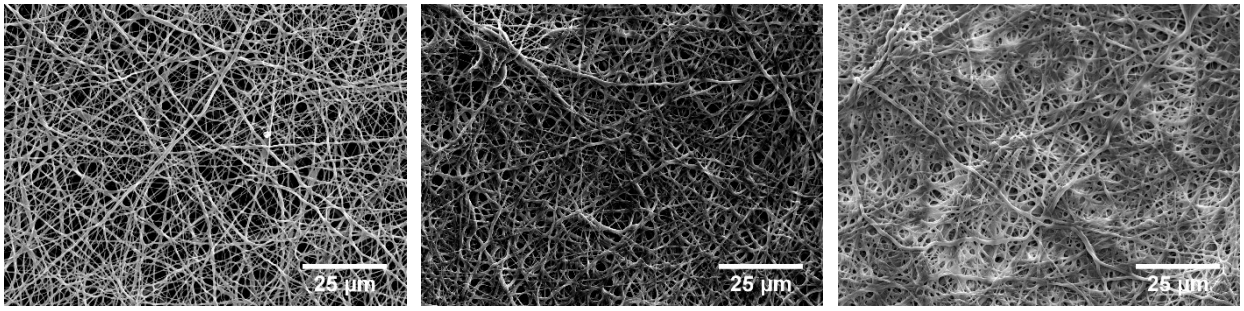

Figure 3.1.1: SEM images of DBM nanofiber scaffolds at 1,000x magnification: (a) DBM nanofiber scaffolds, (b) DBM nanofiber scaffolds after glutaraldehyde vapor treatment, before exposure to water, (c) DBM nanofiber scaffolds after glutaraldehyde vapor treatment, after exposure to water.

Having DBM lots from the same source showing different properties is an expected situation. In Gruskin's study, it was mentioned that individual DBM lots that are processed by the same tissue bank may not be the same since these lots are obtained from different donor bones [4].

ImageJ software was used to calculate the diameters of the DBM nanofibers. The nanofibers were quite uniform, and the average diameter of the nanofibers was 902 nm, as shown in Figure 3.1.2. The nanofiber with the smallest diameter had approximately 500 nm, and the thickest nanofiber had a diameter of 1,300 nm.

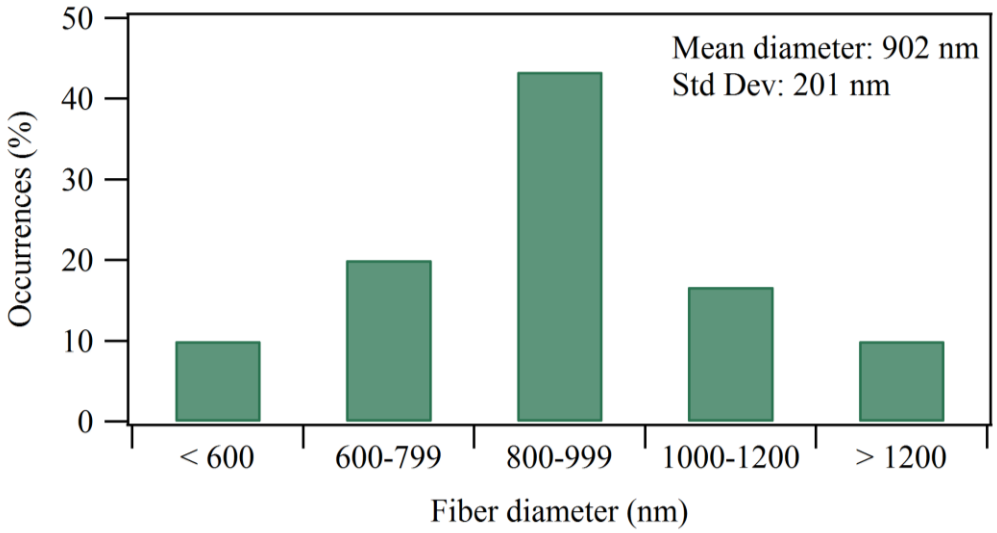

Figure 3.1.2: Fiber diameter occurrences of DBM nanofibers calculated using the SEM image of DBM nanofibers.

After one week in osteogenic media, DBM nanofibers were imaged by using SEM. Figure 3.1.3 presents these nanofibers. The fibers swelled after one week in the osteogenic media and the diameters of the nanofibers became unmeasurable.

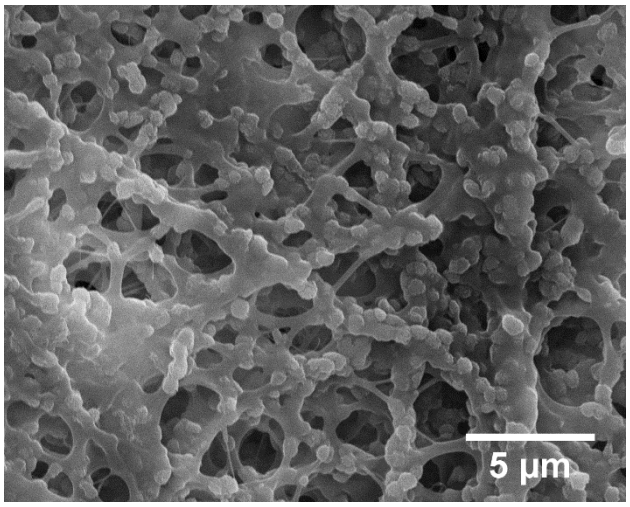

Figure 3.1.3: SEM image of DBM nanofibers without cells after one week in osteogenic differentiation media.

Electrospun PCL scaffolds are fabricated as they have a potential to be used as bone and cartilage scaffolds [5-7]. In 2010, Ruckh demonstrated that PCL nanofibers support the osteogenic differentiation of bone marrow stromal cells [8]. The same technique as well as parameters of Ruckh's study were used here, and PCL nanofibers were achieved as shown Figure 3.1.4.

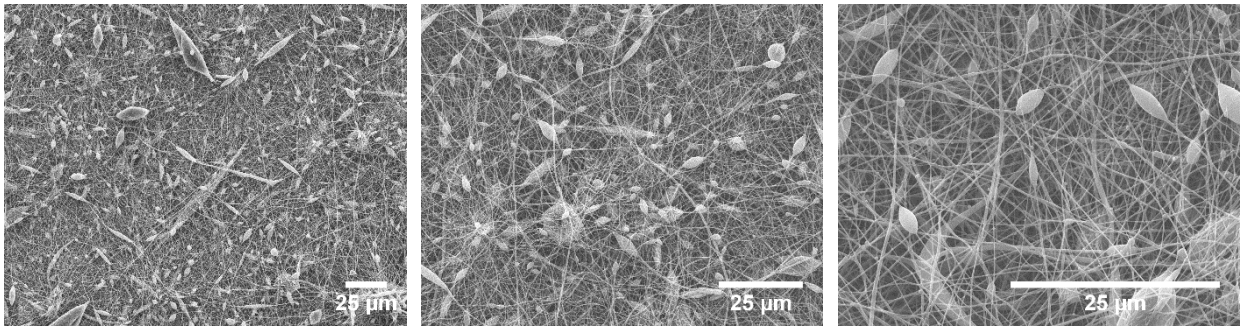

a **b** **c**

Figure 3.1.4: SEM images of PCL nanofiber scaffolds under different magnifications: (a) 500x, (b) 1,000x, (c) 2,500x.

ImageJ software was used to calculate the diameters of the PCL nanofibers. Most of the PCL nanofibers were uniform. The thickest nanofiber had a diameter of approximately 650 nm. The average of the nanofiber diameters was approximately 265 nm as presented in Figure 3.1.5.

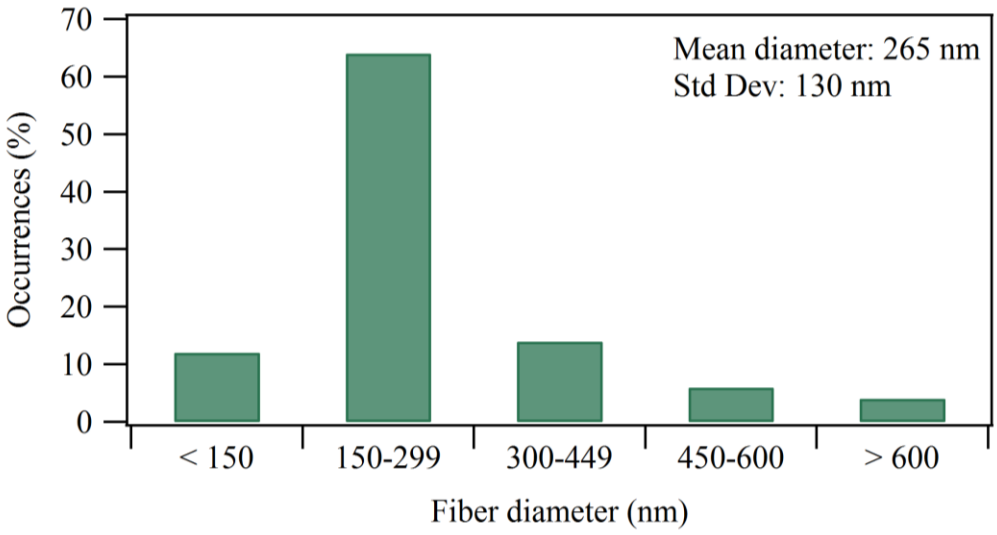

Figure 3.1.5: Fiber diameter occurrences of PCL nanofibers calculated using the SEM image of PCL nanofibers.

After one week in osteogenic media, PCL nanofibers were imaged by using SEM. Figure 3.1.6 shows these nanofibers.

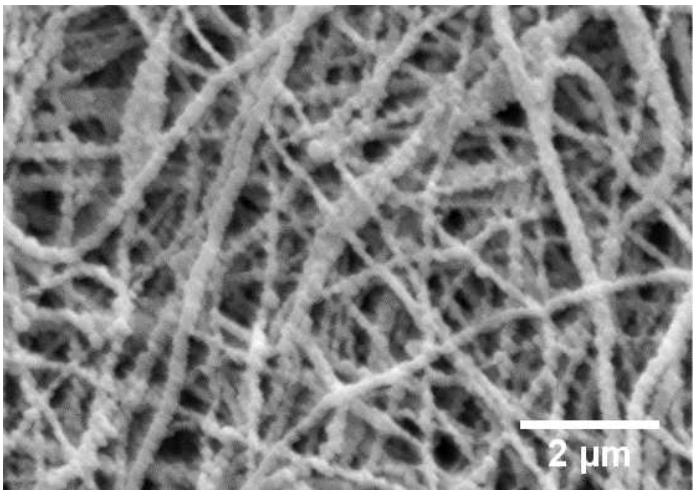

Figure 3.1.6: SEM image of PCL nanofiber scaffold without cells after one week in osteogenic differentiation media.

When the diameters were calculated by using ImageJ software, it was seen that the PCL nanofiber diameters were quite similar to each other. The thickest nanofiber had a diameter of

approximately 400 nm, and the average of the diameters was approximately 200 nm as shown in Figure 3.1.7. As the PCL nanofibers were exposed to the media, they appeared a little bit thinner than before.

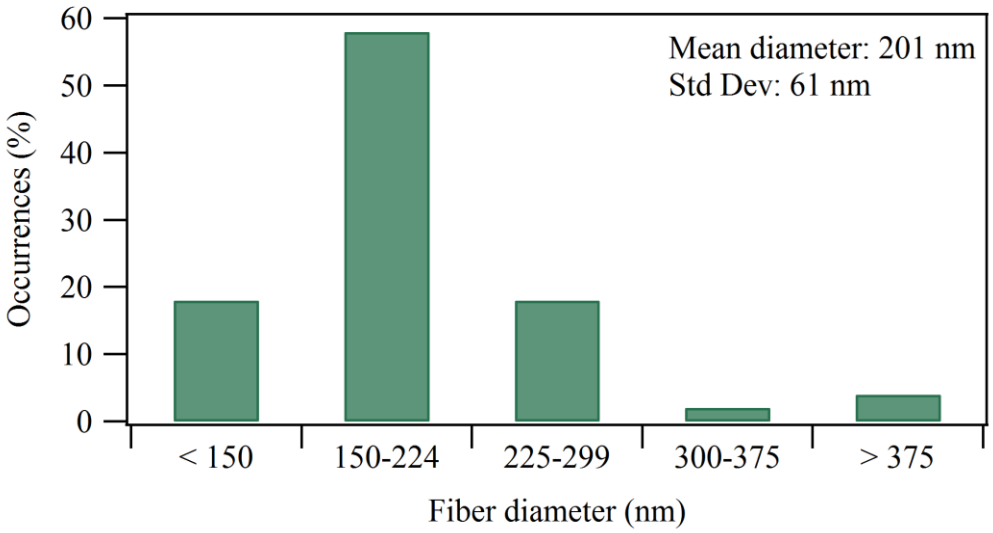

Figure 3.1.7: Fiber diameter occurrences of PCL nanofibers after one week in osteogenic media calculated using the SEM image of PCL nanofibers.

3.2 Short-term AD-MSC response on DBM and PCL Scaffolds

After one, four, and seven days of culture, adipose-derived mesenchymal stem cells' (AD-MSCs) response to demineralized bone matrix (DBM) and poly (ε-caprolactone) (PCL) nanofiber scaffolds were investigated through cell adhesion and cell proliferation. Live cell stain calcein-AM and CellTiter 96® Non-Radioactive Cell Proliferation assays were used to evaluate the ability of DBM and PCL nanofiber scaffolds to support AD-MSC adhesion and proliferation, respectively.

In 2012, Khanna-Jain et al. investigated the adhesion, viability, and proliferation morphology of human dental pulp stem cells (DPSCs) cultured in human serum medium seeded

on β-tricalcium phosphate/poly(L-lactic acid/caprolactone) scaffold (β-TCP/P(LLA/CCL)), and proved that human DPSCs can proliferate and differentiate into osteogenic lineage within β-TCP/P(LLA/CL) scaffolds [9]. Calcein-AM staining study was used to evaluate the cell adhesion of DPSCs on β-TCP/P(LLA/CL) scaffold. It was shown that as time progresses, more cells can be observed on the surfaces. Calcein-AM staining is a common technique to evaluate cell adhesion of cells on surfaces.

Calcein-AM was used to evaluate the cell adhesion of AD-MSCs on DBM and PCL nanofiber scaffolds. Two groups were examined qualitatively by using this fluorescent assay: DBM nanofiber scaffolds (8 mm diameter) seeded with 25,000 AD-MSCs and PCL nanofiber scaffolds (8 mm diameter) seeded with 25,000 AD-MSCs. Figure 3.2.1 on the following page shows fluorescence microscopy images of the adhesion of AD-MSCs on both DBM and PCL nanofiber scaffolds. After one day of culture, there are more AD-MSCs on DBM nanofiber scaffolds than on PCL nanofiber scaffolds. More cells were observed on day four and day seven in comparison to day one for both cases. Highly populated colonies of cells were formed on both types of nanofiber scaffolds on day seven. These results are consistent with the results of Khanna-Jain et al. [9].

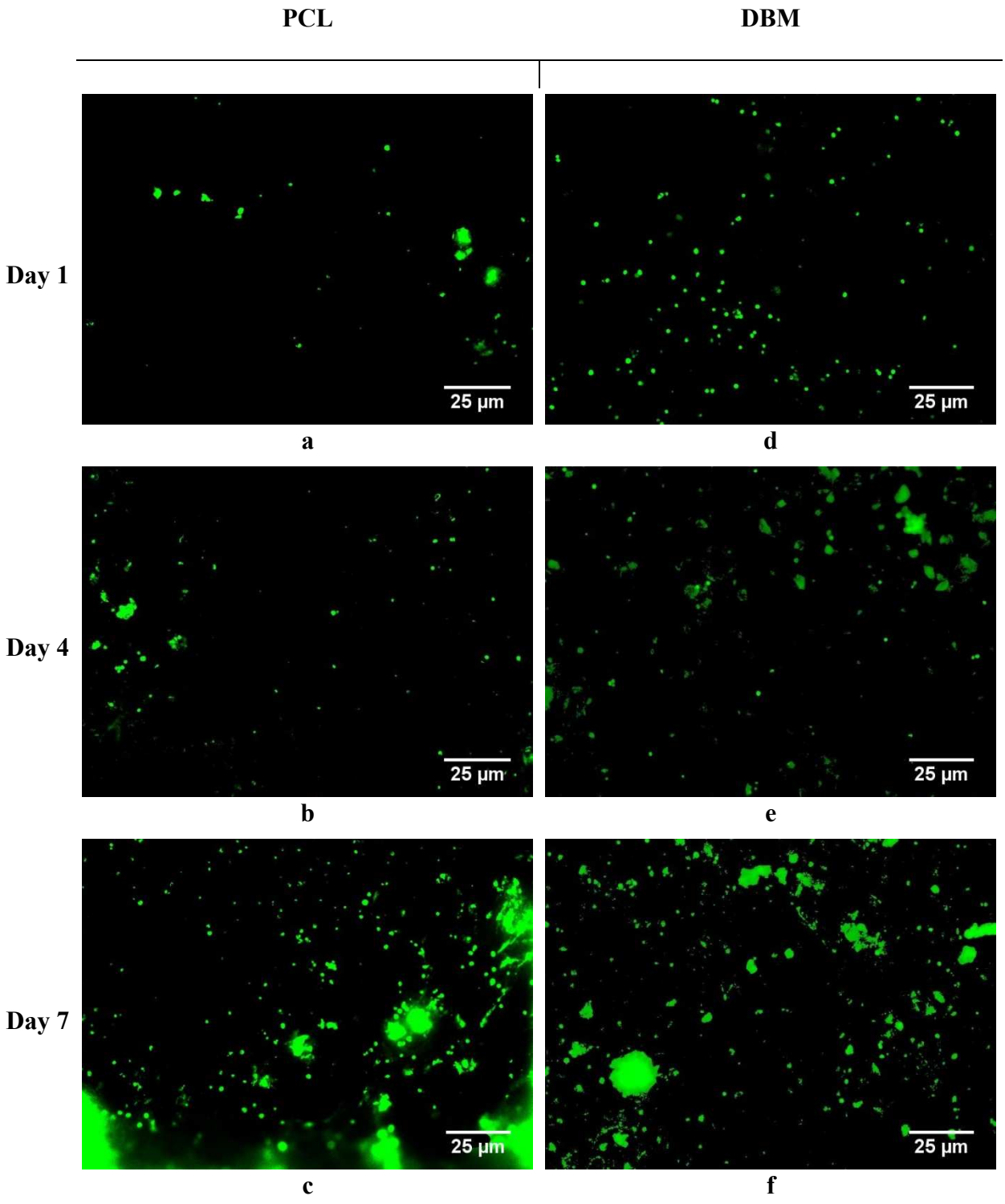

Figure 3.2.1: Live cells stained with calcein-AM on control surfaces (a, b, c) and DBM nanofiber scaffolds (d, e, f) after one, four, and seven days of culture, respectively.

CellTiter 96® Non-Radioactive Cell Proliferation assay was used to evaluate the ability of DBM and PCL nanofiber scaffolds to support viable cell proliferation. In this assay, MTT is converted into a purple colored formazan product with an absorbance maximum near 570 nm by viable cells with active metabolism. The quantity of formazan is directly proportional to the mitochondrial activity, which is often a direct measure of cell viability. Two different groups were examined in this study: DBM nanofiber scaffolds seeded with 25,000 AD-MSCs and PCL nanofiber scaffolds seeded with 25,000 AD-MSCs. After one day of culture, cell metabolic activity on DBM and PCL nanofiber scaffolds was similar. But, after four days of culture, cell metabolic activity on PCL nanofiber scaffolds was found to be significantly higher than cell metabolic activity on DBM nanofiber scaffolds ($p < 0.05$). After seven days of culture, cell metabolic activity on DBM and PCL nanofiber scaffolds was similar to cell metabolic activity after one day of culture. Figures 3.2.2 and 3.2.3 illustrate these results.

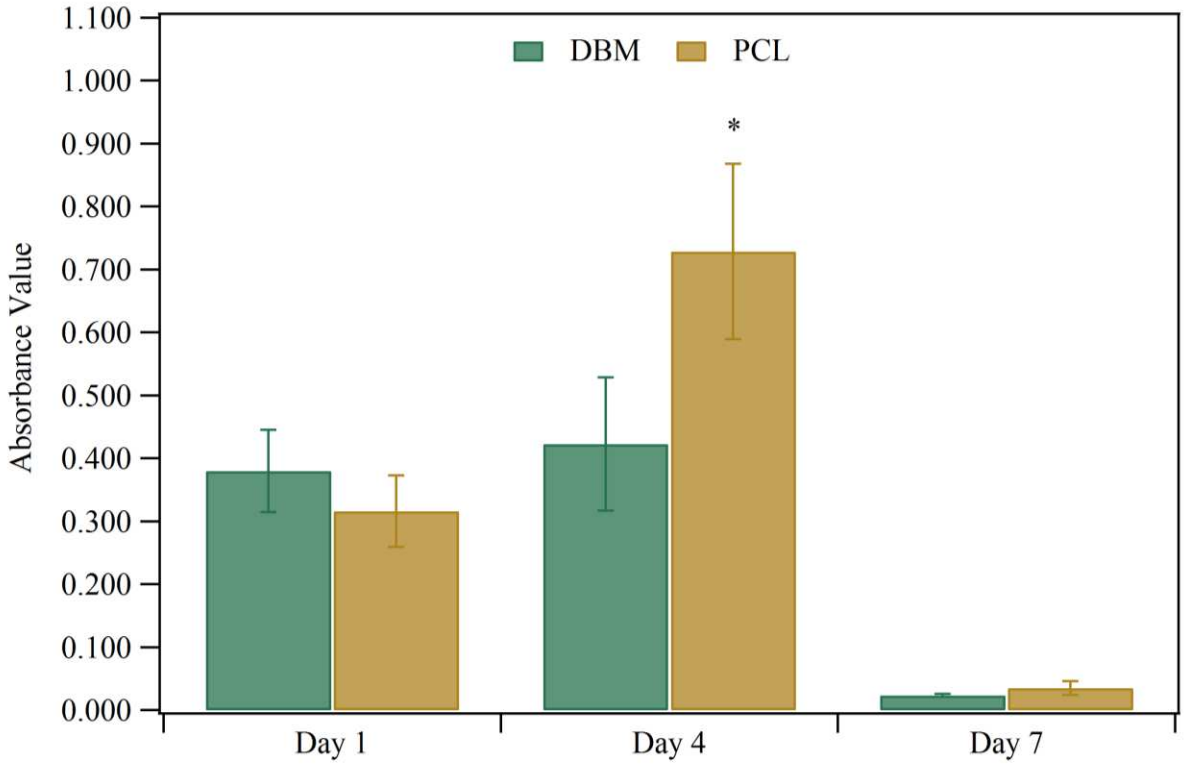

Figure 3.2.2: Average cell viability on DBM and PCL nanofiber scaffolds seeded with 25,000 AD-MSCs, measured using CellTiter 96® Non-Radioactive Cell Proliferation assay. Cell viability was significantly different on PCL nanofiber scaffolds than DBM nanofiber scaffolds only on day four (* → $p < 0.05$).

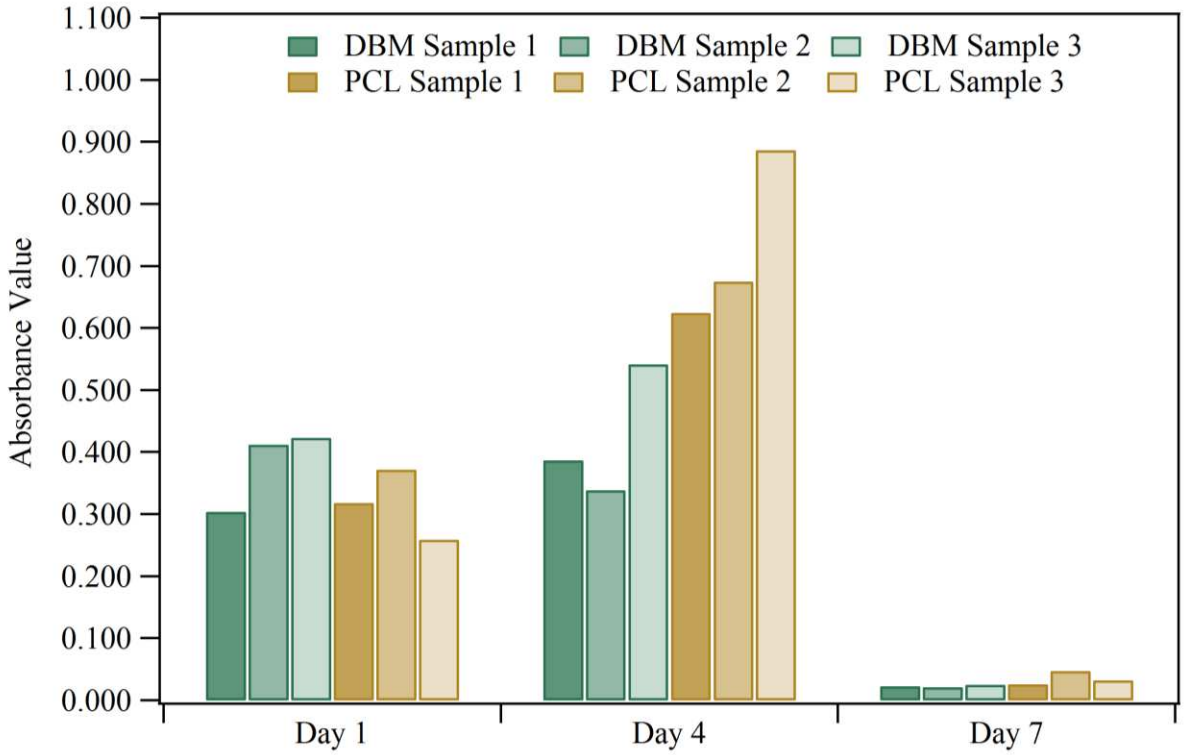

Figure 3.2.3: Cell viability on DBM and PCL nanofiber scaffolds seeded with 25,000 AD-MSCs, for all samples, measured using CellTiter 96® Non-Radioactive Cell Proliferation assay.

The aforementioned study was repeated using 100,000 of AD-MSCs. This time, cell metabolic activity on both DBM and PCL nanofiber scaffolds were similar after one and four days of culture. After seven days of culture, cell metabolic activity on DBM nanofiber scaffolds were significantly higher than cell metabolic activity on PCL nanofiber scaffolds. Figures 3.2.4 and 3.2.5 present these results.

Cell differentiation is associated with an increase in mitochondrial content and activity and inhibiting mitochondrial function promotes pluripotency and prevents differentiation [22]. When 25,000 cells were used, the mitochondrial activity of the cells on DBM and PCL nanofiber were both decreased, which may indicate progression of osteoblastic differentiation after seven days of

culture. When cell numbers were increased to 100,000, again the mitochondrial activity was high at day one, but decreased with time.

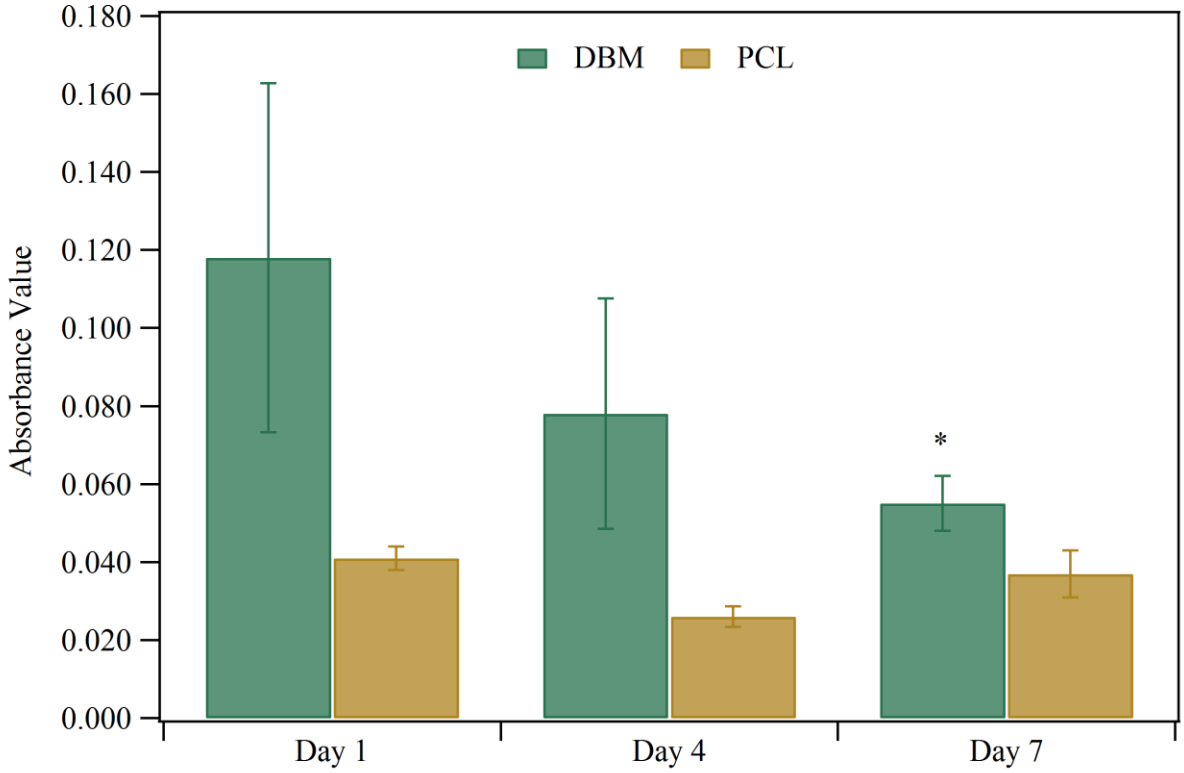

Figure 3.2.4: Average cell viability on DBM and PCL nanofiber scaffolds seeded with 100,000 AD-MSCs, measured using CellTiter 96® Non-Radioactive Cell Proliferation assay. After seven days of culture, average cell viability on DBM nanofiber scaffolds was significantly higher when compared to the average cell viability on PCL nanofiber scaffolds (* → $p < 0.05$).

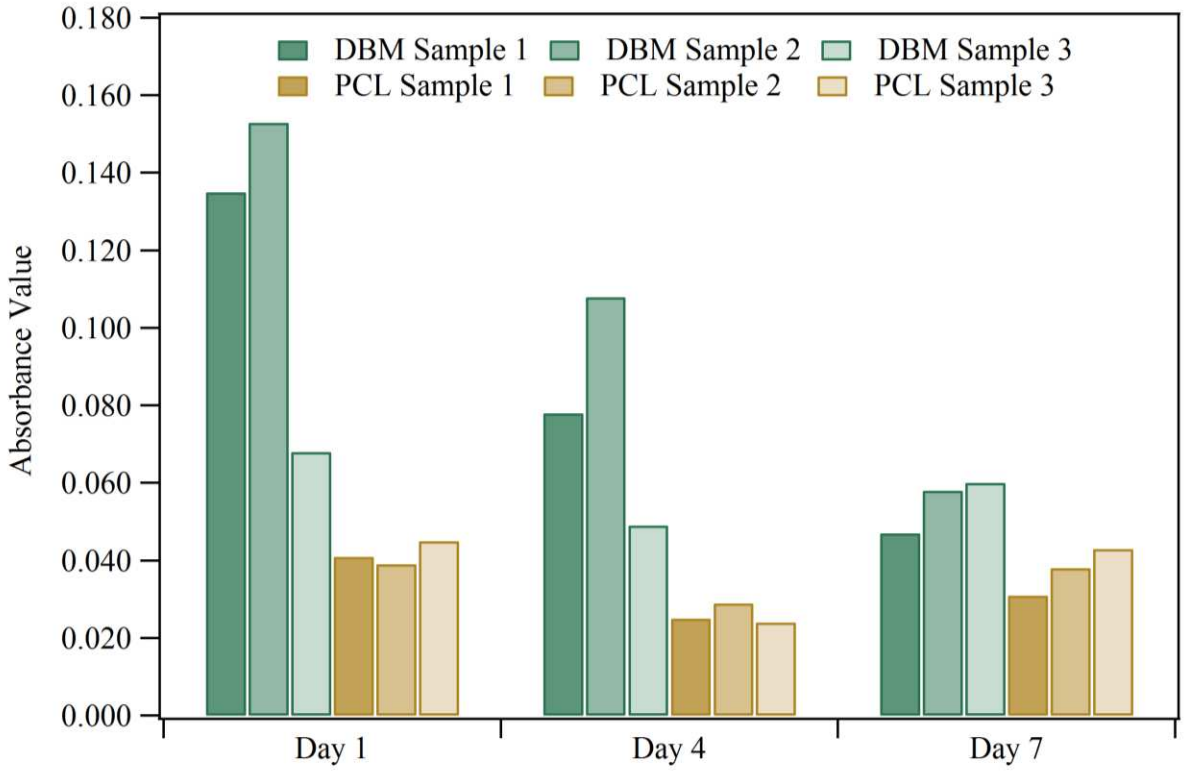

Figure 3.2.5: Cell viability on DBM and PCL nanofiber scaffolds seeded with 100,000 AD-MSCs, for all samples, measured using CellTiter 96® Non-Radioactive Cell Proliferation assay.

3.3 Long-term AD-MSC response on DBM and PCL Scaffolds

3.3.1 Total Protein Content

In 2005, Popat investigated the influence of nanoporous alumina membranes on long-term osteoblast response, and bicinchoninic acid (BCA) protein assay was used to evaluate the protein content of the viable cells on nanoporous alumina in comparison to other surfaces such as glass and aluminum. The study demonstrated that for long time periods, cells on nanoporous alumina membranes produce more protein than cells on other surfaces, suggesting that the nanoporous structure provides favorable surface architecture for osteoblast function [10]. Popat's study inspired this study to use BCA assay and evaluate the total protein content of viable adipose-derived

mesenchymal stem cells (AD-MSCs) on both demineralized bone matrix (DBM) and poly (ε-caprolactone) (PCL) nanofibers.

BCA protein assay was used to evaluate the total protein content of viable AD-MSCs on the scaffolds. A FLUOstar Omega plate reader was used to compare the absorbance values of protein standards to resulting solutions after cell lysis at 562 nm. Figure 3.3.1 shows the total protein content of AD-MSCs on DBM and PCL nanofiber scaffolds without cells compared to DBM and PCL nanofiber scaffolds seeded with cells. Cells on both nanofiber scaffolds acted similarly. Only at week 2, PCL nanofibers seeded with cells had significantly more proteins than PCL nanofibers without cells. Furthermore, the total protein content of the scaffolds dropped after one week for all cases. DBM and PCL nanofibers were seeded with 100,000 cells/cm^2. The cells competed with each other and this led the protein content to decrease over time.

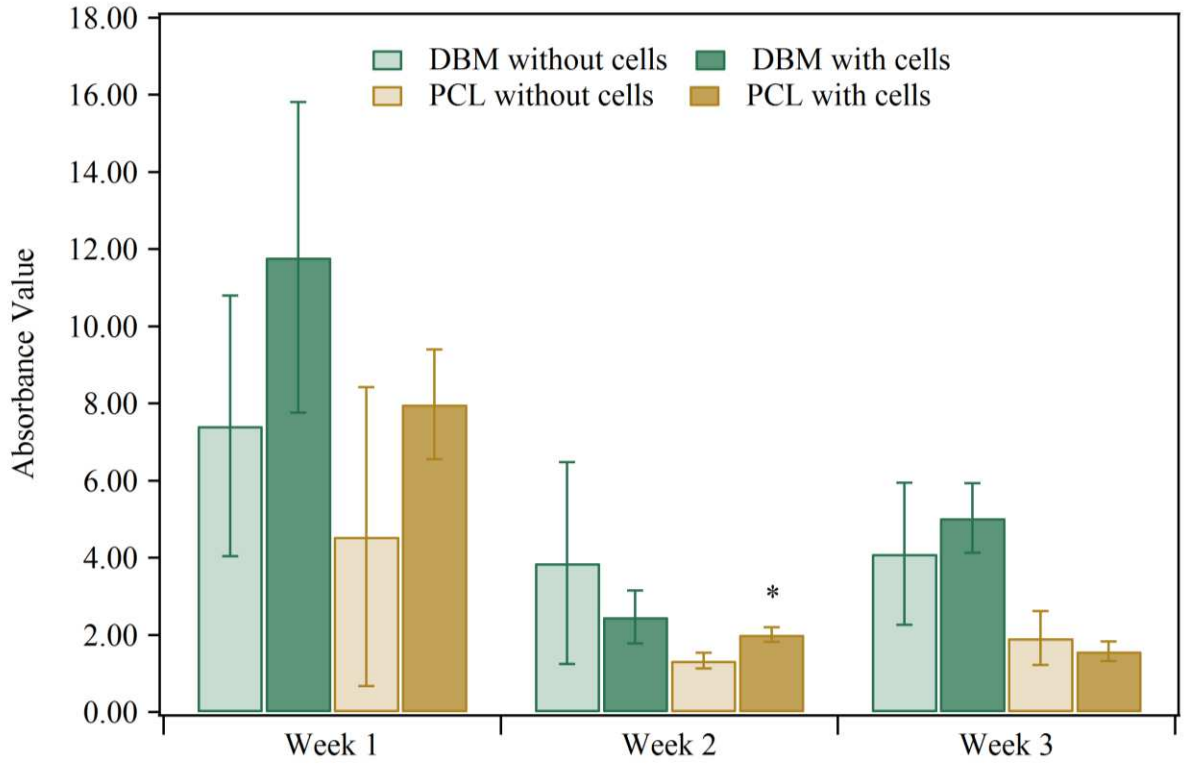

Figure 3.3.1: Total protein content on various surfaces for three weeks measured using BCA assay. Only at week 2, PCL nanofibers seeded with cells had significantly more proteins than PCL nanofibers without cells (* → $p < 0.05$).

This assay results at one and two weeks of culture showed no statistical significance when the difference between DBM nanofiber scaffolds with cells and without cells were compared to the difference between PCL nanofiber scaffolds with cells and without cells, as shown in Figure 3.3.2.

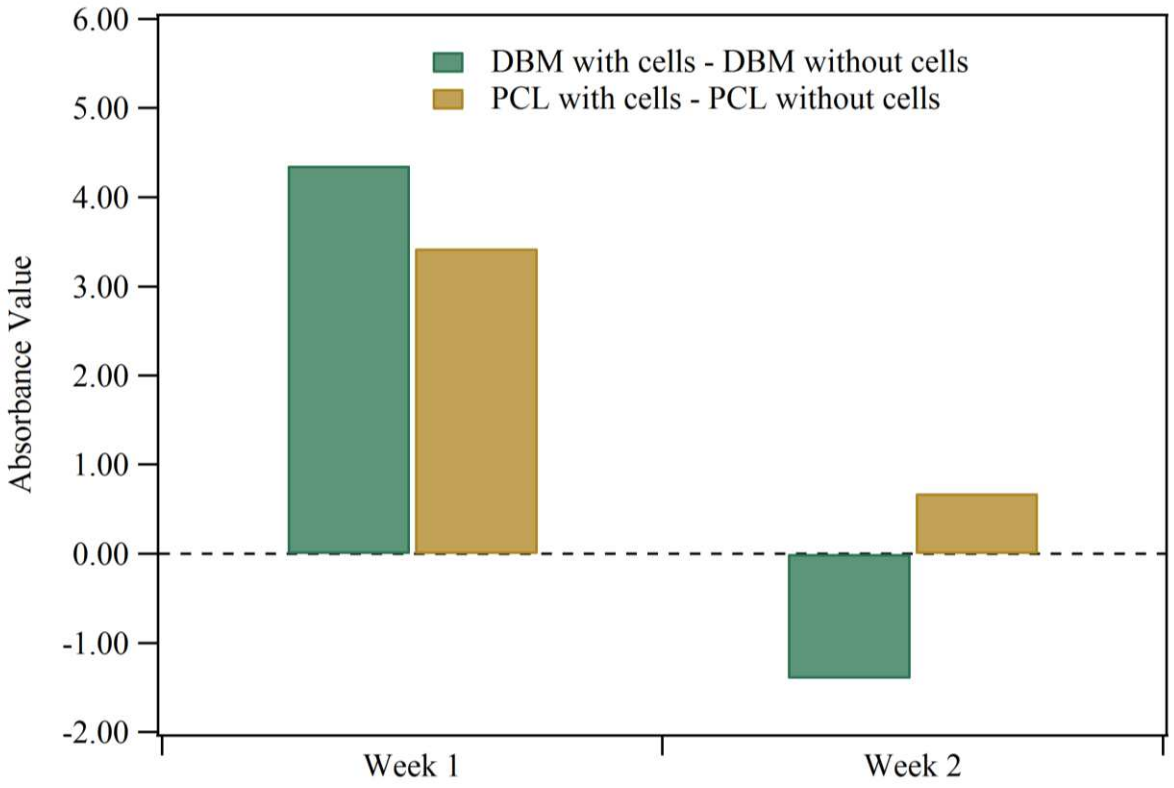

Figure 3.3.2: BCA assay results. The difference between DBM nanofiber scaffolds with cells and without cells compared to the difference between PCL nanofiber scaffolds with cells and without cells.

3.3.2 Alkaline phosphatase (ALP) Activity

Alkaline phosphatase (ALP), a membrane-bound glycoprotein, is one of the key components in the process of osteogenesis. ALP activity is a very early marker of differentiation of mesenchymal stem cells to osteoblasts [11, 12].

There are different hypotheses on how alkaline phosphatase could stimulate biomineralization. In 1926, Robison proposed that alkaline phosphatase in bone hydrolyzes organic phosphate esters, thus generating orthophosphate so that calcium phosphate mineral can grow [13]. Blitterswijk also defined the activity of alkaline phosphatase as during ossification

(osteogenesis) process, alkaline phosphatase enzyme hydrolyzes organic phosphate and calcium-containing substrate in order to use them to obtain supersaturated concentrations for the aim of enhancing mineral deposition [14].

Yohay mentions that cessation of proliferation, which also indicates the start of differentiation, expresses high levels of alkaline phosphatase, whereas active proliferation is associated with low levels of alkaline phosphatase early in culture [15]. Bellow's study also supports this idea, proving that organic phosphate and alkaline phosphatase play a significant part in the initiation of mineralization, but are not required for the continuation of mineralization of bone nodules [16].

Another hypothesis is that alkaline phosphatase promotes skeletal mineralization and the main function of alkaline phosphatase is to hydrolyze inorganic pyrophosphate at the site of mineral crystal proliferation [17]. Wutti states that ALP is believed to provide inorganic phosphate for mineralization, although ALP's exact function is not known [6]. In 2007, Popat demonstrated the ability of titania nanotubular surfaces to promote osteoblast differentiation and bone matrix production, and also observed elevated levels of ALP during the initial phase of bone matrix deposition in vitro [18].

ALP activity, as assessed by colorimetric ALP assay, was measured after one, two and three weeks of culture. The colorimetric ALP assay results at one week of culture showed that there was statistical significance when DBM nanofiber scaffolds with cells and DBM nanofiber scaffolds without cells were compared. But after two weeks of culture there was no significant difference between these two. The results of the assay were very similar for PCL nanofiber scaffolds with cells and without cells. There was a significant difference between these two conditions after one week of culture, but after two weeks of culture there was no significant

difference, as shown in Figure 3.3.3. The ALP activity dropped after week one, because ALP activity is an early differentiation marker. When differentiation starts, there is a lot of ALP, but then the amount of ALP goes down since cells start functioning.

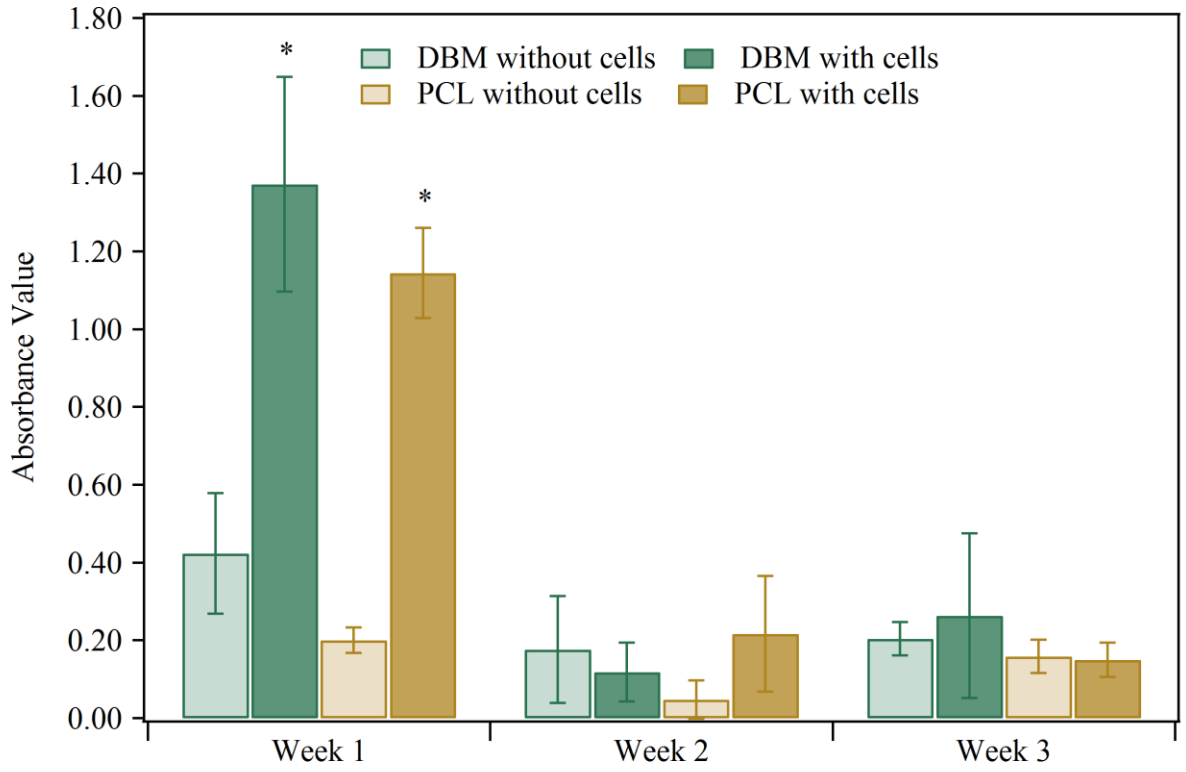

Figure 3.3.3: ALP activity measured on DBM nanofibers with no cells, DBM nanofibers seeded with cells, PCL nanofibers with no cells, and PCL nanofibers seeded with cells, after one, two and three weeks of differentiation. ALP activity after week 1 on DBM nanofibers seeded with cells and PCL nanofibers seeded with cells are significantly higher than on DBM nanofibers with no cells and PCL nanofibers with no cells, respectively (* → $p < 0.05$).

The difference between DBM nanofiber scaffolds with cells and without cells versus the difference between PCL nanofiber scaffolds with cells and without cells in ALP activity was also compared for week 1 and 2. The results of the assay showed that there was no significant difference between the two conditions (Figure 3.3.4). A prior study that was conducted in our lab demonstrated that PCL scaffolds have the ability to enhance osteoblastic behavior of marrow stromal cells in osteogenic media. Since there is no significant difference between the behavior of

DBM and PCL nanofiber scaffolds, it can be concluded that DBM nanofiber scaffolds can also enhance osteoblastic differentiation of cells in osteogenic media.

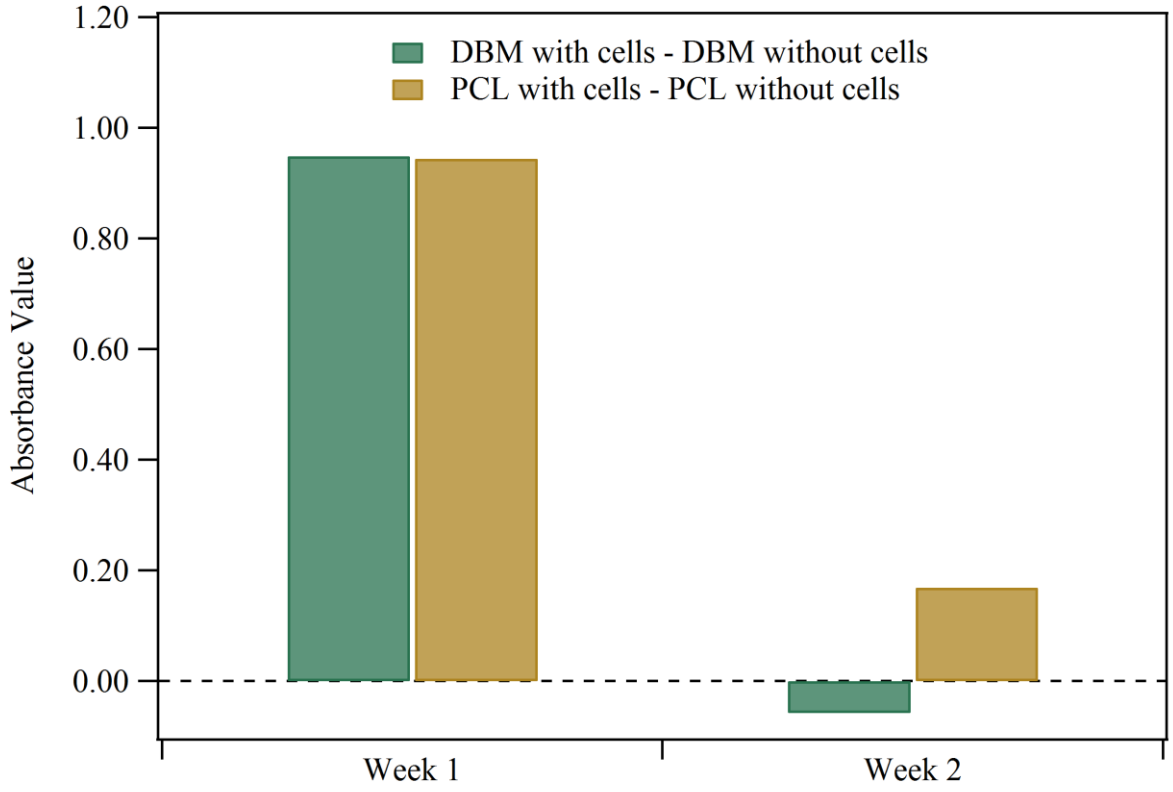

Figure 3.3.4: ALP assay results. The difference between DBM nanofiber scaffolds with cells and without cells compared to the difference between PCL nanofiber scaffolds with cells and without cells.

3.3.3 Mineralization

Calcium deposition is initiated during matrix maturation and slowly increased. A bony structure is formed from the mineralized matrix. This process occurs at the end of osteoblast differentiation [19, 20]. In studies that use osteogenic cultures in vitro, mineralization is considered a terminal stage for cell differentiation. Alizarin red staining is a common technique to detect calcium [21]. SEM and alizarin calcium staining were used to examine mineralization patterns

qualitatively on demineralized bone matrix (DBM) and poly (ε-caprolactone) (PCL) nanofiber scaffolds. Alizarin stains calcium and calcium compounds red. Figure 3.3.5 shows stained scaffolds of DBM and PCL with cells and without cells.

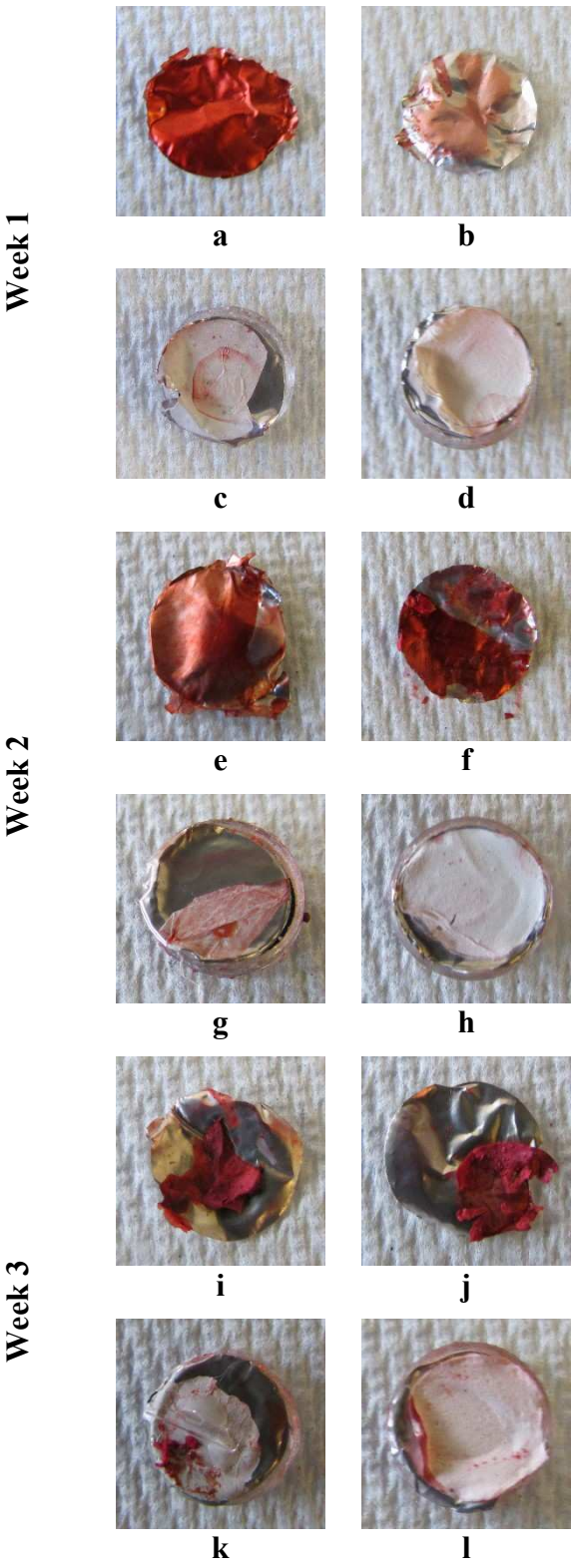

Figure 3.3.5: Calcium staining of cells on DBM and PCL nanofiber scaffolds. (a), (e), (i): DBM with cells, (b), (f), (j): DBM no cells, (c), (g), (k): PCL with cells, (d), (h), (l): PCL no cells.

According to the figure, DBM scaffolds deposited more calcium mineral than PCL scaffolds during three-week experiments. At one week of culture, DBM nanofibers that were seeded with cells deposited more calcium minerals than DBM nanofibers with no cells. After two and three weeks of culture, mineral deposition was still higher on the scaffolds with cells, but the difference was not as pronounced. Mineralization on PCL scaffolds seeded with cells were more than PCL scaffolds without cells at each time point. After staining with alizarin, PCL nanofiber scaffolds looked very similar to the PCL scaffolds that had been tested at the same time points with the same assay in the study of Ruckh et al. [8].

After one, two and three weeks of culture in osteogenic media, mineralization patterns were examined qualitatively by SEM, as shown in Figure 3.3.6. It appears that DBM nanofibers without cells swell during three-week experiments. Furthermore, cells on DBM and PCL nanofiber scaffolds organized the nanofibers during three weeks. The nanofibers seeded with cells did not swell as DBM nanofibers without cells did.

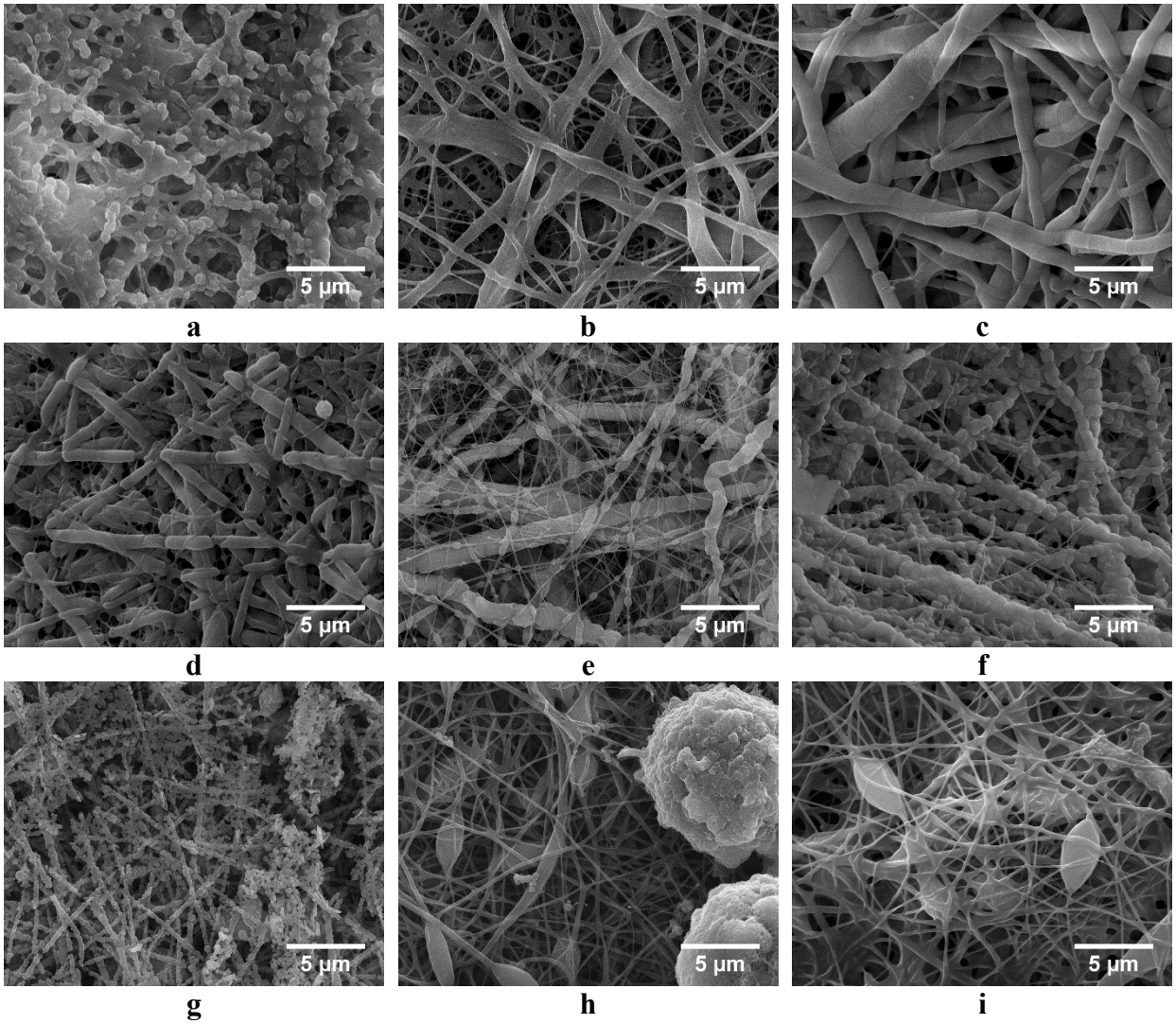

Figure 3.3.6: SEM images of DBM nanofiber scaffolds with no cells (a, b, c), DBM nanofiber scaffolds seeded with cells (d, e, f), and PCL nanofiber scaffolds seeded with cells (g, h, i), after one, two, and three weeks in osteogenic media, respectively.

Mineralization was quantified by energy-dispersive X-ray spectroscope (EDS). After one week of culture, the EDS scans showed higher calcium and phosphorous peaks for mineral deposit on DBM nanofiber scaffolds compared to PCL controls, as demonstrated in Figure 3.3.7 and Figure 3.3.8. There were almost no calcium and phosphorous peaks for mineral deposit on PCL nanofiber scaffolds both with cells and without cells (Figure 3.3.8).

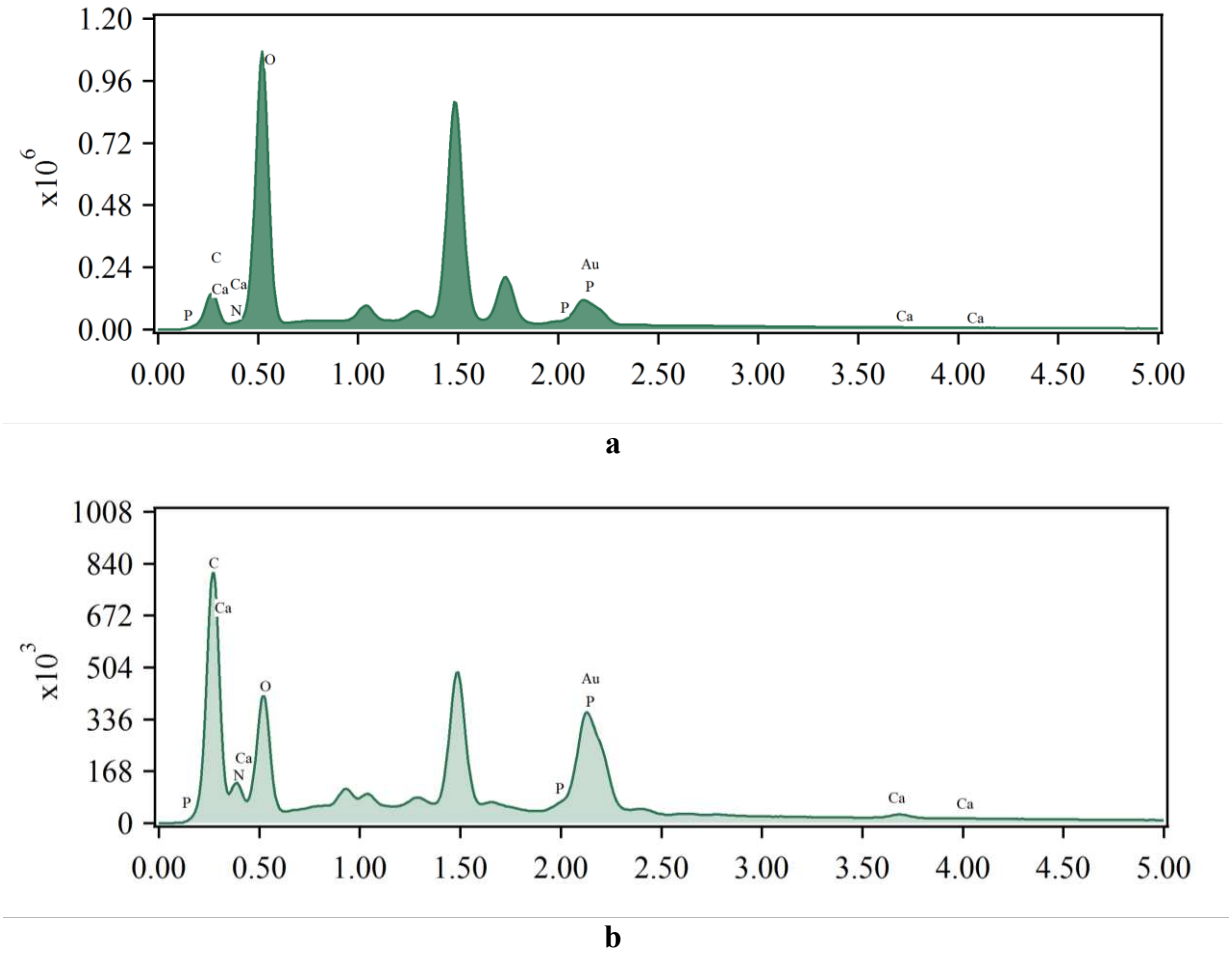

Figure 3.3.7: EDS scans of mineralization for (a) DBM with cells (week 1) and (b) DBM no cells (week 1).

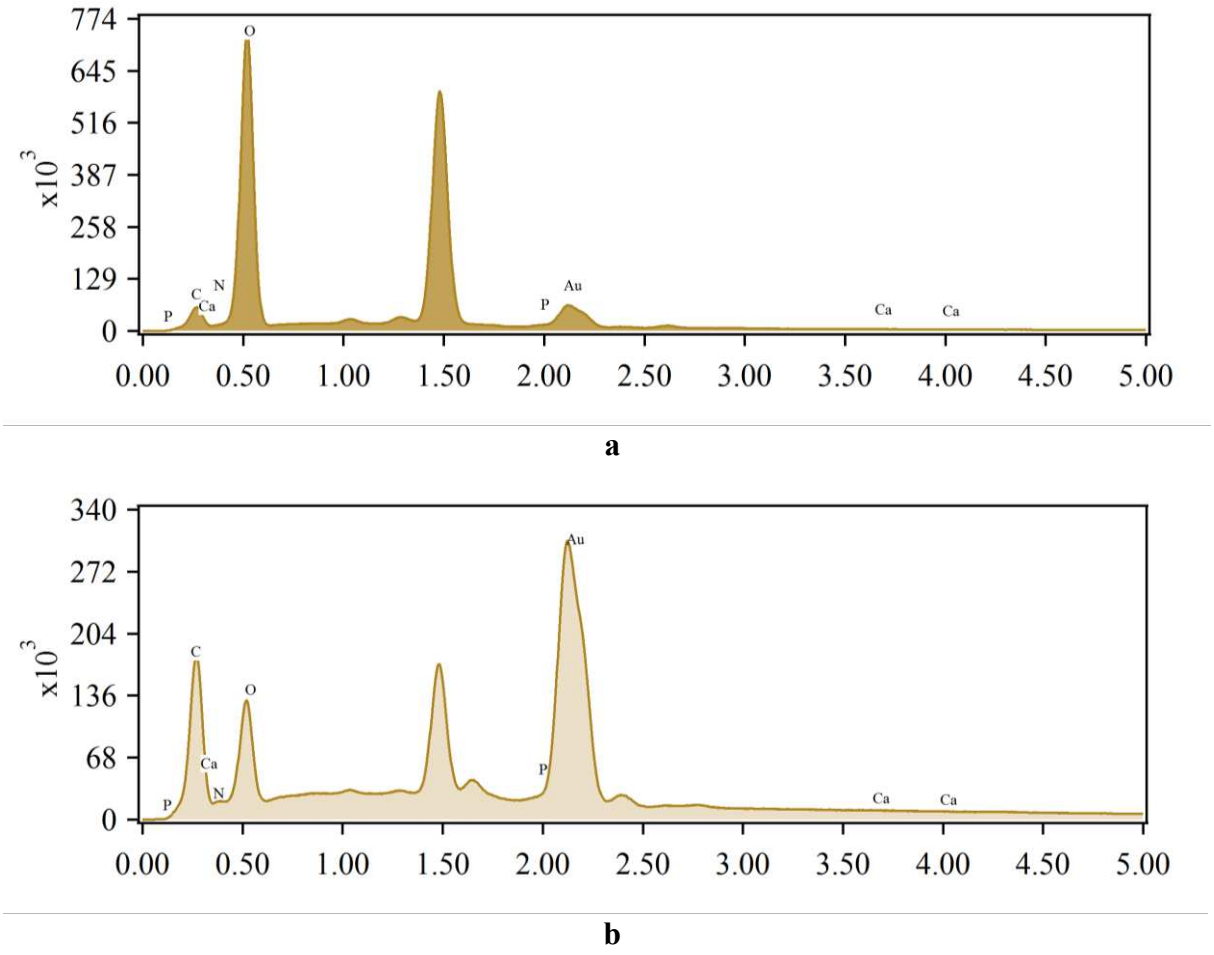

Figure 3.3.8: EDS scans of mineralization for (a) PCL with cells (week 1) and (b) PCL no cells (week 1).

After two weeks of culture in osteogenic media, DBM nanofiber scaffolds that were seeded with cells revealed more mineralization, whereas mineralization on DBM nanofiber scaffolds that were not seeded with cells did not increase at all (Figure 3.3.9). According to the EDS scans, there were no calcium and phosphorous peaks for mineral deposit on PCL nanofiber scaffolds that were seeded with cells. But there were a little calcium and phosphorous peaks for mineral deposit for PCL nanofiber scaffolds that were not seeded with cells (Figure 3.3.10).

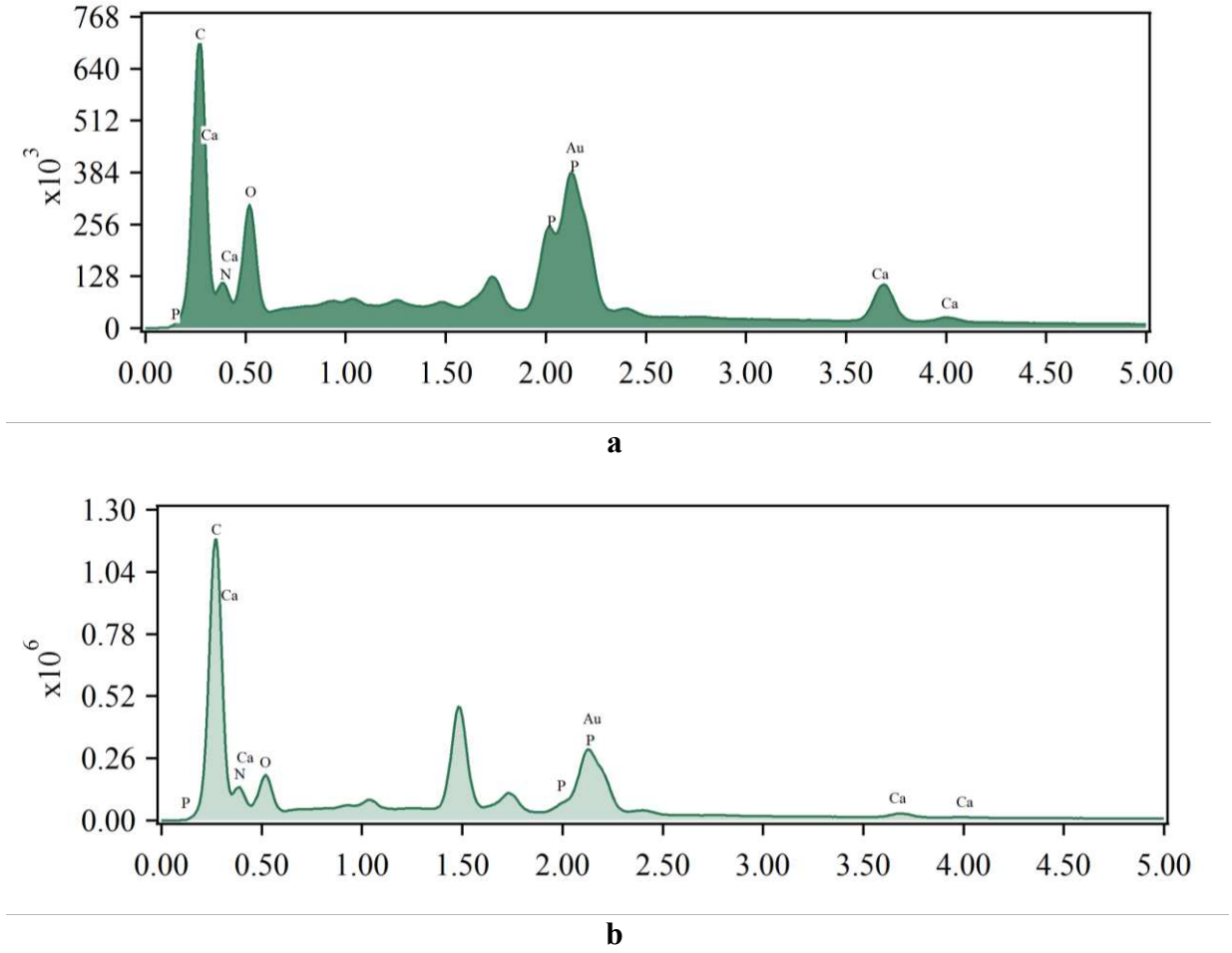

Figure 3.3.9: EDS scans of mineralization for (a) DBM with cells (week 2) and (b) DBM no cells (week 2).

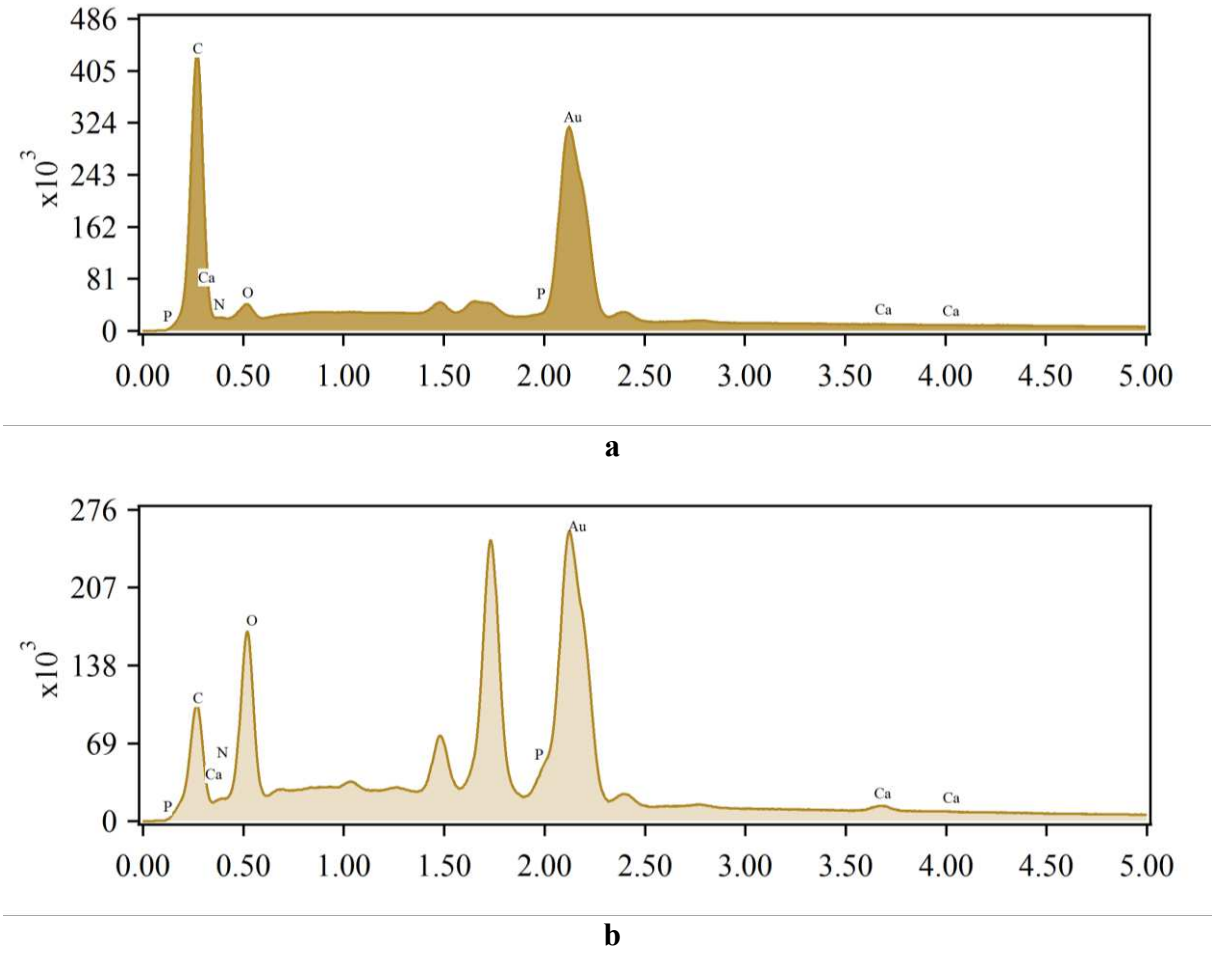

Figure 3.3.10: EDS scans of mineralization for (a) PCL with cells (week 2) and (b) PCL no cells (week 2).

After three weeks of culture in osteogenic media, the EDS scans also showed much higher calcium and phosphorous peaks for mineral deposit on DBM nanofiber scaffolds that were both with cells and without cells. But the nanofibers that were exposed to cells exhibited more surface mineralization when compared to the control surfaces, according to the EDS results (Figure 3.3.11). PCL nanofiber scaffolds that were not seeded with cells showed a little calcium and phosphorous peaks for mineral deposits, while there were no peaks for PCL nanofiber scaffolds that were seeded with cells (Figure 3.3.12).

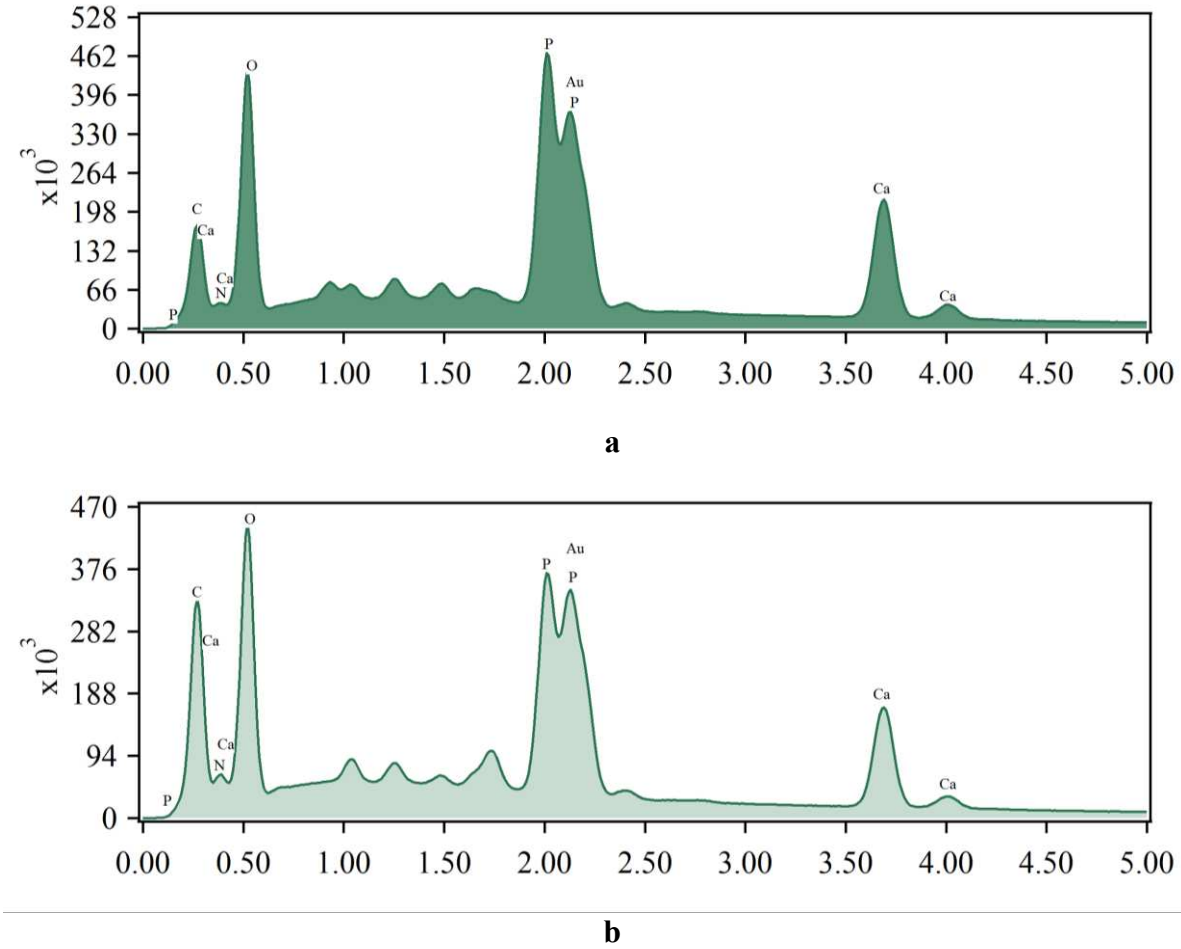

Figure 3.3.11: EDS scans of mineralization for (a) DBM with cells (week 3) and (b) DBM no cells (week 3).

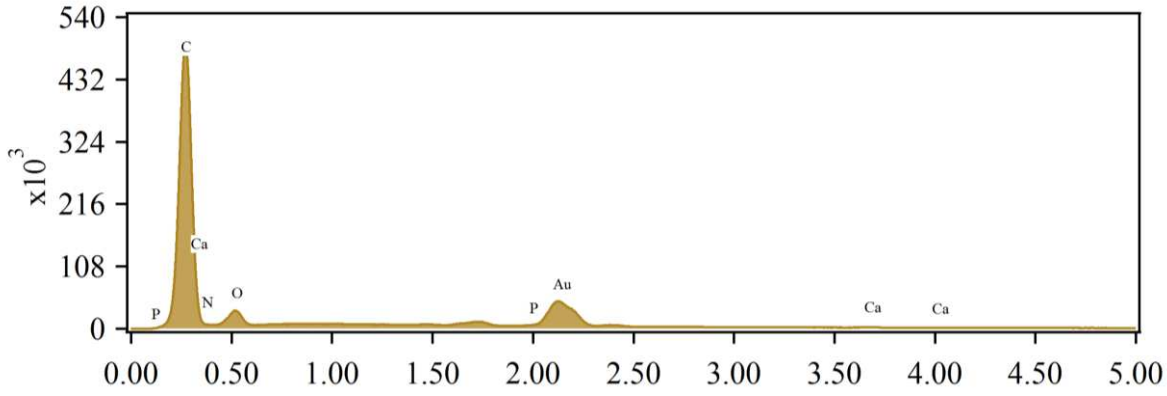

a. PCL with cells Week 3

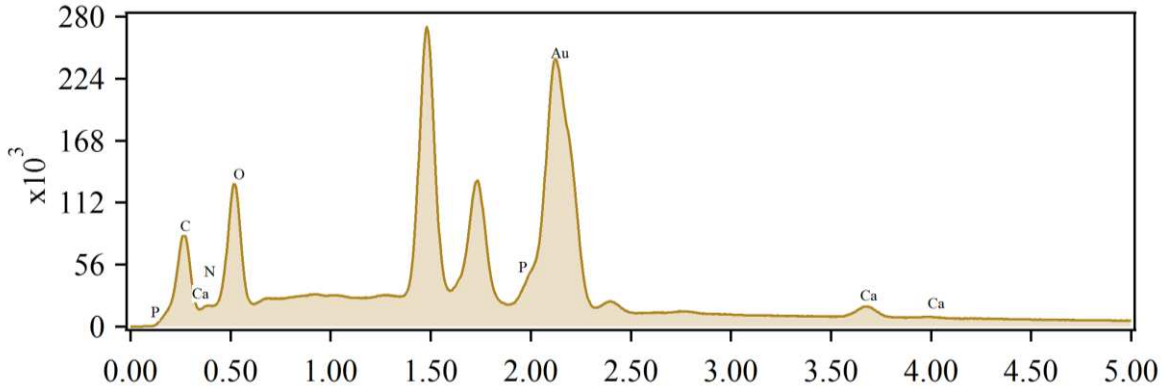

b. PCL no cells Week 3

Figure 3.3.12: EDS scans of mineralization for (a) PCL with cells (week 3) and (b) PCL no cells (week 3).

In summary, after three weeks of culture, EDS revealed high calcium and phosphorus deposition on DBM scaffolds compared to PCL controls, as further illustrated in Figure 3.3.13. The DBM scaffolds exhibited increased mineralization over three weeks, both with and without cells.

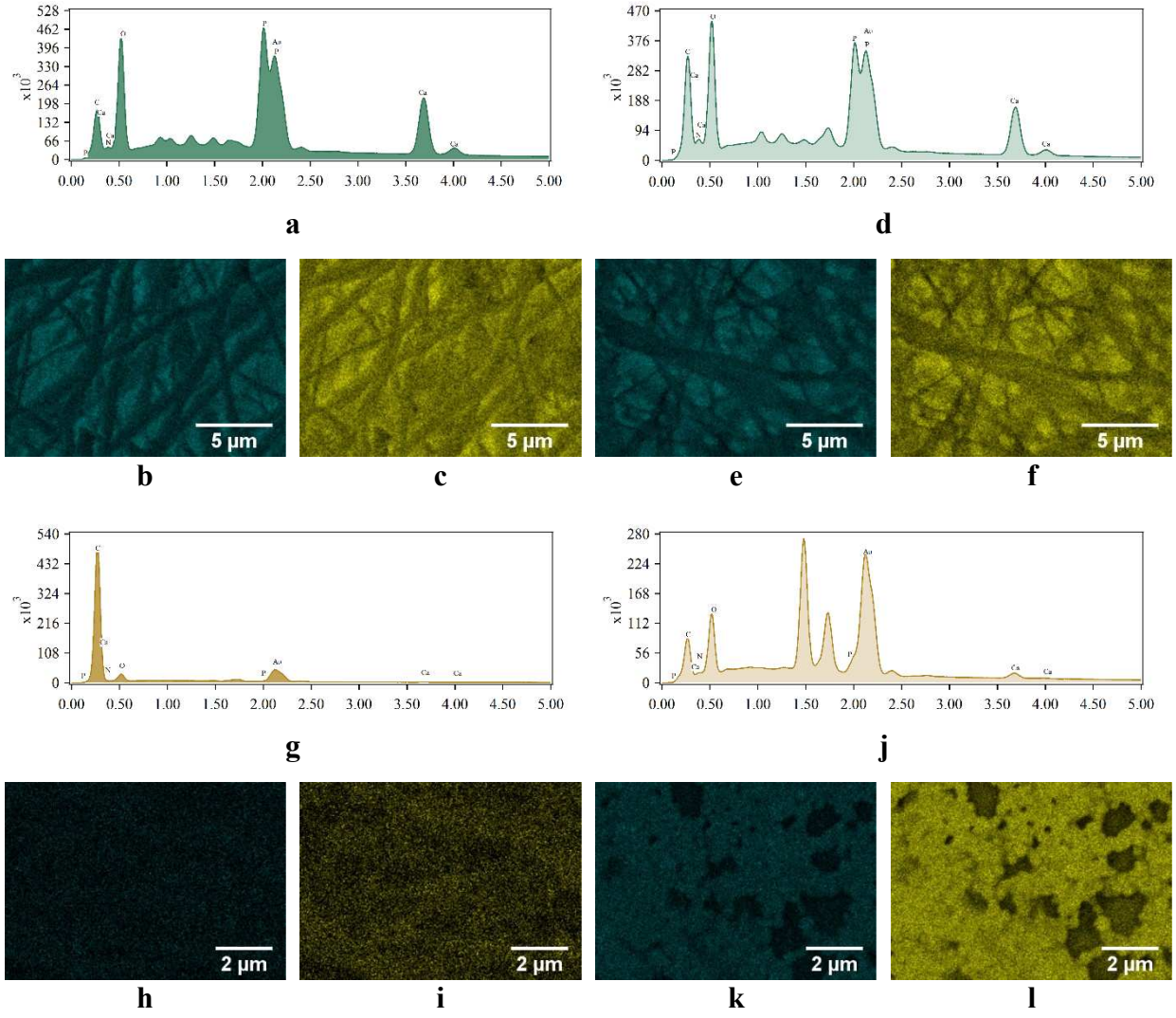

Figure 3.3.13: EDS scan of mineral deposition showing CA, P, O, C, N and Au peaks for (a) DBM with cells, (d) DBM no cells, (g) PCL with cells, and (j) PCL no cells. Elemental map of mineral deposition showing Ca and P, respectively for DBM with cells (b, c), DBM no cells (e, f), PCL with cells (h, i), and PCL no cells (k, l). After three weeks in osteogenic media.

Ca and P are parts of bone matrix and recognized as markers of osteoblast phenotype expression. The EDS scans showed high calcium and phosphorous peaks for mineral deposit for DBM nanofiber scaffolds seeded with cells and also DBM nanofiber scaffolds without cells. It appears that adipose-derived mesenchymal stem cells (AD-MSCs) support Ca and P mineralization on DBM nanofiber scaffolds. Based on these findings, it can be claimed that

osteogenic differentiation media exposure for three weeks results in Ca and P accumulation, because osteogenic differentiation media includes both of these minerals. P can be provided from β-glycerol phosphate L-ascorbic acid 2-phosphate, and Ca can be provided from DMEM and FBS. Proteins in the DBM are capable of mineralizing even in the absence of cells. This was not observed on the PCL nanofiber scaffolds.

The DBM scaffolds exhibited increased mineralization over three weeks, both with and without cells. For both DBM with cells and without cells, C and O elements were deposited on fibers, whereas P and Ca minerals were deposited on places in between the fibers (Figure 3.3.14, Figure 3.3.15).

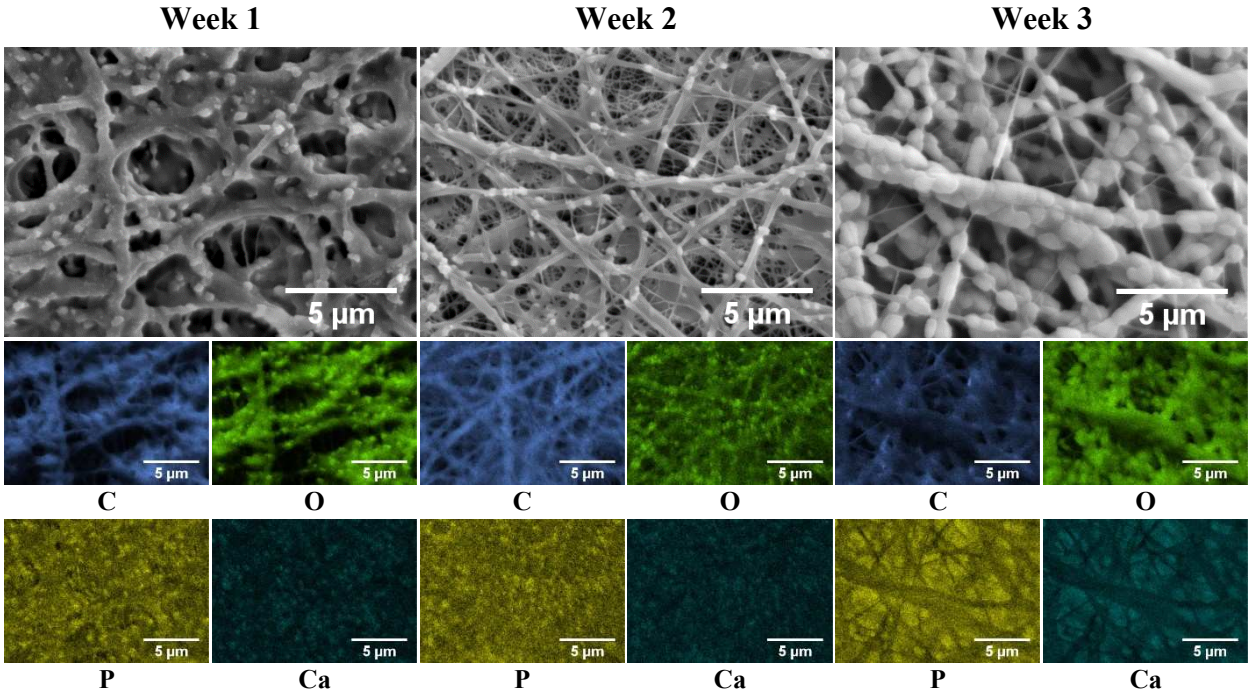

Figure 3.3.14: SEM images and elemental maps of DBM nanofibers without cells during three weeks of culture in osteogenic differentiation media.

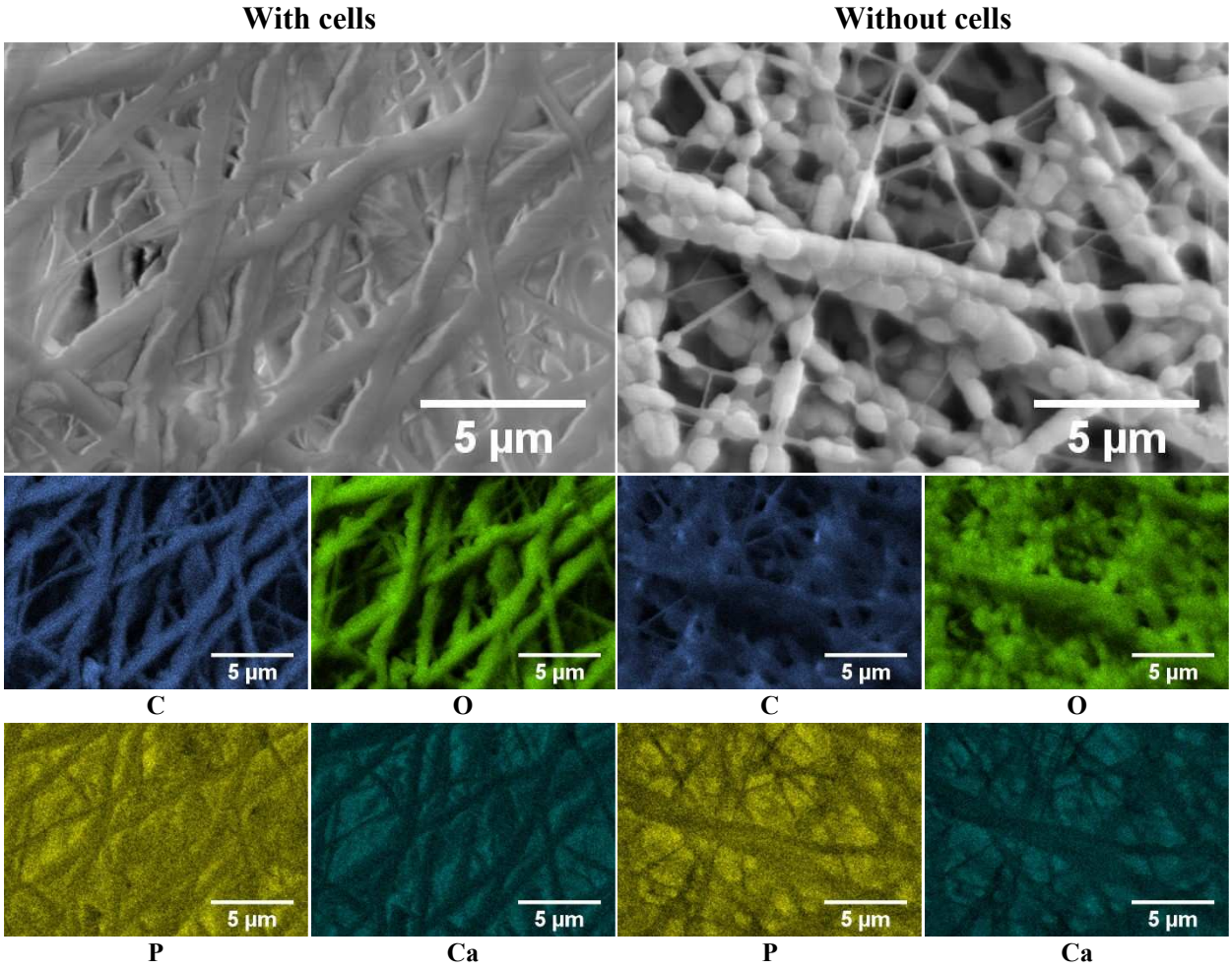

Figure 3.3.15: SEM images and elemental maps of DBM nanofibers with cells and without cells after three weeks of culture in osteogenic differentiation media.

3.3.4 Thermal Analysis of Demineralized Bone Matrix (DBM)

Demineralized bone matrix (DBM) is an acellular composite material that is obtained from donor allograft. Composition and also osteoinductivity of individual DBM lots that are processed by the same tissue bank may not be the same since these lots were obtained from different donor bones [4]. In this study, electrospinning was used to obtain DBM nanofibers. In order to obtain electrospun DBM nanofibers, first, 1.1 g of DBM lot 104063-605 in a 10 mL solvent blend of of hexafluoro-2-propanol / trifluoroacetic acid (70:30) was prepared at 40 ºC, but it could not be

dissolved. Then, DBM lot 115561-601 was used and uniform nanofibers were achieved by electrospinning. These results led to a need for further research about DBM's properties. Thermal properties of DBM were investigated through TGA (Thermogravimetric Analysis) equipment.

TGA is a thermal analysis method that measures weight changes of a sample as a function of temperature. Six DBM lots were characterized with this method with regard to their composition. Their decomposition temperatures were not significantly different as can be seen from Table 3.3.1 below.

Table 3.3.1: Dissolution of DBMs in 70:30 HFIP:TFA (11% DBM at 40 ºC for 22h).

DBM Lots		**Decomposition temperatures °C**
115561-601	Dissolved	236.82
132270-6505	Dissolved	246.24
115679-601	Not dissolved	249.04
104063-605	Not dissolved	248.50
116719-603	Dissolved	-
9/21/12	Not dissolved	243.89

Thermogravimetric analysis of the DBM lot 115679-601 is presented in Figure 3.3.16, which represents the general behavior of all lots between 500 ºC and 600 ºC, except for DBM lot 115561-601.

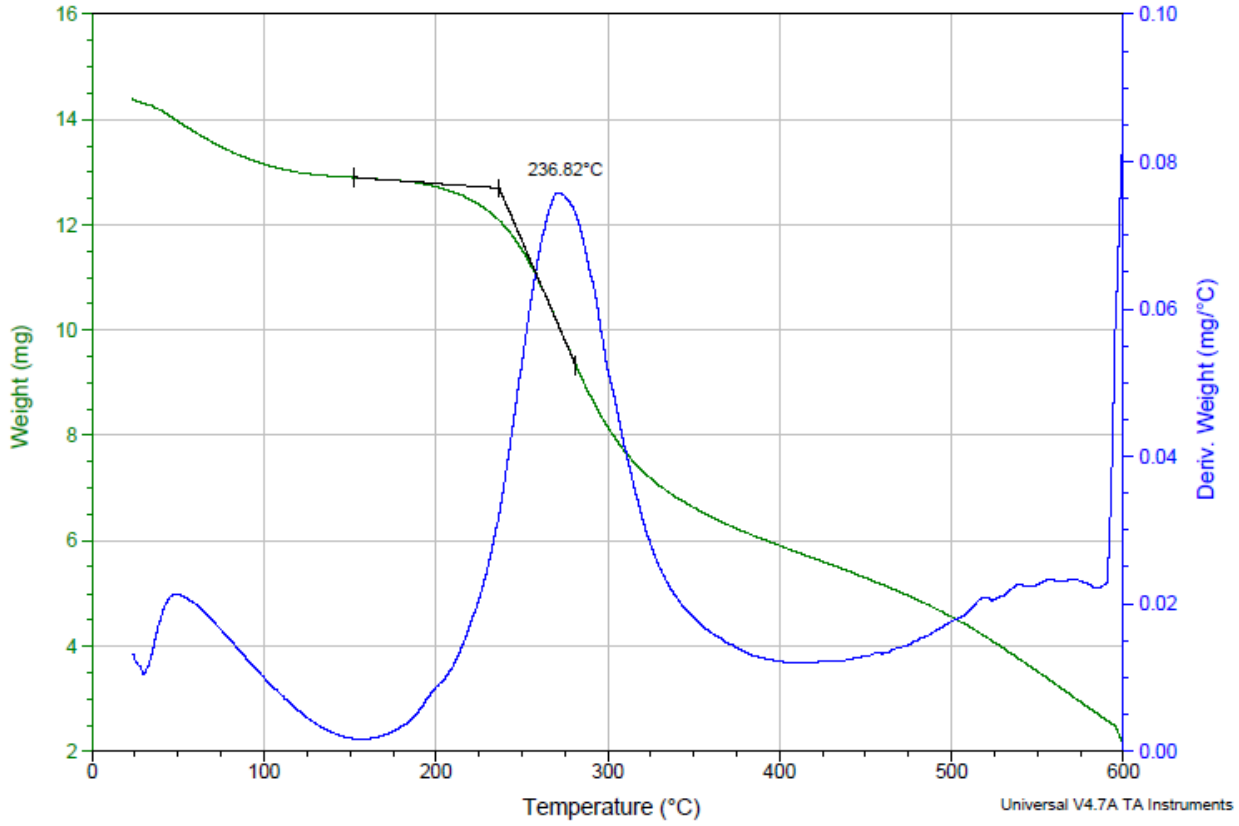

Figure 3.3.16: Thermogravimetric analysis (TGA) of the DBM powder 115561-601 performed in a N_2 atmosphere.

Thermogravimetric analysis of the DBM lot 115561-601, shown in Figure 3.3.17, displayed a different behavior. That is, there was an endotherm in this temperature range. It absorbed energy and lost mass, whereas the other lots did not show such behavior.

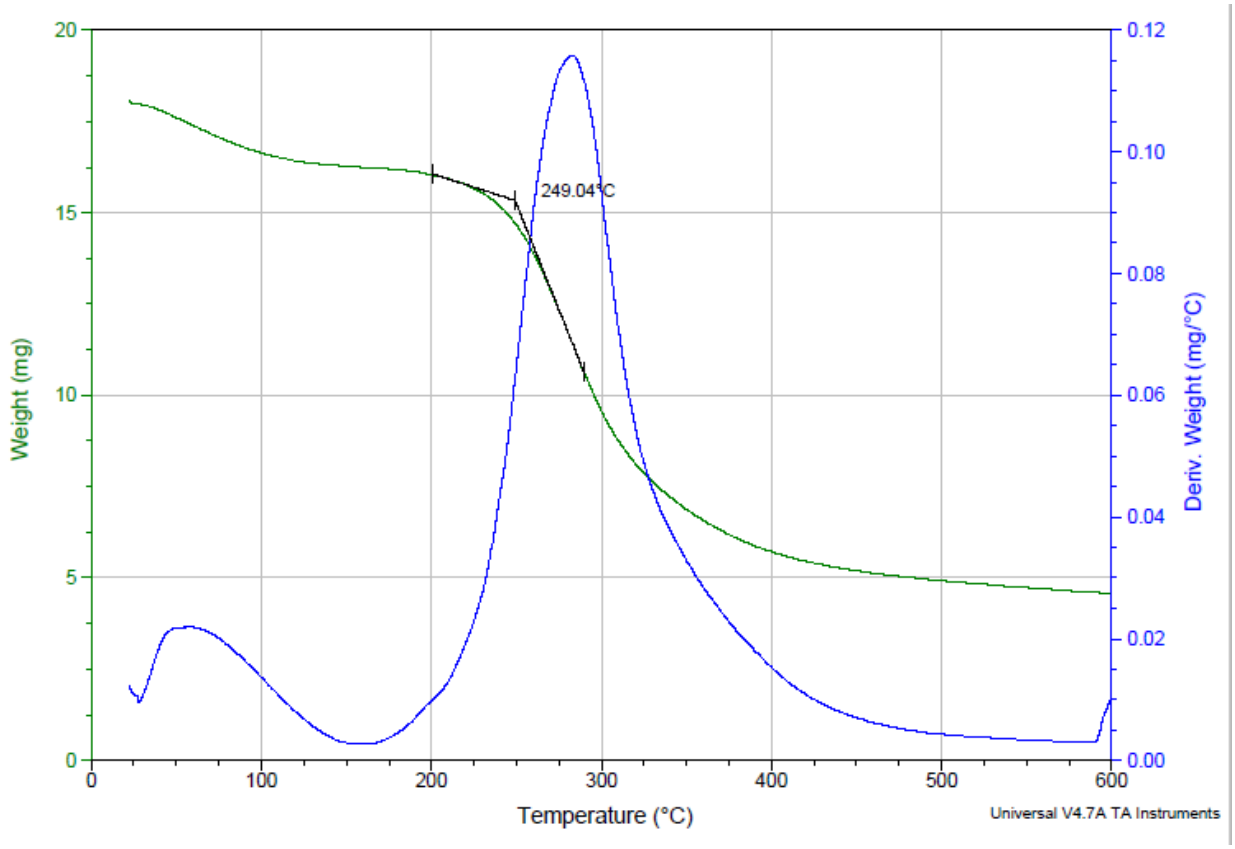

Figure 3.3.17: Thermogravimetric analysis (TGA) of the DBM powder 115679-601 performed in a N_2 atmosphere.

The morphology of the DBM nanofibers from different DBM lots were characterized by SEM imaging. The fibers' properties seemed different than each other. Electrospun nanofibers from DBM lot 115561-601 was uniform, but the other two DBMs formed less uniform nanofibers, as can be seen in Figure 3.3.18.

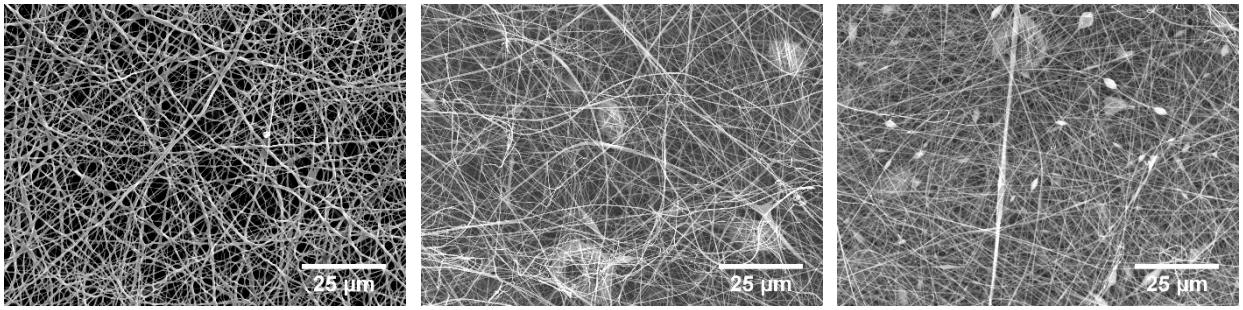

Figure 3.3.18: SEM Images of DBM lots: (a) 115561-601, (b) 116719-603, (c) 132270-6505.

REFERENCES

1. Heydarkhan-Hagvall, S., Schenke-Layland, K., Dhanasopon, A. P., Rofail, F., Smith, H., Wu, B. M., . . . MacLellan, W. R. (2008). Three-dimensional electrospun ECM-based hybrid scaffolds for cardiovascular tissue engineering. *Biomaterials, 29*(19), 2907-2914.

2. Murugan, R., & Ramakrishna, S. (2006). Nano-featured scaffolds for tissue engineering: a review of spinning methodologies. *Tissue Engineering, 12*(3), 435-447.

3. Leszczak, V., Place, L. W., Franz, N., Popat, K. C., & Kipper, M. J. (2014). Nanostructured biomaterials from electrospun demineralized bone matrix: a survey of processing and crosslinking strategies. *ACS Appl Mater Interfaces, 6*(12), 9328-9337.

4. Gruskin, E., Doll, B. A., Futrell, F. W., Schmitz, J. P., & Hollinger, J. O. (2012). Demineralized bone matrix in bone repair: History and use. *Advanced Drug Delivery Reviews, 64*(12), 1063-1077.

5. Yoshimoto, H., Shin, Y. M., Terai, H., & Vacanti, J. P. (2003). A biodegradable nanofiber scaffold by electrospinning and its potential for bone tissue engineering. *Biomaterials, 24*(12), 2077-2082.

6. Wutticharoenmongkol, P., Pavasant, P., & Supaphol, P. (2007). Osteoblastic phenotype expression of MC3T3-E1 cultured on electrospun polycaprolactone fiber mats filled with hydroxyapatite nanoparticles. *Biomacromolecules, 8*(8), 2602-2610.

7. Nam, J., Huang, Y., Agarwal, S., & Lannutti, J. (2007). Improved cellular infiltration in electrospun fiber via engineered porosity. *Tissue Engineering, 13*(9), 2249-2257.

8. Ruckh, T. T., Kumar, K., Kipper, M. J., & Popat, K. C. (2010). Osteogenic differentiation of bone marrow stromal cells on poly(ε-caprolactone) nanofiber scaffolds. *Acta Biomaterialia, 6*(8), 2949-2959.

9. Khanna-Jain, R., Mannerström, B., Vuorinen, A., Sándor, G. K., Suuronen, R., & Miettinen, S. (2012). Osteogenic differentiation of human dental pulp stem cells on β-tricalcium phosphate/poly (l-lactic acid/caprolactone) three-dimensional scaffolds. *Journal of Tissue Engineering, 3*(1), 2041731412467998.

10. Popat, K. C., Leary Swan, E. E., Mukhatyar, V., Chatvanichkul, K.-I., Mor, G. K., Grimes, C. A., & Desai, T. A. (2005). Influence of nanoporous alumina membranes on long-term osteoblast response. *Biomaterials, 26*(22), 4516-4522.

11. Owen, T. A., Aronow, M., Shalhoub, V., Barone, L. M., Wilming, L., Tassinari, M. S., . . . Stein, G. S. (1990). Progressive development of the rat osteoblast phenotype in vitro: reciprocal relationships in expression of genes associated with osteoblast proliferation and differentiation during formation of the bone extracellular matrix. *J Cell Physiol, 143*(3), 420-430.

12. Liu, F., Malaval, L., & Aubin, J. E. (2003). Global amplification polymerase chain reaction reveals novel transitional stages during osteoprogenitor differentiation. *J Cell Sci, 116*(Pt 9), 1787-1796.

13. Robison, R. (1926). The Possible Significance of Hexosephosphoric Esters in Ossification: A Reply to Shipley, Kramer and Howland. *Biochem J, 20*(2), 388-391.

14. Blitterswijk, C. V. (2008). *Tissue engineering*. Burlington, MA: Elsevier.

15. Yohay, D. A., Zhang, J., Thrailkill, K. M., Arthur, J. M., & Quarles, L. D. (1994). Role of serum in the developmental expression of alkaline phosphatase in MC3T3-E1 osteoblasts. *J Cell Physiol, 158*(3), 467-475.

16. Bellows, C. G., Aubin, J. E., & Heersche, J. N. (1991). Initiation and progression of mineralization of bone nodules formed in vitro: the role of alkaline phosphatase and organic phosphate. *Bone Miner, 14*(1), 27-40.

17. Anderson, H. C., Sipe, J. B., Hessle, L., Dhanyamraju, R., Atti, E., Camacho, N. P., & Millan, J. L. (2004). Impaired calcification around matrix vesicles of growth plate and bone in alkaline phosphatase-deficient mice. *Am J Pathol, 164*(3), 841-847.

18. Popat, K. C., Eltgroth, M., LaTempa, T. J., Grimes, C. A., & Desai, T. A. (2007). Decreased Staphylococcus epidermis adhesion and increased osteoblast functionality on antibiotic-loaded titania nanotubes. *Biomaterials, 28*(32), 4880-4888.

19. Lian, J. B., & Stein, G. S. (1992). Concepts of osteoblast growth and differentiation: basis for modulation of bone cell development and tissue formation. *Crit Rev Oral Biol Med, 3*(3), 269-305.

20. Shin, H., Zygourakis, K., Farach-Carson, M. C., Yaszemski, M. J., & Mikos, A. G. (2004). Modulation of differentiation and mineralization of marrow stromal cells cultured on biomimetic hydrogels modified with Arg-Gly-Asp containing peptides. *J Biomed Mater Res A, 69*(3), 535-543.

21. Hoemann, C. D., El-Gabalawy, H., & McKee, M. D. (2009). In vitro osteogenesis assays: Influence of the primary cell source on alkaline phosphatase activity and mineralization. *Pathologie Biologie, 57*(4), 318-323.

22. Wanet, A., Arnould, T., Najimi, M., & Renard, P. (2015). Connecting Mitochondria, Metabolism, and Stem Cell Fate. *Stem Cells and Development, 24*(17), 1957–1971.

CHAPTER 4: CONCLUSION AND FUTURE WORK

4.1 Summary and Overall Conclusion

Bone tissue engineering is an ideal way to heal severe bone injuries and defects by using the body's natural biological response in conjunction with many fields like biology, engineering, material science, and medicine [1, 2]. Cells, scaffold and cell-matrix (scaffold) interactions are the three important factors that contribute to the success of tissue engineering applications [1, 3, 4]. This work demonstrated the ability to produce demineralized bone matrix (DBM) nanofiber scaffolds. First, nanofiber DBM scaffolds were fabricated by electrospinning method. In order to stabilize the nanostructure, the nanofibers were crosslinked by glutaraldehyde vapor. The nanofibers were imaged by using scanning electron microscopy (SEM). Some fiber structure and porosity were successfully preserved. The same structure was also achieved after exposure to DI water. DBM nanofiber scaffolds' ability to support cell adhesion and cell viability of adipose-derived mesenchymal stem cells (AD-MSCs) for short-term in culture media was investigated. Poly (ε-caprolactone) (PCL) scaffolds were used as control surfaces. Live cell stain calcein-AM was used to assess cell adhesion, and CellTiter 96® Non-Radioactive Cell Proliferation assays were used to assess cell proliferation. DBM scaffolds supported greater cell adhesion compared to PCL nanofiber scaffolds. For cell viability, the two types of scaffolds behaved similarly. The results led us to further research on DBM scaffolds. The ability to support osteoblastic differentiation of AD-MSCs for long-term (three weeks) in osteogenic differentiation media was also investigated. This time, both PCL scaffolds and DBM scaffolds seeded with no cells were used as control surfaces. The total protein content of viable AD-MSCs on the scaffolds was assessed by Pierce™ BCA Protein assay kit. Cells behaved similarly on both DBM and PCL nanofiber scaffolds and the total

protein content of scaffolds dropped after one week for all cases. In order to determine alkaline phosphatase (ALP) activity, a commercially available alkaline phosphatase colorimetric assay kit was used. Nanofiber scaffolds displayed increased levels of ALP activity for the first week for all cases. ALP activity dropped after one week. SEM and alizarin calcium staining techniques were used to examine mineralization patterns qualitatively on DBM and PCL nanofiber scaffolds. DBM scaffolds deposited more calcium mineral than PCL scaffolds during three-week experiments. Mineralization was quantified by energy-dispersive X-ray spectroscope (EDS). After three weeks of culture, EDS revealed high calcium and phosphorus deposition on DBM scaffolds compared to PCL controls. The DBM scaffolds exhibited increased mineralization over three weeks, both with and without cells. These results demonstrate that the adhesion, proliferation, and osteogenic differentiation of AD-MSCs were influenced by DBM scaffolds.

4.2 Recommendations for Future Work

In this study, demineralized bone matrix (DBM) was dissolved in a mixture of hexafluoro-2-propanol / trifluoroacetic acid (70/30). HFIP is a halogenated alcohol [5] which is very toxic and renders the nanofibers water-soluble. It is challenging to find an ideal method to crosslink these nanofibers. Hence, instead of TFA and HFIP, other solvents and solvent blends can be searched to be mixed with DBM. In 2014, Leszczak et al. created electrospun DBM nanofibers and demonstrated that the concentration of DBM and the viscosity of the solution influence the fibers' structure and uniformity [6]. 11% DBM (56 cP) was selected after some trials.

Based on this set of information, 10% DBM was dissolved in 33:66, 25:75, 20:80, 10:90 and 0:100 acetic acid : formic acid solution blends and the viscosities of these solution blends were

measured at different time points (Table 4.2.1, Figure 4.2.1). The viscosities of these blends were too low to electrospin.

Table 4.2.1: Viscosity of 10% DBM at different ratios of acetic acid : formic acid at different time points.

		Avg Viscosities (cP)				
	10% DBM	33% Ac	25% Ac	20% Ac	10% Ac	0% Ac
Hours	0	10.6	18.9	18.9	17.4	16.6
	6	17.3	16.6	15.6	14.7	14.4
	12	16.3	16.0	14.9	14.2	13.3
	18	15.3	14.5	14.5	13.1	12.4

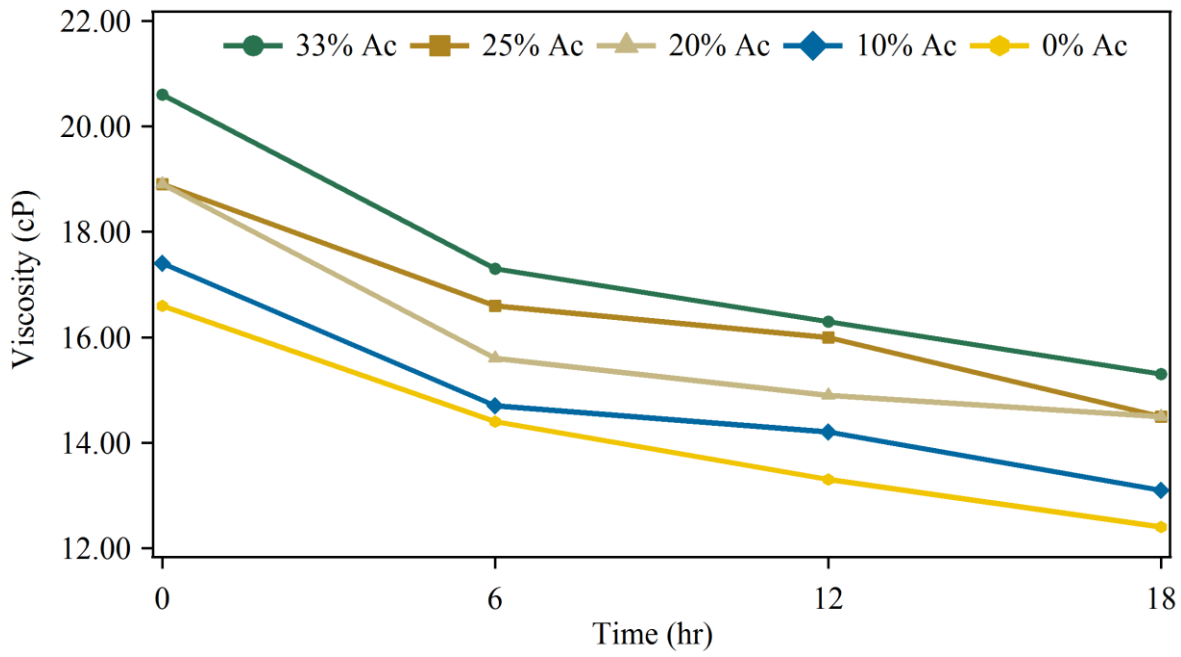

Figure 4.2.1: Viscosity of 10% DBM at different ratios of acetic acid : formic acid at different time points.

Next, 13% DBM was dissolved in 30:70 acetic acid: formic acid, and directly electrospun. No fibers were achieved, as demonstrated in Figure 4.2.2.

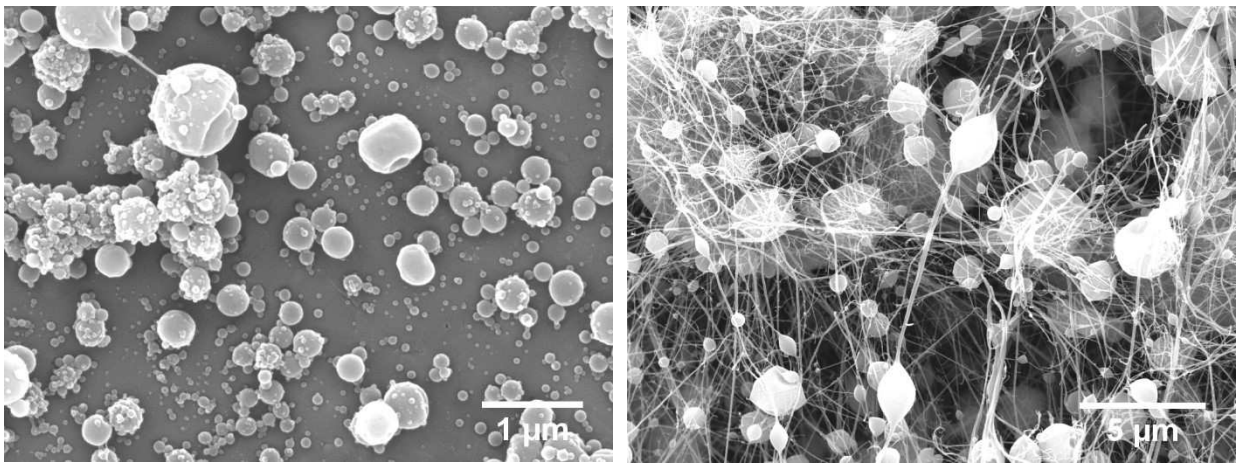

a **b**

Figure 4.2.2: SEM images of 13% (a) and 18% (b) DBM dissolved in 70:30 formic acid : acetic acid solvent blend.

Then 15% DBM was dissolved in 33:66 acetic acid: formic acid. The viscosities of the solutions at different time points were again very low.

Table 4.2.2: Viscosity of 15% DBM 33:66 acetic acid : formic acid, at different time points, at different rpm values.

		33% Ac			
	Time	rpm	V (cP)	T (°C)	Base Scale	
Hours	6	40	51.6	17.3	68.0	*TL5*
		50	51.3	17.3	85.5	
	12	40	38.5	18.0	50.6	
		50	38.5	18.0	64.2	
		70	39.0	18.0	91.2	
	18	40	36.0	17.2	47.9	
		50	36.2	17.2	60.2	
		70	36.6	17.2	85.4	
	24	40	29.0	17.5	38.6	
		50	29.3	17.5	48.8	
		70	29.5	17.5	68.5	

When DBM concentration was increased to 20%, the solution concentration was too high as can be seen in Figure 4.2.3.

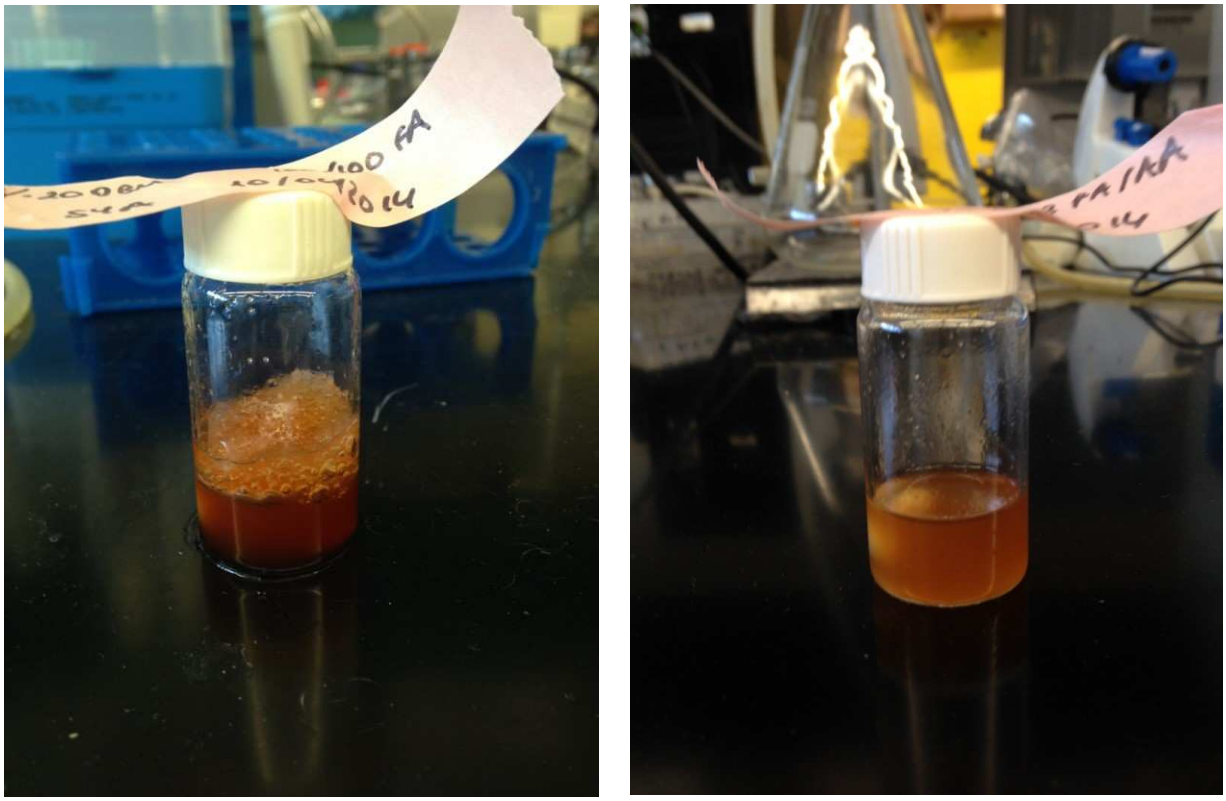

a **b**

Figure 4.2.3: 20% DBM (a) and 18% DBM (b) dissolved in 30:70 acetic acid : formic acid.

Next, DBM concentration was decreased to 18%. The polymer solution that was obtained by using 18% of DBM and 30:70 acetic acid : formic acid was electrospun. The nanofibers were imaged through SEM. Nanofibers were achieved, but they were not uniform, with some very small fibers. Future work may focus on optimizing nanofiber structure by arranging the solvent blend ratio and DBM concentration.

REFERENCES

1. Langer, R., & Vacanti, J. P. (1993). Tissue engineering. *Science, 260*(5110), 920-926.

2. Mistry, A. S., & Mikos, A. G. (2005). Tissue Engineering Strategies for Bone Regeneration. In I. V. Yannas (Ed.), *Regenerative Medicine II: Clinical and Preclinical Applications* (pp. 1-22). Berlin, Heidelberg: Springer Berlin Heidelberg.

3. Murugan, R., & Ramakrishna, S. (2007). Design strategies of tissue engineering scaffolds with controlled fiber orientation. *Tissue Engineering, 13*(8), 1845-1866.

4. Renth, A. N., & Detamore, M. S. (2012). Leveraging "Raw Materials" as Building Blocks and Bioactive Signals in Regenerative Medicine. *Tissue Engineering Part B-Reviews, 18*(5), 341-362.

5. Simpson, D. G., Bowlin, G. L., Wnek, G. E., Stevens, P. J., Carr, M. E., Matthews, J. A., & Rajendran, S. (2013). Electroprocessed collagen and tissue engineering: Google Patents.

6. Leszczak, V., Place, L. W., Franz, N., Popat, K. C., & Kipper, M. J. (2014). Nanostructured biomaterials from electrospun demineralized bone matrix: a survey of processing and crosslinking strategies. *ACS Appl Mater Interfaces, 6*(12), 9328-9337.